

# **ANNUAL REPORT**

## **2006**



**RESEARCH INSTITUTE FOR SOLID STATE  
PHYSICS AND OPTICS**  
Hungarian Academy of Sciences, Budapest, Hungary

# **Research Institute for Solid State Physics and Optics**

**Hungarian Academy of Sciences**

**Director: Dr. János Kollár**

*Address:* Budapest XII., Konkoly-Thege M. út 29-33, Hungary

*Letters:* H-1525 Budapest, P.O.B. 49

*Phone:* (36-1-) 392 2212

*Fax:* (36-1-) 392 2215

*E-Mail:* szfki@szfki.hu

*URL:* <http://www.szfki.hu/>

## **ANNUAL REPORT 2006**

*Edited by* **L. Csillag, G. Konczos, B. Selmeçi, I. Túttó**

*Closed on* 7<sup>th</sup> December, 2006

*ISSN* 1418-4559

*Dear Reader,*

It is my pleasure to hand over the 13rd, 2006 edition of the Annual Report of the Research Institute for Solid State Physics and Optics.

Our institute was founded by the *Hungarian Academy of Sciences* in 1981 as part of the *Central Research Institute for Physics*. In 1992 we became an independent institute under the name of *Research Institute for Solid State Physics*. The present profile of the institute took shape in 1998 when the *Crystal Physics Laboratory* of the Hungarian Academy of Sciences joined us, and our name changed to *Research Institute for Solid State Physics and Optics*.

The primary mission of the institute is conducting basic research in the fields of theoretical and experimental solid state physics and materials science including metal physics, crystal physics and liquid crystal research, theoretical and experimental optics including laser physics, quantum optics and the interaction of light with matter. Our experimental research activity is connected to unique methodologies like X-ray diffraction, NMR-, Mössbauer-, and optical spectroscopy and neutron scattering experiments at the *Budapest Neutron Centre*. Some of our research activities are closely related to applications, e.g., in the fields of optical thin films, laser applications, crystal growing technologies and metallurgy.

About 65 % of our funding is provided by the Hungarian Academy of Sciences; the rest originates from a variety of funding agencies in the form of competitive projects. Basic research is financed mostly by the *Hungarian Research Fund* (OTKA, 52 projects). Our staff consists of 188 employees with 133 scientists among them. Thanks to a long tradition of our graduate and postgraduate training programmes, more and more young researchers are joining us. We are involved in several international projects in collaboration with a great number of research institutions and universities. More than half of our publications (about 65 %) feature co-authors from foreign countries indicating an essential role of these partnerships. Various EU, ESF and COST and other international projects play an important role in our research activity. The share of these international resources in our budget is about 9 % (see Key figures).

This year we have published 195 papers in high quality peer-reviewed international journals as well as 36 papers in conference proceedings or books. These numbers are similar to those in previous years.

We are proud that Professor Norbert Kroó, our former director, has been elected as a member of the *Scientific Council of the European Research Council*. One of our scientists, Patrik Fazekas won the *Physics Prize* of the Hungarian Academy of Sciences. Another researcher, Gábor Oszlányi became *Doctor of the Hungarian Academy of Sciences* (DSc) this year.

It is a tradition in our institute to present awards for outstanding publication activity. In 2006 the *publication prize* was won by Imre Bakonyi for his work in the field of electrodeposited multilayers with giant magnetoresistance (GMR) behaviour and amorphous metastable phases. The *applied research prize* was awarded to three young researchers, Sára Tóth, Miklós Füle and Miklós Veres for their results in the development of super capacitors.

I hope that this booklet gives useful information to the reader. The key figures will help you to get a general overview of our institute. In addition to the description of the research activities, the Annual Report contains the e-mail addresses of our scientists as well for an easier contact. For further information please visit our WEB page at <http://www.szfki.hu>.

Budapest, November 30, 2006

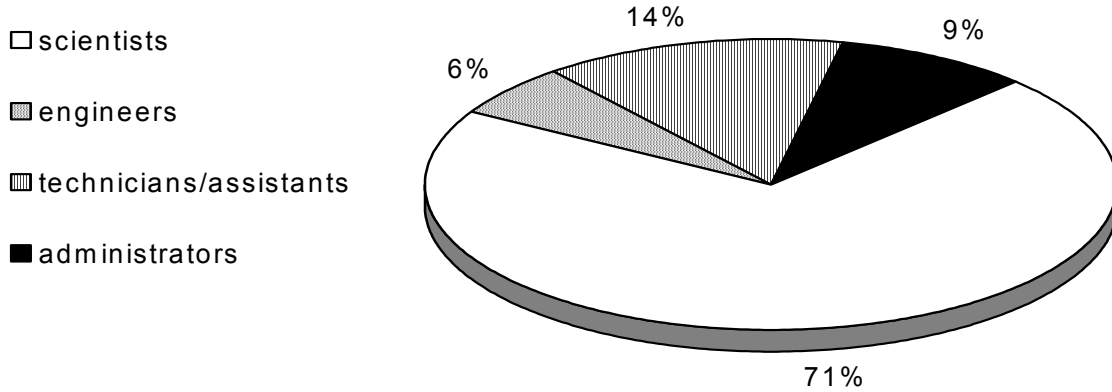
*János Kollár*

Director

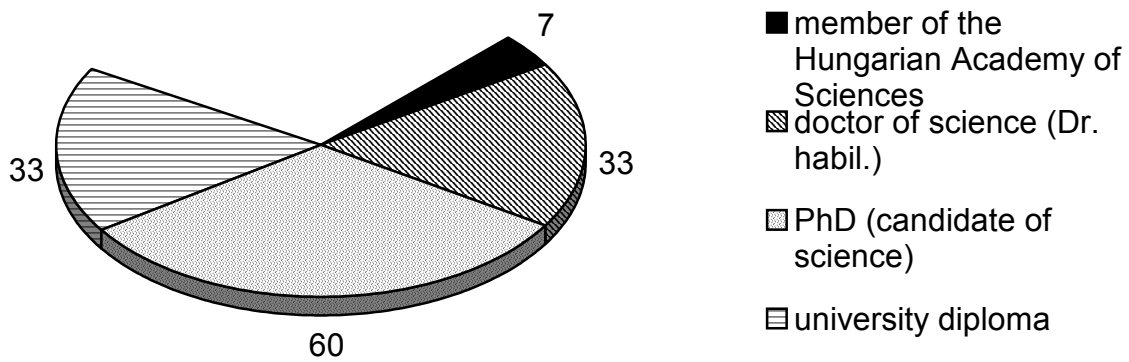
# Key figures

**Permanent staff of the Institute: 188 employees. Its distribution:**

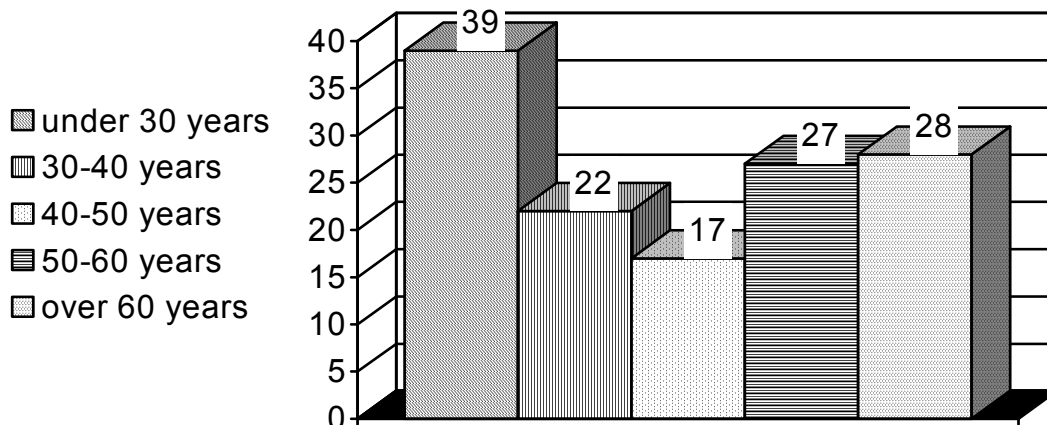
a) by professions:



b) by scientific titles/degrees:



c) by ages:



## Financial management

a) Sources of operation costs:

□ MTA (Hungarian Academy of Sciences)

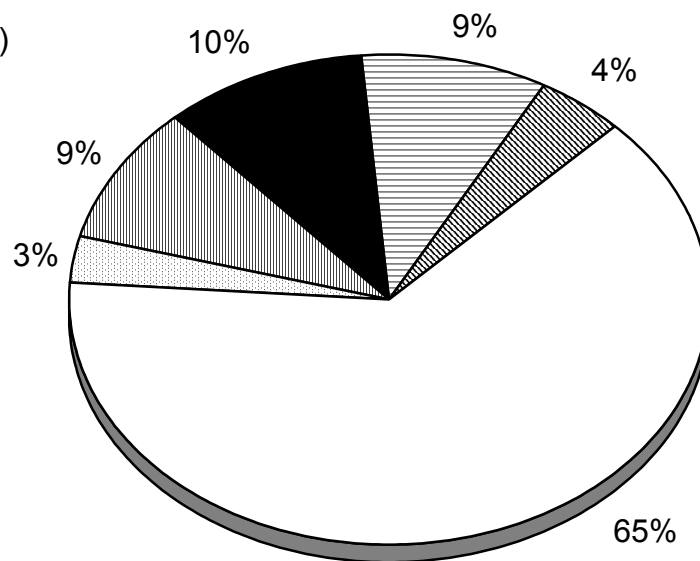
▨ MTA Research grant

▨ OTKA (Hungarian Scientific Research Fund)

■ Government

▨ EU

▨ Others



b) Distribution of expenditures:

□ wages and salaries

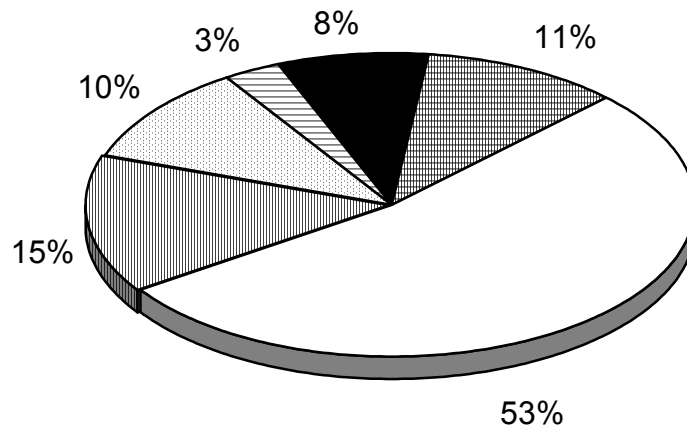
▨ overhead, labour (health service, etc.)

▨ overhead, other (energy, etc.)

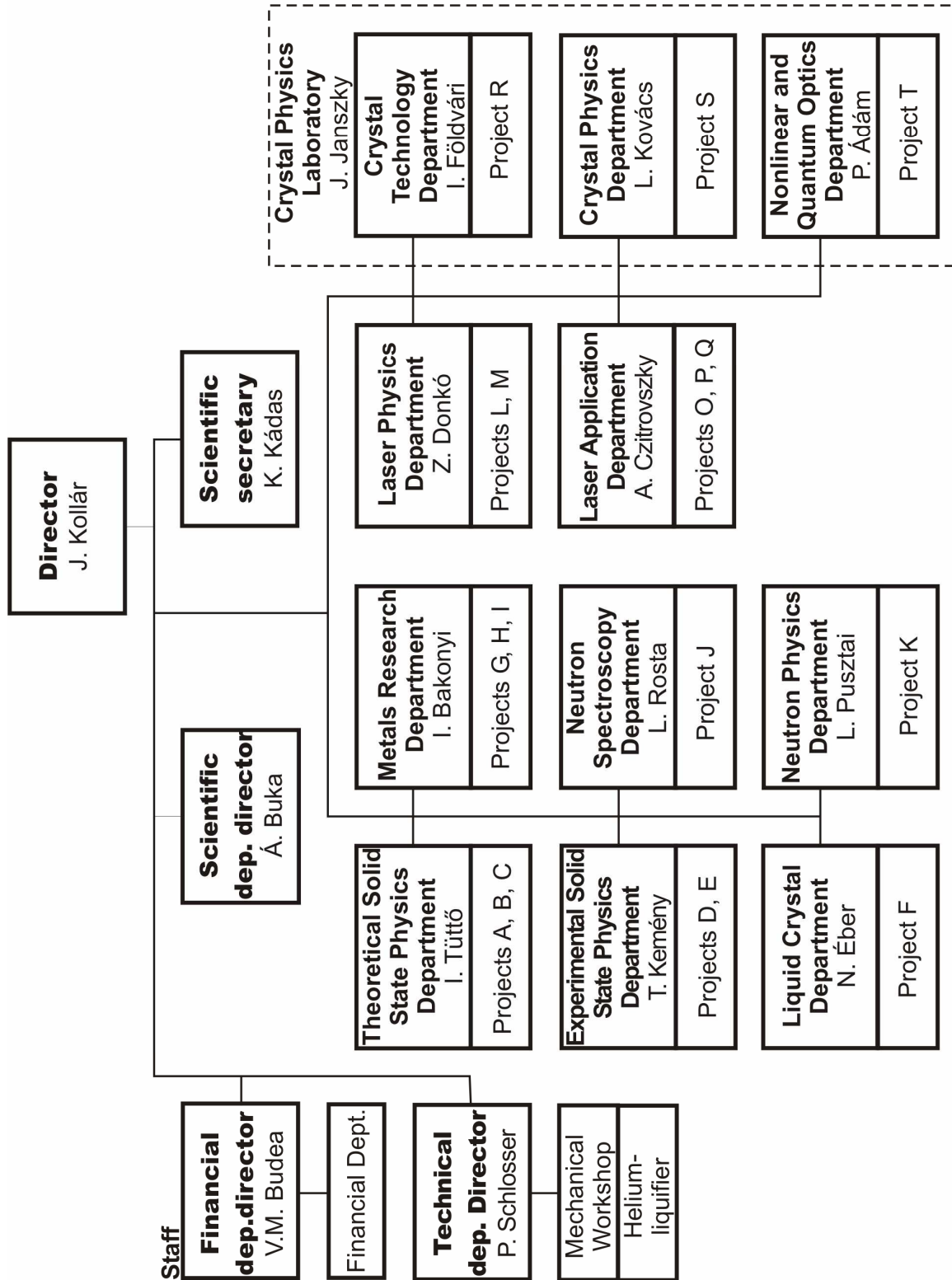
▨ consumables

■ others (incl. travel costs)

▨ investments



## Structure of the Research Institute for Solid State Physics and Optics



## A. STRONGLY CORRELATED SYSTEMS

*J. Sólyom, K. Buchta<sup>#</sup>, G. Fáth, Ö. Legeza, K. Penc, E. Szirmai<sup>#</sup>, K. Vladár, F. Woynarovich, A. Zawadowski<sup>+</sup>*

**Low dimensional fermionic and spin models.** — We have continued the application of the density-matrix renormalization-group (DMRG) method to study quantum phase transitions in spin and fermionic systems by analyzing the behavior of quantum information entropies for sites and blocks, a method that we have developed recently. It was shown that in the half-filled one-dimensional  $SU(n)$  Hubbard model, except for  $n=2$ , finite spin and charge gaps are found for arbitrary positive  $U$ , the transition to the gapped phase at  $U_c=0$  is of Kosterlitz-Thouless type and is accompanied by a bond dimerization both for even and odd  $n$ . In the  $1/n$ -filled case, the transition has similar features as the transition at  $U=0$  in the half-filled  $SU(2)$  Hubbard model. The charge gap opens exponentially slowly for  $U>U_c=0$  and the spin sector remains gapless.

A new entropy based approach has been proposed to study quantum phase transitions in low-dimensional models undergoing a transition from uniform to spatially inhomogeneous phases, such as dimerized, trimerized, or incommensurate phases. It is based on studying the length dependence of the von Neumann entropy and its corresponding Fourier spectrum for finite segments in the ground state or first excited state of finite chains. Peaks at a nonzero wave vector are indicators of oscillatory behavior in decaying correlation functions.

The quantum fluctuations in finite segments of the zero-temperature XX chain resulting from entanglement of the block with the rest of the chain has also been studied. We have found that the rest of the chain acts as a thermal environment and an effective temperature can be introduced to describe fluctuations.

A two-leg ladder with  $n$ -component fermionic fields in the chains has been considered using an analytic renormalization group method. The fixed points and possible phases have been determined for generic band filling as well as for half-filled systems and for the case when one of the subbands is half-filled. A weak-coupling Luttinger-liquid phase and several strong-coupling gapped phases have been found.

We calculated the surface spin correlations in the  $S=3/2$  antiferromagnetic Heisenberg chain using the DMRG method. These correlations decay to zero logarithmically slowly due to a bulk and a surface marginal operator. The localized edge excitations determine the first gap, which vanishes as  $\Delta_1 \sim 1/(L \ln L)$ . This supports the suggestion that this model belongs to the same universality class as the  $S=1/2$  chain having  $S=1$  impurity end spins.

**Low dimensional and frustrated magnetic systems.** — When discussing quantum magnets, it is useful to classify models according to whether or not the ground state breaks the  $SU(2)$  symmetry. While simple examples of both cases are well known [long-range magnetic order for broken  $SU(2)$  symmetry, spin ladders for nonbroken  $SU(2)$  symmetry], a lot of activity is currently devoted to the problem of identifying more exotic ground states of either type. Regarding  $SU(2)$  broken ground states, the existence of nematic (quadrupolar) order is well documented in a number of models, and it has been proposed that some kind of antiferroquadrupolar order might be at the origin of the anomalous properties of the recently investigated  $NiGa_2S_4$ . For that reason, we have investigated the

---

<sup>#</sup> PhD student

<sup>+</sup> Permanent position: Budapest University of Technology and Economics

$S=1$  Heisenberg model with bilinear and biquadratic exchange on the triangular lattice. Using mean-field theory, exact diagonalizations, and  $SU(3)$  flavor theory, we have precisely mapped out the phase diagram in a magnetic field (see Fig. 1). In particular, we show that ferroquadrupolar order can coexist with short-range helical magnetic order, and that the antiferroquadrupolar phase is characterized by a remarkable  $2/3$  magnetization plateau, in which one site per triangle retains quadrupolar order while the other two are polarized along the field.

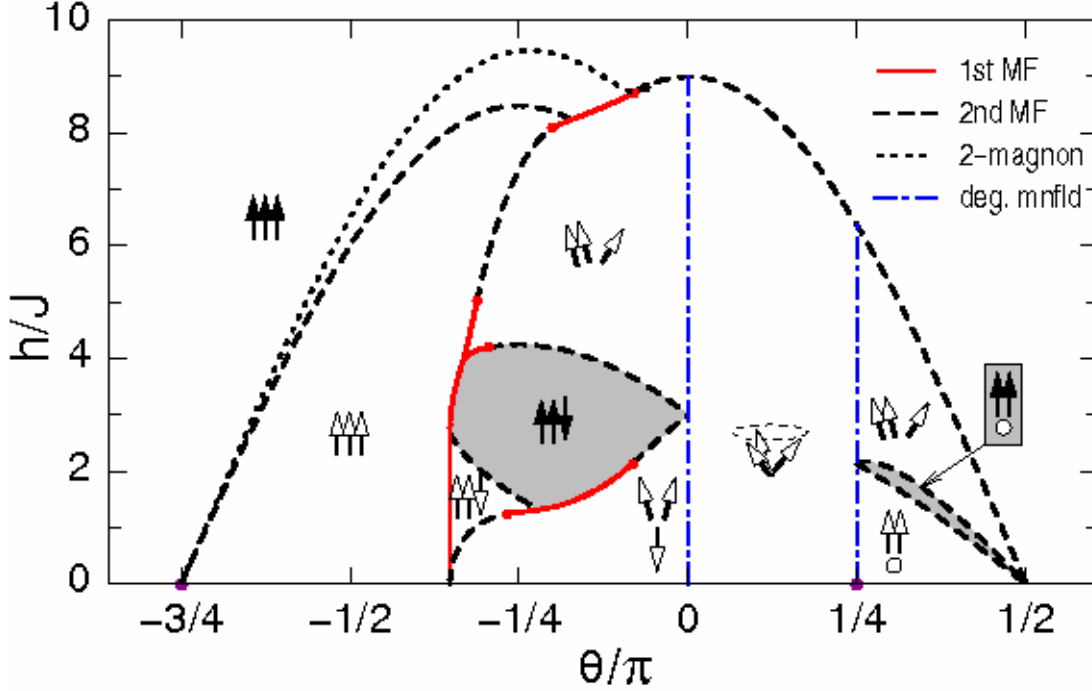


**Figure 1.** Magnetic phase diagram of the  $S=1$  Heisenberg model on triangular lattice. The strength of the bilinear coupling is  $\cos(\theta)$ , of the biquadratic one is  $\sin(\theta)$ . Solid (dashed) lines denote 1st (2nd) order phase boundaries in the variational (mean-field) approach.

The dotted line shows the exact boundary of the ferroquadrupolar phase. Along the dashed-dotted lines the variational solution is highly degenerate. The plateaux are shaded in gray. Filled arrows represent fully polarized magnetic moments, empty arrows partially polarized ones.

The dynamical response functions of the one-dimensional conductors show nonanalytical, power-law behavior of the intensity near the Fermi-points, as predicted by the Luttinger liquid theory. The power-law behaviour is, however, not limited to the vicinity of the Fermi points, but is also present along the lower edges of the excitation continua. The relevant exponents are related to the phase shifts associated with the excitation. In the case of the Hubbard model, the phase shifts can be calculated from a particular form of the Bethe Ansatz equations. Using this technique, we have calculated the edge exponents for the Hubbard model, and compared it to the experimentally measured photoemission spectra of TTF-TCNQ quasi one-dimensional material.

**Other problems.** — Game theory is one of the key paradigms behind many scientific disciplines from biology to behavioral sciences and to economics. In its evolutionary form and especially when the interacting agents are linked in a specific social network the underlying solution concepts and methods are very similar to those applied in non-equilibrium statistical physics. We have written a review that gives a tutorial-type overview of the field for physicists.

## E-Mail:

Krisztián Buchta	buchta@szfki.hu
Gábor Fáth	fath@szfki.hu
Örs Legeza	olegeza@szfki.hu
Karlo Penc	penc@szfki.hu
Jenő Sólyom	solyom@szfki.hu
Edina Szirmai	eszirmai@szfki.hu
Károly Vladár	vk@szfki.hu
Ferenc Woynarovich	fw@szfki.hu
Alfréd Zawadowski	zawa@phy.bme.hu

## Grants

- OTKA\* T043330 Theoretical study of strongly correlated low-dimensional systems (J. Sólyom, 2003–2006)
- OTKA F046356 Development and application of the momentum-space density-matrix renormalization group method for fermionic systems (Ö. Legeza, 2004–2007)
- OTKA T047003 Statistical physics of evolutionary games (Participant: G. Fáth, 2004–2007)
- OTKA T049607 Exotic phases and excitation in frustrated electron systems with charge, spin and orbital degrees of freedom (K. Penc, 2005–2007)
- NKFP 2/051/2004 Language Miner (Participant: G. Fáth, 2005–2007)

## Publications

### Articles

- A.1. Legeza Ö, Sólyom J; Two-site entropy and quantum phase transitions in low-dimensional models; *Phys Rev Lett*; **96**, 116401/1–4, 2006
- A.2. Läuchli\* A, Mila\* F, Penc K; Quadrupolar phases of the S=1 bilinear-biquadratic Heisenberg model on the triangular lattice; *Phys Rev Lett*; **97**, 087205/1–4, 2006
- A.3. Carmelo\* JMP, Penc K; Correlation-function asymptotic expansions: Universality of prefactors of the one-dimensional Hubbard model; *Phys Rev B*; **73**, 113112/1–4, 2006
- A.4. Legeza Ö, Buchta K, Sólyom J; Unified phase diagram of models exhibiting neutral-ionic transition; *Phys Rev B*; **73**, 165124/1–11, 2006
- A.5. Fáth G, Legeza Ö, Lajkó\* P, Iglói F; Logarithmic delocalization of end spins in the S=3/2 antiferromagnetic Heisenberg chain; *Phys Rev B*; **73**, 214447/1–11, 2006
- A.6. Szirmai E; Sólyom J; Possible phases of two coupled  $n$ -component fermionic chains determined using an analytic renormalization group method; *Phys Rev B*; **74**, 155110/1–17, 2006
- A.7. Carmelo\* JMP, Penc K; General spectral function expressions of a 1D correlated model; *Eur Phys J*; **51**, 477–499, 2006

---

\* OTKA = Hungarian Scientific Research Fund

- A.8. Carmelo\* JMP, Penc K; Spectral microscopic mechanisms and quantum phase transitions in a 1D correlated problem; *J Phys: Condens Matter*; **18**, 2881–2895, 2006
- A.9. Carmelo\* JMP, Penc K, Sacramento\* PD, Sing\* M, Claessen\* R; The Hubbard model description of the TCNQ related singular features in photoemission of TTF-TCNQ; *J Phys: Condens Matter*; **18**, 5191–5212, 2006
- A.10. Motome\* Y, Penc K, Shannon\* N; Monte Carlo study of half-magnetization plateau and magnetic phase diagram in pyrochlore antiferromagnetic Heisenberg model; *J Magn Magn Mater*; **300**, 57–61, 2006
- A.11. Carmelo\* JMP, Martelo\* LM, Penc K; The low-energy limiting behavior of the pseudofermion dynamical theory; *Nucl Phys B*; **737**, 237–260, 2006
- A.12. Eisler\* V, Legeza Ö, Rácz\* Z; Fluctuations in subsystems of the zero temperature XX chain: Emergence of an effective temperature; *J Stat Mech*; P11013, 2006
- A.13. Legeza Ö, Gebhard\* F, Rissler\* J; Entanglement production by independent quantum channels; *Phys Rev B*; **74**, 195112/1-11, 2006
- A.14. Buchta K, Legeza Ö, Szirmai E, Sólyom J; Mott transition and dimerization in the one-dimensional  $SU(n)$  Hubbard model; accepted for publication; cond-mat/0607374
- A.15. Legeza Ö, Sólyom J, Tincani\* L, Noack\* RM; Entropic analysis of quantum phase transitions from uniform to spatially inhomogeneous phases; accepted for publication; cond-mat/0610499.
- A.16. Szabó\* G, Fáth G; Evolutionary games on graphs; accepted for publication; cond-mat/0607344

### ***Conference proceeding***

- A.17. Fáth G, Sarvary\* M; Towards an economic theory of meaning and language; In: *Proc. of ECCS'05, Nov 14-18, 2005, Paris*; Eds.: P. Bourguine, F. Kepes, M. Schoenauer; pp. 669–697, 2005.

### ***Book chapter***

- A.18. Fáth G, Sarvary\* M; Cultural Evolution in a Population of Heterogeneous Agents; In: *The Complex Networks of Economic Interactions: Essays in Agent-Based Economics and Econophysics*, Lecture Notes in Economics and Mathematical Systems; Eds.: A. Namatame, T. Kaizouji, Y. Aruka, Springer, Berlin; Vol. 567, pp. 193–205, 2006.

***See also: C.30., C.31.***

## B. COMPLEX SYSTEMS

*F. Iglói, R. Juhász, N. Menyhárd, A. Sütő, Zs. Szép, P. Szépfalusy*

The principal interest of this group is the theoretical investigation of different aspects of equilibrium and non-equilibrium statistical physics and quantum systems.

**Phase transitions and critical behaviour.** — We have considered interacting many particle systems with quenched disorder having strong Griffiths singularities, which are characterized by the dynamical exponent,  $z$ , such as random quantum systems and exclusion processes. In several  $d = 1$  and  $d = 2$  dimensional problems we have calculated the inverse time-scales,  $\tau^{-1}$ , in finite samples of linear size,  $L$ , either exactly or numerically. In all cases, having a discrete symmetry, the distribution function,  $P(\tau^{-1}, L)$ , is found to depend on the variable,  $u = \tau^{-1}L^z$ , and to be universal given by the limit distribution of extremes of independent and identically distributed random numbers. This finding is explained in the framework of a strong disorder renormalization group approach when, after fast degrees of freedom are decimated out the system is transformed into a set of non-interacting localized excitations. The Fréchet distribution of  $P(\tau^{-1}, L)$  is conjectured to hold for all random systems having a strong disorder fixed point, in which the Griffiths singularities are dominated by disorder fluctuations.

We have studied the critical behavior at an interface which separates two semi-infinite subsystems belonging to different universality classes, thus having different set of critical exponents, but having a common transition temperature. We have solved this problem analytically in the frame of  $\phi^k$  mean-field theory, which is then generalized using phenomenological scaling considerations. A large variety of interface critical behavior is obtained which is checked numerically on the example of two-dimensional  $q$ -state Potts models with  $2 \leq q \leq 4$ . We have found that weak interface couplings are generally irrelevant, resulting in the same critical behavior at the interface as for a free surface. With strong interface couplings, the interface is found to remain ordered at the bulk transition temperature. More interesting is the intermediate situation, the special interface transition, when the critical behavior at the interface involves new critical exponents, which however can be expressed in terms of the bulk and surface exponents of the two subsystems.

An investigation of the effect of quenched disorder in a one-dimensional nonequilibrium kinetic Ising cellular automaton model has been carried out with the help of large-scale computer simulations. It has been found that weak disorder causes irrelevant perturbation, contradicting the Harris criterion. In the strong disorder limit, however, a continuously changing density decay exponent was observed.

**Quantum systems.** — We have studied the spin and particle dynamics in the phases originating from the polar phase of a Bose-Einstein condensed spin-1 gas when a magnetic field is switched on. Two species Fermi gas has been investigated on the BCS side up to the Feshbach resonance taking into account gradient corrections. Ground state structure of the partly filled 1-shell of a fermion gas of atoms of spin  $s$  in a spherically symmetric trap potential has been determined.

In a complete one-loop parametrization of the  $SU(3)_R \times SU(3)_L$  linear sigma model the boundary of the first order chiral transition region in the  $m_\pi$ - $m_K$  plane is determined using resummed perturbation theory. Based on the scaling region of the tricritical point on the  $m_\pi = 0$  axis, its location is estimated.

In the leading order of the large  $N$  expansion to a  $O(N) \times Z_2$  symmetric scalar model, which represents an extension of the Standard Model with an  $n$ -component "phantom" field, the possibility of phantom field fluctuations induced symmetry breaking of  $Z_2$  symmetry is demonstrated even when all iteratively renormalized parameters of the model are positive.

**Other researches.** — Ground states of classical pair interactions in continuous space were studied in two papers. For interactions having a non-negative and finite-range Fourier transform the existence of periodic and aperiodic ground states was proven for high enough densities. This is the first result on this problem, valid in three dimensions.

Efficiency of the charge flipping (CF) method of crystallographic phase retrieval, introduced in 2004, was demonstrated on experimental data coming from an X-ray diffraction measurement on a molecular crystal containing 271 non-hydrogen atoms in its unit cell. Because of an awkward pseudo-symmetry, earlier determination of the structure presented considerable difficulty to other methods. Structure solution with the CF algorithm was shown to be much faster and more complete.

## E-Mail:

Ferenc Iglói	igloi@szfki.hu
Róbert Juhász	juhasz@szfki.hu
Nóra Menyhárd	menyhard@szfki.hu
András Sütő	suto@szfki.hu
Zsolt Szép	szepzs@achilles.elte.hu
Péter Szépfalusy	psz@galahad.elte.hu

## Grants and international cooperations

OTKA T048721 Statistical physics of disordered systems (F. Iglói, 2005-2008)  
OTKA T046129 Dynamics of phase transitions and symmetry breaking phases (P. Szépfalusy, 2004-2007)  
DAAD-MÖB 26/2006 Statistical physics of nonequilibrium and disordered systems (F. Iglói, 2006-2007)  
KPI Öveges grant ASEP1111 Transport and condensation in interacting and reacting systems (F. Iglói, 2006-2007)

## Publications

### Articles

- B.1. Sütő A; Crystalline ground states for classical particles; *Phys Rev Lett*; **95**, 265501/1-4, 2005
- B.2. Karsai\* M, Juhász R, Iglói F; Nonequilibrium phase transitions and finite size scaling in weighted scale-free networks; *Phys Rev E*; **73**, 036116/1-6, 2006
- B.3. Környei\* L, Pleimling\* M, Iglói F; Reentrance during nonequilibrium relaxation; *Europhys Lett*; **73**, 197-203, 2006
- B.4. Mercaldo\* MT, Anglés d'Auriac\* J-Ch, Iglói F; Critical and tricritical singularities of the three-dimensional random-bond Potts model for large  $q$ ; *Phys Rev E*; **73**, 026126/1-12, 2006

- B.5. Bagaméry\* FÁ, Turban\* L, Iglói F: Critical behavior at the interface between two systems belonging to different universality classes; *Phys Rev B*; **73**, 144419/1-15, 2006
- B.6. Juhász R, Lin\* Y-C, Iglói F; Strong Griffiths singularities in random systems and their relation to extreme value statistics; *Phys Rev B*; **73**, 224206/1-10, 2006
- B.7. Lin\* Y-C, Rieger\* H, Laflorencie\* N, Iglói F; Strong disorder renormalization group study of  $S = 1/2$  Heisenberg antiferromagnet layers/bilayers with bond randomness, site dilution and dimer dilution; *Phys Rev B*; **74**, 024427/1-12, 2006
- B.8. Mélin\* R, Iglói F; Strongly disordered Hubbard model in one dimension: spin and orbital infinite randomness and Griffiths phases; *Phys Rev B*; **74**, 155104/1-8, 2006
- B.9. Sütő A; From bcc to fcc: interplay between oscillating long-range and repulsive short-range forces; *Phys Rev B*; **74**, 104117/1-8, 2006
- B.10. Ódor\* G, Menyhárd N; Critical behavior of an even-offspringed branching and annihilating random-walk cellular automaton with spatial disorder; *Phys Rev E*; **73**, 036130/1-5, 2006
- B.11. Herpay\* T, Szép Zs: Resummed one-loop determination of the phase boundary of the  $SU(3)_R \times SU(3)_L$  linear sigma model in the  $m_\pi - m_K -$  plane; *Phys Rev D*; **74** 025008/1-11, 2006
- B.12. Patkós\* A, Szép Zs; Phantom field fluctuation induced Higgs effect; *Phys Lett B*; **642**, 384-388, 2006
- B.13. Csordás\* A, Szőke\* E, Szépfalusy P; Cluster states of Fermions in the single 1-shell model; *Eur Phys J D*; accepted for publication
- B.14. Kis-Szabó\* K, Szépfalusy P, Szirmai\* G; Phases of a polar spin-1 Bose gas in a magnetic field; *Phys Lett A*; accepted for publication

***See also A.5., E.15., E.30***

## C. ELECTRONIC STATES IN SOLIDS

*J. Kollár, P. Fazekas, K. Kádas, B. Lazarovits, I. Tüttő, B. Újfalussy, A. Virosztek<sup>+</sup>, L. Vitos, V. Zólyomi*

The surprisingly low magnetic transition temperatures in **austenitic stainless steels** indicate that in these Fe-based alloys **magnetic disorder** might be present at room temperature. Using a first-principles approach, we have obtained a theoretical description of the stacking fault energy in Fe-Cr-Ni alloys as a function of composition and temperature. Comparison of our results with experimental databases provides a strong evidence for large magnetic fluctuations in these materials. We demonstrate that the effects of alloying additions on the structural properties of steels contain a dominant magnetic contribution, which stabilizes the most common austenitic steels at normal service conditions. The **stacking fault energy** (SFE) of **austenitic stainless** steels has been determined using a quantum mechanical first-principles approach. We identify the electronic, magnetic and volume effects responsible for the compositional dependence of the SFE. We find that both the alloying element and the composition of the host material are important for understanding the alloying effects. Our results show that no simple and universally valid composition equations exist for the SFE.

We present a first-principles description of the **temperature-dependent elastic constants in random alloys**. The substitutional disorder is treated using the coherent potential approximation implemented within the frameworks of exact muffin-tin orbitals theory. The temperature effects are approximated as the sum of electronic and thermal expansion contributions. Calculations on pure Nb demonstrate that this approach correctly accounts for the main temperature dependence of cubic elastic constants. When extended to Nb-Zr solid solution, the theoretical results show good agreement with experiments at temperatures  $< 300$  K.

We put forward a technique for calculating the **surface segregation profile in substitutional disordered alloys**. The surface internal energy and the effective bulk and surface chemical potentials are calculated using the full charge density exact muffin-tin orbitals method, combined with the coherent potential approximation. The application of our approach is demonstrated to the close-packed surface of  $\text{Ag}_c\text{Pd}_{1-c}$  random alloys with  $0 < c < 1$ . The surface concentration profile, surface energy and segregation energy are investigated as functions of bulk composition. The present results are compared with former theoretical and experimental data. It is found that at low temperature, Ag segregates to the surface layer for the entire bulk composition range. At 0 K, the subsurface layer contains 100% Pd for  $c < 0.4$ , and somewhat more than  $(2c-1)$  Ag in alloys with  $c > 0.5$ . The temperature dependence of the segregation profile is significant for Pd rich alloys and for alloys with intermediate concentrations. At temperatures 1600 K, the subsurface layer is obtained to be almost bulk like.

Using the density functional theory formulated within the framework of the exact muffin-tin orbitals method, we have investigated the **stability of the body centered cubic phase of Be** ( $\beta$ -Be). We calculated the elastic constants and Debye temperature of  $\beta$ -Be over a wide volume range and compared to those obtained for the low temperature hexagonal phase ( $\alpha$ -Be). We obtained a significant difference in anisotropy of the bcc and hcp structures. In line with experiments, we predict that the hcp  $\rightarrow$  bcc phase transition occurs at 240 GPa at 0 K and 239 GPa at ambient temperature. We find that the bcc phase rapidly

---

<sup>+</sup> Permanent position: Budapest University of Technology and Economics

loses its stability above the zero temperature equilibrium volume ( $V_0$ ) and becomes mechanically unstable at  $1.17 V_0$ , where the stability condition  $C_{11} > C_{12}$  is violated. We demonstrated that at 0 K the lattice instability of bcc Be near its experimental volume is related to an electronic topological transition due to the increased number of occupied  $s$  states near the Fermi level compared to that at  $V_0$ . The mechanism is found to be present in other hexagonal metals and alloys as well.

In order to find the ground state configuration of a **magnetic cluster** it is necessary to know the interactions between the individual atoms. These interactions can lead to a **non-collinear magnetic ground state**. In particular, two strategies can be followed: (i) the interaction parameters of a classical Heisenberg model can be calculated by using the magnetic force theorem and then the motion of the spins can be traced by solving the Landau-Lifshitz-Gilbert equation or (ii) an ab-initio spin-dynamics technique can be applied where the ground state can be found in a self-consistent way. The magneto-crystalline anisotropy, the anisotropic exchange as well as the Dzyaloshinskii-Moria interaction between the magnetic atoms can play an important role in the formation of a non-collinear ground state configuration. Therefore we made relativistic calculations for small anti-ferromagnetic clusters on a non-magnetic surface (Cr/Au) with both methods. By comparing the Heisenberg model results with the ab-initio ones can find the limitations and problems which can arise from the simple model calculations.

We started to study **non-linear transport** properties of **strongly correlated electron systems** by using the so-called Keldysh Green's function technique. First we investigate some simple model systems to enable us to develop a method (combined with ab-initio electronic structure calculations) which can be applied for realistic problems in the future.

Driven by its potential application in the design of ultra-high density magnetic recording devices, we are engaged in large calculations aimed to calculate the **magneto-crystalline anisotropy of surface nanostructures**. A comprehensive study for various geometries of different kinds of magnetic atoms (and their alloys) on a variety of substrates was performed.

Nuclear magnetic resonance measurements on isotope engineered **double walled carbon nanotubes** (DWCNTs) suggest a uniformly metallic character of all nanotubes. Such an effect can only be explained by the interaction between the inner and outer shell. We have performed an extensive study of the inter-layer interaction in DWCNTs by density functional theory and inter-molecular Hückel model. We have found that it is possible for two layers of semiconducting single walled nanotubes to form a metallic DWCNT, but not necessarily in every case. For most metallic DWCNTs, a high density of states can be expected at the Fermi level.

The smallest possible inner tube diameter in a DWCNT is the zero diameter inner tube, in other words, an infinite linear carbon chain. We have performed a first principles study of the vibrational properties of the infinite carbon chain, employing a novel linear/exponential scaling scheme based on the intrinsic behavior of the long range force constant couplings in quasi one-dimensional chains. We obtained the longitudinal optical Raman active frequency at  $1870-1877 \text{ cm}^{-1}$ , in contrast to the widely accepted values in the  $2000-2200 \text{ cm}^{-1}$  range. Our results provided further evidence for the assignment of the characteristic Raman peaks near  $1850 \text{ cm}^{-1}$  of the recently discovered long linear carbon chains encapsulated inside multi-walled or DWCNTs.

We studied **non-local order in correlated electron systems**. The order parameter cannot be defined at a single lattice site, because the spin and/or orbital states of at least two sites are entangled due to quantum resonance. Dimer states and plaquette states are well-known

examples. It is furthermore possible that the dimers and plaquettes themselves are resonating, forming quantum liquid type phases. We investigated the competition of such non-local phases with conventional magnetic and orbital ordering.

In close collaboration with experimentalist colleagues at the Budapest University of Technology and Economics, we worked on the interpretation of recent experimental results on the correlated system BaVS<sub>3</sub>. In particular, we discussed the ARPES determination of the electronic structure, and magnetic-field induced metal-insulator transitions and quantum criticality at high pressures.

We have continued to investigate theoretically various properties of **unconventional density waves** (UDW) in quasi-one- and two-dimensional systems. Our calculations of the angular dependent magnetoresistance (ADMR) indicate that UDW may be responsible for the observed experimental behavior in the pseudogap phase of the heavy fermion material CeCoIn<sub>5</sub>. We have worked out the theory of UDW driven by electron-phonon coupling, and suggested a unified description of UDW and superconductivity explaining the qualitative features of the phase diagram of high temperature superconductors. Based on UDW theory we have also suggested an explanation of the pseudogap phase in (TaSe<sub>4</sub>)<sub>2</sub>I. Moreover, we determined the optical conductivity in superconductors with various nodal gap structures.

## E-Mail:

Patrik Fazekas	pf@szfki.hu
Krisztina Kádas	kadas@szfki.hu
János Kollár	jk@szfki.hu
Bence Lazarovits	bl@szfki.hu
István Tüttő	tutto@szfki.hu
Balázs Újfalussy	bu@szfki.hu
Attila Virosztek	viro@szfki.hu
Levente Vitos	lv@szfki.hu
Viktor Zólyomi	zachary@szfki.hu

## Grants and international cooperations

OTKA T048827 First principles calculations for surfaces; surface stress and segregation (J. Kollár, 2005-2008)

EFS Programme: Towards atomistic materials design (J. Kollár, 2003-2007)

OTKA 46773 Investigation of metals, alloys and oxides using the density functional theory (L.Vitos, 2004-2007)

OTKA K62280 Phase transitions in correlated electron systems: Theory and NMR experiments (P. Fazekas, 2006-2009 )

## Publications

### Articles

C.1. Dubrovinskaia\* N, Dubrovinsky\* L, Kantor\* I, Crichton\* W A, Dmitriev\* V, Prakapenka\* V, Shen\* G, Vitos L, Ahuja\* R, Johansson\* B, Abrikosov\* I A; Beating the miscibility barrier between iron and magnesium by high-pressure alloying; *Phys Rev Lett*; **95**, 245502/1-4, 2005

- C.2. Kádas K, Nabi\* Z, Kwon\* SK, Vitos L, Ahuja\* R, Johansson\* B, Kollár J; Surface relaxation and surface stress of 4d transition metals; *Surface Science*; **600**, 395-402, 2006
- C.3. Kwon\* SK, Nabi\* Z, Kádas K, Vitos L, Kollár J, Johansson\* B, Ahuja\* R; Surface energy and stress release by layer relaxation; *Phys Rev B*; **72**, 235423/1-5, 2005
- C.4. Vitos L, Larsson\* K, Johansson\* B, Hanson\* M, Hogmark\* S; An atomistic approach to the initiation mechanism of galling; *Comp Mat Sci*; **37**, 193-197, 2006
- C.5. Vitos L, Magyari-Köpe\* B, Kollár J, Grimvall\* G, Johansson\* B; Phase separation in Ca-bearing minerals; *Physics of the Earth and Planetary Interiors*; **156**, 108-116, 2006
- C.6. Kissavos\* AE, Simak\* SI, Olsson\* P, Vitos L, Abrikosov\* IA; Total energy calculations for systems with magnetic and chemical disorder; *Comp Mat Sci*; **35**, 1-5, 2006
- C.7. Landa\* A, Klepeis\* J, Söderlind\* P, Naumov\* I, Velikokhatnyi\* O, Vitos L, Ruban\* A; Fermi surface nesting and pre-martensitic softening in V and Nb at high pressures; *J Phys Condens Matter*; **18**, 5079-5085, 2006
- C.8. Punkkinen\* MPJ, Kokko\* K, Ropo\* M, Väyrynen\* IJ, Vitos L, Johansson\* B, Kollár J; Magnetism of (FeCo)Si alloys: Extreme sensitivity on crystal structure; *Phys Rev B*; **73**, 024426/1-10, 2006
- C.9. Vitos L, Nilsson\* JO, Johansson\* B; Alloying effects on the stacking fault energy in austenitic stainless steels from first-principles theory; *Acta Materialia*; **54**, 3821-3826, 2006
- C.10. Huang\* L, Vitos L, Kwon\* SK, Johansson\* B, Ahuja\* R; Thermo-elastic properties of random alloys from first-principles theory; *Phys Rev B*; **73**, 104203/1-4, 2006
- C.11. Vitos L, Korzhavyi\* PA, Johansson\* B; Evidence of large magnetostructural effects in austenitic stainless steels; *Phys Rev Lett*; **96**, 117210/1-4 2006
- C.12. Ropo\* M, Kokko\* K, Vitos L, Kollár J, Johansson\* B; The chemical potential in surface segregation calculations: AgPd alloys; *Surf Sci*; **600**, 904-913, 2006
- C.13. Landa\* A, Klepeis\* J, Söderlind\* P, Naumov\* I, Velikokhatnyi\* O, Vitos L, Ruban\* A; Ab initio calculations of elastic constants of the bcc V–Nb system at high pressures; *Journal of Physics and Chemistry of Solids*; **67**, 2056-2064, 2006
- C.14. Faulkner\* JS, Pella\* S, Rusanu\* A, Puzyrev\* Y, Leventouri\* Th, Stocks\* GM, Ujfalussy B; Mean-field approximations for the electronic states in disordered alloys; *Phil Mag*; **86**, 2661-2671, 2006
- C.15. Radnóczy\* K, Fazekas P; Orbital order and spin-orbit coupling in BaVS<sub>3</sub>; *Physica B: Condens matter*; **378-380**, 663-664, 2006
- C.16. Lazarovits B, Szunyogh\* L, Weinberger\* P; Spin-polarized surface states close to adatoms on Cu(111); *Phys Rev B*; **73**, 045430/1-5, 2006

- C.17. Zólyomi V, Ruzsnyák\* Á, Kürti\* J, Gali\* Á, Simon\* F, Kuzmany\* H, Szabados\* Á, Surján\* PR; Semiconductor-to-metal transition of double walled carbon nanotubes induced by inter-shell interaction; *physica status solidi (b)*; **243**, 3476-3479, 2006
- C.18. Pfeiffer\* R, Simon\* F, Kuzmany\* H, Popov\* VN, Zólyomi V, Kürti\* J; Tube-tube interaction in double-wall carbon nanotubes; *physica status solidi (b)*; **243**, 3268-3272, 2006
- C.19. Schaman\* Ch, Pfeiffer\* R, Zólyomi V, Ayami\* D, Herges\* R, Dubay\* O, Sloan\* J; The transformation of open picotubes to a closed molecular configuration; *physica status solidi (b)*; **243**, 3151-3154, 2006
- C.20. Kürti\* J, Zólyomi V, Yang\* S, Kertesz\* M; Double walled carbon nanotube with the smallest inner diameter: a first principles study; *physica status solidi (b)*; **243**, 3464-3467, 2006
- C.21. Dóra\* B, Maki\* K, Virosztek A; D-wave density waves in CeCoIn<sub>5</sub> and high T<sub>c</sub> cuprates; *J Phys IV*; **131**, 319-322, 2005
- C.22. Ványolos\* A, Virosztek A; Unconventional charge density wave in coupled electron-phonon system; *J Phys IV*; **131**, 347-348, 2005
- C.23. Won\* H, Haas\* S, Maki\* K, Parker\* D, Dóra\* B, Virosztek A; Gossamer superconductivity, new paradigm?; *physica status solidi (b)*; **243**, 37-45, 2006
- C.24. Dóra\* B, A. Ványolos\* A, Virosztek A; Pseudogap phase in (TaSe<sub>4</sub>)<sub>2</sub>I: Mean-field calculation; *Phys Rev B*; **73**, 125110/1-6, 2006
- C.25. Ványolos\* A, Dóra\* B, A. Virosztek A; Unconventional charge density wave driven by electron-phonon coupling; *Phys Rev B*; **73**, 165127/1-10, 2006
- C.26. Dóra\* B, K. Maki\* K, Virosztek A; Optical conductivity of nodal superconductors; *Current Applied Physics*; **6**, 903-908, 2006
- C.27. Landa\* A, Söderlind\* P, Vitos L; Density-functional calculations of  $\alpha$ -Pu-Ga(Al) alloys; *J Alloys and Compounds*; accepted for publication
- C.28. Zander\* J, Sandström\* R, Vitos L; Modeling mechanical properties for non-hardenable aluminium alloys; *Materials science and Engineering*; accepted for publication
- C.29. Stocks\* GM, Eisenbach\* M, Ujfalussy B, Lazarovits, Szunyogh\* L, Weinberger\* P; On calculating the magnetic state of nanostructures; *Progress in Materials Science*; accepted for publication
- C.30. Mila\* F, Vernay\* F, Ralko\* A, Becca\* F, Fazekas P, Penc K; The emergence of Resonating Valence Bond physics in spin-orbital models; *J Phys: Cond Mat*; accepted for publication; cond-mat/0609455
- C.31. Fazekas P, Penc K, Radnóczy\* K, Barisic\* N, Berger\* H, Forró\* L, Mitrovic\* S, Gauzzi\* A, Demkó\* L, Kézsmárki\* I, Mihály\* G; The electronic structure and the phases of BaVS<sub>3</sub>; *J Magn and Magn Mater*; accepted for publication

### **Conference proceedings**

- C.32. Vitos L, Korzhavyi\* PA, Nilsson\* JO, Johansson\* B; Theoretical evidence of large magneto-structural effects in austenitic stainless steels; In: *International Conference on Magnetism, Kyoto, Japan, August 20-25, 2006*; J Magn and Magn Mat; accepted for publication
- C.33 Vitos L, Johansson\* B; Mechanical properties of random alloys from quantum mechanical simulations; In: *Workshop on state-of-the-art in scientific and parallel computing Umeå, Sweden, June 18-21, 2006*; Springer series: Lecture Notes in Computer Science; accepted for publication

### **Book chapter**

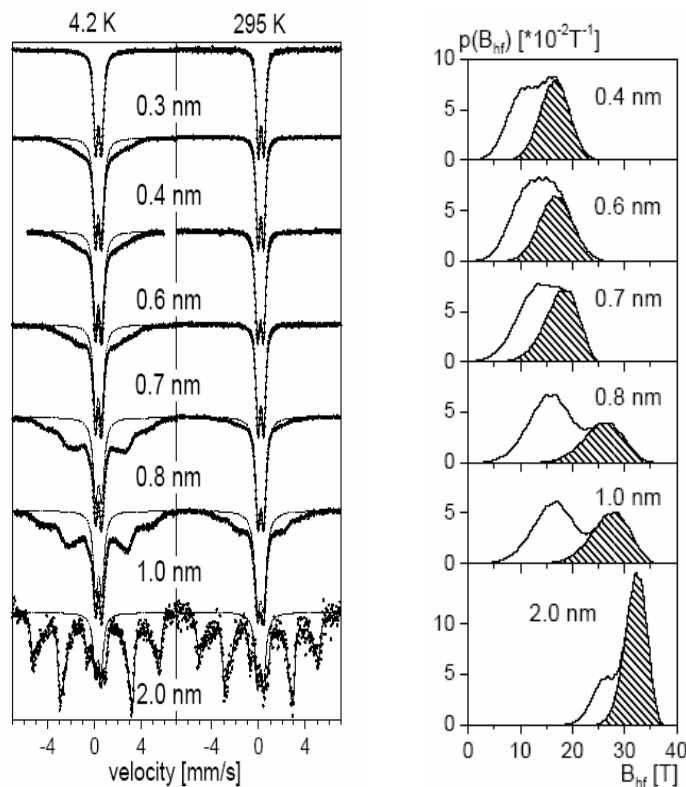
- C.34. Palotás\* K, Lazarovits B, Szunyogh\* L, Weinberger\* P; Electric properties of nanostructures; In: *Handbook of Theoretical and Computational Nanotechnology*; Eds.: M. Rieth and W. Schommers, Volume 10, Chapter 6; American Scientific Publishers, Los Angeles; pp. 363-408, 2006

## D. NON-EQUILIBRIUM ALLOYS

*I. Vincze, J. Balogh, L. Bujdosó, D. Kaptás, T. Kemény, L.F. Kiss*

**The magnetism of multilayers with ultra-thin Fe layers.** — The magnetism of ultrathin layers raises many interesting questions, but in most cases it is difficult to separate the effects of dimensionality from the effects of intermixing between the magnetic and non-magnetic layers. Fe/Al and Fe/Ag multilayers have been investigated by  $^{57}\text{Fe}$  Mössbauer spectroscopy to gain information both on the magnetic properties and on the local neighborhood of the magnetic atoms.

The Fe-Al system is well suited for such a study since the magnetic moment and the hyperfine field of the Fe atoms depends strongly on the number of Al first neighbors. The temperature and magnetic field dependences of the Fe hyperfine fields were studied in ultra-thin Fe/Al multilayers with constant Al (3 nm) and varying (between 0.3 and 2.0 nm) Fe layer thickness. The room temperature and the 4.2 K Mössbauer spectra can be seen in *Fig. 1*. Interface mixing results in the formation of a non-magnetic alloy phase. Its amount, calculated from the 4.2 K spectra, is  $t_D=0.3$  nm in equivalent thickness for all the samples. The effective thickness of the magnetic Fe layers,  $t_{eff}$ , was calculated by subtracting  $t_D$  from the nominal thickness. The observed change in the shape of the hyperfine field distributions, as shown in *Fig. 2*, and the related jump of the average parameters with increasing effective thickness is explained by the building up of the magnetic Fe layers and by the respective roles of the two- and three or more monolayer thick Fe regions. A markedly different temperature and magnetic field dependence of the magnetic behavior was observed below and above  $t_{eff}=0.5$  nm, where the formation of Fe regions consisting of three and more atomic planes starts. At and above this thickness  $T_c$  is well above room temperature, the Fe hyperfine fields show a Bloch-type  $T^{3/2}$ -law decrease with increasing temperature. In magnetic fields applied perpendicularly to the sample plane a rather large magnetic anisotropy, i.e. slow approach to magnetic saturation, is observed. In 3 T field, full collinearity of the magnetic moments is reached only in the thickest ( $t_{eff}=1.7$  nm) sample.



slow approach to magnetic saturation, is observed. In 3 T field, full collinearity of the magnetic moments is reached only in the thickest ( $t_{eff}=1.7$  nm) sample.

**Figure 1. (left)** Mössbauer spectra of Fe/Al multilayers measured at 4.2 K and at room temperature as a function of the nominal Fe layer thickness

**Figure 2. (right)** Distribution of the Fe hyperfine field of the magnetically split component of the Mössbauer spectra at 4.2 K as a function of the nominal Fe layer thickness. The lightly shaded area marks the high field component (see text for details).

Below  $t_{eff}=0.5$  nm the formation of two layers thick magnetic platelets was deduced from the hyperfine field distribution. The magnetically split component of the spectra disappears well below room temperature. It is a kind of freezing at  $T_f=15$  K and 40 K for  $t_{nom}=0.4$  and 0.7 nm, respectively. The hyperfine field increases linearly with decreasing temperature below  $T_f$ . The superparamagnetic nature of the transition was verified by the application of a 1 T magnetic field above the freezing temperature which resulted in the reappearance of the magnetic splitting.

Fe/Ag multilayers also show superparamagnetic properties when the nominal Fe layer thickness is in the few monolayer range, but mixing of the elements is much less significant due to the large positive heat of mixing. The average cluster size was determined both from SQUID magnetization and from in-field Mössbauer spectroscopy measurements. For  $d_{Fe}=0.2$  nm nominal thickness, it is in the 1-2 nm range depending on  $d_{Ag}$ , as well. Increasing  $d_{Ag}$  was found to decrease the magnetic grain size. The spectra of two samples with  $d_{Ag}=2.6$  (A) and 5.4 nm (B) are shown in *Fig. 3*, as measured at 4.2 K in zero and in different applied fields. For both samples the spectra exhibit broad but definitely structured lines, which allows a separation into two components, also shown in the figure. Application of an external field at 4.2 K does not influence the shape of the distributions and the measured spectra correspond to a ferromagnetic behavior. In accordance with a saturating bulk magnetization the intensity of the second and fifth lines goes to zero above 3 T at 4.2 K, i.e. the magnetic moments are aligned along the applied field. The average value of the full hyperfine field distribution and the two sub-distributions are shown in *Fig. 4* for the two samples. Since the hyperfine field is aligned opposite to the magnetization, the saturation of  $B_{hf} + B_{ext}$ , i.e. the sum of the measured hyperfine field and the external field, also indicates ferromagnetic alignment of the magnetic moments along the applied field. This behavior proves that the significant differences observed in the 4.2K spectra of the two samples are not due to different superparamagnetic relaxation rates or to the presence of magnetically different sites, but reflect differences of the hyperfine field of Fe atoms sitting in different neighborhoods. Our analysis has shown that the ratio of the low field components can be supposed proportional to the number of interface atoms. The 50-70 % ratio of the interface atoms, as can be estimated from the ratio of the low field components, is in line with the 1-2 nm average grain size deduced from the SQUID measurements.

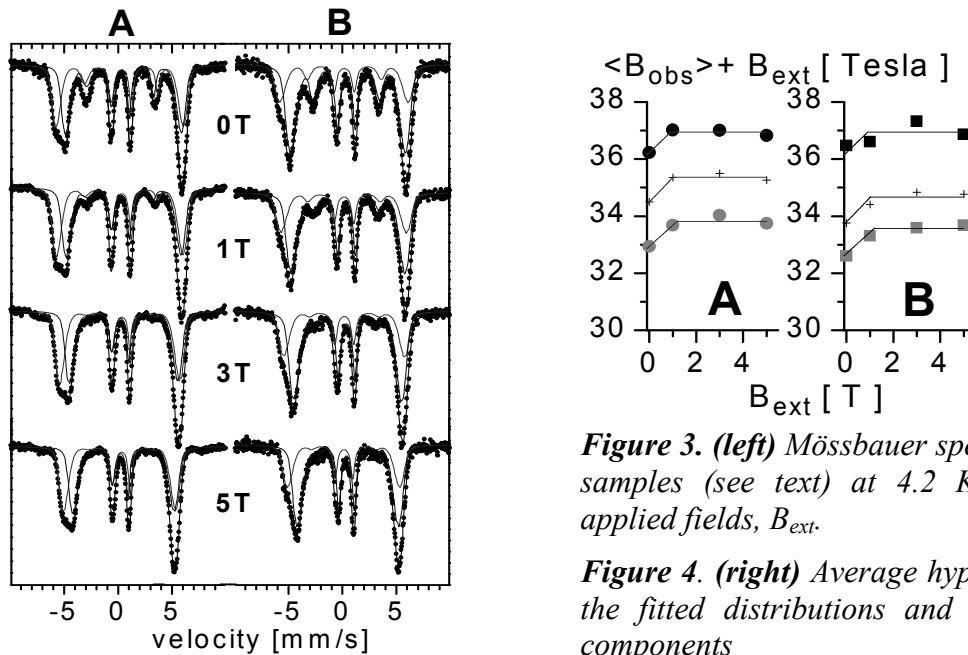


**Figure 3. (left)** Mössbauer spectra of Fe/Ag samples (see text) at 4.2 K in different applied fields,  $B_{ext}$ .

**Figure 4. (right)** Average hyperfine field of the fitted distributions and the two sub-components

## E-Mail:

Imre Vincze	vincze@szfki.hu
Sára Judit Balogh	baloghj@szfki.hu
László Bujdosó	bujdi@szfki.hu
Dénes Kaptás	kaptas@szfki.hu
Tamás Kemény	kemeny@szfki.hu
László Ferenc Kiss	kissl@szfki.hu

## Grants and international cooperations

OTKA T 048965	Magnetic properties of multilayer structures (J. Balogh, 2005-2008)
OTKA T046795	Superferromagnetism in nanostructures (I. Vincze, 2004-2007)
TÉT E-21/04	Magnetic interactions in nanocomposites (L.F. Kiss, 2005-2006)
TÉT GR-6/03	Bulk amorphous and nanophase alloys (T.Kemény, 2005-2006)

## Publications

### Articles

- D.1. Zentková\* M J, Mihalik\* M, Kováč\* J, Zentko\* A, Mitróová\* Z, Lukáčová\* M, Kavečanský\* V, Kiss LF; Magnetic properties of  $\text{TM}_3[\text{Cr}(\text{CN})_6]_2 \cdot n\text{H}_2\text{O}$ ; *Phys Status Solidi (b)*; **243**, 272-276, 2006
- D.2. Kaptás D, Sváb E, Somogyvári\* Z, André\* G, Kiss LF, Balogh J, Bujdosó L, Kemény T, Vincze I; Incommensurate antiferromagnetism in  $\text{FeAl}_2$ : magnetic, Mössbauer and neutron diffraction measurements; *Phys Rev B*; **73**, 012401/1-4, 2006
- D.3. Csontos\* M, Balogh J, Kaptás D, Kiss LF, Kovács\* A; Mihály G; Magnetic and transport properties of Fe-Ag granular multilayers; *Phys Rev B*; **73**, 184412/1-9, 2006
- D.4. Balogh J, Kaptás D, Kiss LF, Kemény T, Vincze I, Temst\* K, Van Haesendonck\* C; Fe-Ag granular multilayers and heterostructures studied in applied magnetic field ; *Hyperfine Interactions*; accepted for publication
- D.5. Balogh J, Kaptás D, Kiss LF, Kemény T, Bujdosó L, Vincze I; Thickness dependence of the magnetic anisotropy of Fe layers separated by Al; *Hyperfine Interactions*; accepted for publication
- D.6. Blázquez\* JS, Franco\* V, Conde\* CF, Conde\* A; Kiss LF; Thermal and microstructural dependence of the initial permeability of  $\text{Co}_{60}\text{Fe}_{18}\text{Nb}_6(\text{B,Cu})_{16}$  alloys; *J Alloys and Compounds*; accepted for publication
- D.7. Kaptás D, Balogh J, Kemény T, Kiss LF, Bujdosó L, Kovács\* A, Hirata\* A, Vincze I; Mössbauer study of ultra-thin Fe/Al multilayer films; *Phys Rev B*; accepted for publication

*See also E.14., H.5., K.7.*

## E. X-RAY DIFFRACTION

*G. Faigel, F. Borondics<sup>#</sup>, G. Bortel, L. Gránásy, A. Jánossy<sup>+</sup>, Z. Jurek, K. Kamarás, G. Klupp<sup>#</sup>, É. Kováts<sup>#</sup>, G. Oszlányi, Á. Pekker<sup>#</sup>, S. Pekker, T. Pusztai, Gy. Tóth<sup>#</sup>, G. Tegze<sup>#</sup>, M. Tegze*

**Fullerenes and related systems.** — The fullerenes are closed shell all carbon atom molecules. The most abundant among them is the C<sub>60</sub> molecule.

Fullerenes can form a large variety of compounds with elements or with other molecules. In the group of A<sub>x</sub>C<sub>60</sub> compounds (A=Na, K, Rb, Cs) there are materials with very interesting properties. Many superconducting materials (A<sub>3</sub>C<sub>60</sub>), and also polymers with different dimensionality (RbC<sub>60</sub>, Na<sub>4</sub>C<sub>60</sub>) were found. We performed infrared measurements on Cs<sub>4</sub>C<sub>60</sub>, Rb<sub>4</sub>C<sub>60</sub>, K<sub>4</sub>C<sub>60</sub> and Na<sub>2</sub>C<sub>60</sub> to investigate the interplay between the molecular Jahn-Teller effect and the crystal field of the cations. We were able to tune the crystal field strength by varying the size of the cations and the temperature. Distortion patterns were derived from the observed splitting of the infrared-active C<sub>60</sub> modes. We concluded that the dynamics of the distortion changes on weakening the crystal field in the following order: static distortion - constrained pseudorotation - free pseudorotation. We also observed a unique nanosegregated form of Na<sub>2</sub>C<sub>60</sub> below 400 K, containing C<sub>60</sub>, metallic Na<sub>3</sub>C<sub>60</sub> and several other minority phases. We studied this material with infrared, ESR, NMR spectroscopy and neutron scattering.

Similarly to fullerenes cubane (C<sub>8</sub>H<sub>8</sub>) is also a cage-molecule. We successfully synthesized high symmetry molecular crystals from C<sub>60</sub> and C<sub>70</sub> with cubane. The two type of molecules form crystals as a result of molecular recognition between the convex surface of fullerenes and the concave cubane. Static cubane occupies the octahedral voids of the face centered cubic structures and acts as a bearing between the rotating fullerene molecules. We extended the family of fullerene-cubane materials to higher fullerenes, such as C<sub>76</sub> and C<sub>84</sub>, and to diethynyl-cubane. These new molecular crystals also consist of alternating arrays of rotating fullerene and static cubane units. The simple intermolecular interactions make possible an efficient crystal engineering: the lattice parameters depend on the sizes of fullerenes and cubane, therefore, related structures can be designed with high accuracy. We determined the phase diagram of the higher fullerene derivatives: the fullerenes of sizes lower than C<sub>88</sub> form rotor-stator crystals with cubane, while the higher ones form a host-guest system.

Like fullerene molecules, carbon nanotubes are also exclusively built from carbon atoms. These nanostructures have many properties, which promise applications in optical, electronic and even biological systems. In order to exploit these properties, one has to characterize these materials. For this reason we measured the wide-range optical transmission (from the far infrared through the ultraviolet) of transparent nanotube networks and determined the optical constants and the effect of charged impurities on the low-frequency spectra. We followed the addition of free carriers on doping with nitric acid, resulting in higher dc conductivity and better infrared transparency.

**Ab initio structure solution.** — In recent years we have developed an *ab initio* structure solution method – named charge flipping (CF). It is based on the existence of extended zero plateaus in the electron density, but not directly on atomicity. This working principle differs a great deal from that of direct methods, and consequently, CF has found special

---

<sup>#</sup> Ph.D. student

<sup>+</sup> Permanent position: Budapest University of Technology and Economics

applications like modulated structures and quasicrystals. We have extended this list by solving a large pseudosymmetric structure that caused serious problems for classical direct methods. The performance of CF was remarkable: it yielded a perfectly complete electron density at a speed of 12 seconds per solution and with 100% success rate. It is likely that similar resistant structures with pseudosymmetries, ambiguous space groups or disorder are the practical applications where the new method could well complement standard software procedures.

The charge flipping algorithm is iterative and works in dual spaces. While in reciprocal space there is a choice of several variants, the real-space modification always changes the sign of electron density below a threshold  $\delta$ . Although positivity was thought to be a crucial precondition for the CF algorithm, recently we have investigated how well negative scattering density can be tolerated. For this purpose we have introduced the band flipping version of the basic algorithm, and found that the basic+band combination allows the solution of structures using neutron diffraction data alone. Initially, these results were thought to be only of theoretical interest, but with more intense neutron sources in sight, it is likely that *ab initio* neutron crystallography shall become more widespread in practice. At least, here is one more algorithm to help this happen.

**Theory of phase transformations.** — A phase field theory with model parameters evaluated from atomistic simulations/experiments has been applied to predict the nucleation and growth rates of solid CO<sub>2</sub> hydrate in aqueous solutions under conditions typical to underwater natural gas hydrate reservoirs. It has been shown that under practical conditions a homogeneous nucleation of the hydrate phase can be ruled out. The growth rate of CO hydrate dendrites has been determined from phase field simulations as a function of composition while using a physical interface thickness ( $0.85 \pm 0.07$  nm) evaluated from molecular dynamics simulations. The growth rate extrapolated to realistic supersaturations is about three orders of magnitude larger than the respective experimental observation. A possible origin of the discrepancy is discussed. It is suggested that a kinetic barrier reflecting the difficulties in building the complex crystal structure is the most probable source of the deviations.

A phase field theory, we proposed recently to describe nucleation and growth in three dimensions (3D), has been used to study the formation of polycrystalline patterns in the alloy systems Al-Ti and Cu-Ni. We have investigated the evolution of polydendritic morphology, present simulated analogies of the metallographic images, and explore the possibility of modeling solidification in thin layers. Transformation kinetics in the bulk and in thin films has been discussed in terms of the Johnson-Mehl-Avrami-Kolmogorov approach.

A phase-field theory of binary liquid phase separation and solidification coupled to fluid flow has been developed. The respective equations of motion and Navier-Stokes equations have been solved numerically. We incorporated composition and temperature dependent capillary forces. The free energies of the bulk liquid phases were taken from the regular solution model. In the simulations, we observed Marangoni motion of the droplets, and direct and indirect hydrodynamic interactions between the droplets. We found that capillary effects dramatically accelerate droplet coagulation and that solidification interacts with liquid phase separation.

## E-Mail:

Gábor Bortel      gb@szfki.hu  
Ferenc Borondics      bf@szfki.hu

Gyula Faigel	gf@szfki.hu
László Gránásy	grana@szfki.hu
András Jánossy	atj@szfki.hu
Zoltán Jurek	jurek@szfki.hu
Katalin Kamarás	kamaras@szfki.hu
Gyöngyi Klupp	klupp@szfki.hu
Éva Kováts	kovatse@szfki.hu
Gábor Oszlányi	go@szfki.hu
Áron Pekker	pekkera@szfki.hu
Sándor Pekker	pekker@szfki.hu
Tamás Pusztai	pusztai@szfki.hu
Gyula Tóth	gytoth@szfki.hu
György Tegze	turpi@szfki.hu
Miklós Tegze	mt@szfki.hu

## Grants and international cooperations

- OTKA T 049338 Optical spectroscopy of molecular carbon structures (K. Kamarás, 2005-2008)
- OTKA T043237 Elastic x-ray scattering in structural research (G. Faigel 2003-2006)
- OTKA T 048298 Holographic methods in structural research (M. Tegze, 2005-2008)
- OTKA T037323 Dynamics of non-equilibrium morphologies (L. Gránásy, 2002-2005)
- OTKA T043494 New methods for solving the phase problem (G. Oszlányi, 2003-2006)
- OTKA K062588 Dynamics of complex systems (L. Gránásy, 2006-2009)
- GVOP - 3.2.1. – 2004 – 04 – 0009/3.0: Acquisition of far-infrared spectrometer (K. Kamarás, 2005-2006)
- GVOP - 3.2.1. – 2004 – 04 – 0008/3.0 : Analitical applications and development of STM and AFM (G.Faigel, 2005-2006)
- ESA PECS 98005 Phase field modeling of magnetic and composite materials (L. Gránásy, 2004–2006)
- ESA PECS 98021 Phase field modeling of solidification in monotectic systems (L. Gránásy, 2005–2007)
- Participation in EU FP6 –500635-8, IMPRESS Intermetallic Materials Processing in Relation to Earth and Space Solidification (L. Gránásy, 2004–2009)
- Alexander-von-Humboldt Foundation Joint Research Project 3-Fokoop-DEU/1009755, 2006-2008: Electronic properties of doped C<sub>60</sub> and nanotube compounds (Principal investigators: K. Kamarás, Hungary and Rudolf Hackl, Walther-Meissner Institute, Bavarian Academy of Sciences, Garching, Germany)
- EU FP6-STREP NMP4-CT-2006-031847, 2006-2009: Towards new generation of neuro-implantable devices: engineering neuron/carbon nanotubes integrated functional units (NEURONANO) (Coordinator: Laura Ballerini, University of Trieste, Italy, representative of Contractor: K. Kamarás)
- EU FP6-Marie Curie Research Training Network MRTN-CT-2006-035810, 2006-2010: Supramolecular hierarchical self-assembly of organic molecules onto surfaces towards bottom-up nanodevices: a host-driven action (PRAIRIES) (Coordinator: Francois Diederich, ETH Zürich, Switzerland, representative of contractor: K. Kamarás)

## Publications

### Articles

- E.1. Pusztaí T, Bortel G, Gránásy L; Phase field theory modeling of polycrystalline freezing; *Mater Sci Eng A*; **413-414**, 412-417, 2005
- E.2. Tegze G, Pusztaí T, Gránásy L; Phase field simulation of liquid phase separation with fluid flow; *Mater Sci Eng*; **413-414**, 418-422, 2005
- E.3. Svandal\* A, Kvamme\* B, Gránásy L, Pusztaí T; The influence of diffusion on hydrate growth; *J Phase Equilib Diff*; **26**, 534-538, 2005
- E.4. Gránásy L, Pusztaí T, Börzsönyi T, Tóth G, Tegze G, Warren\* JA, Douglas\* JF; Polycrystalline patterns in far-from-equilibrium freezing: a phase field study; *Phil Mag*; **86**, 3757-3778, 2006
- E.5. Svandal\* A, Kvamme\* B, Gránásy L, Pusztaí T, Buanes\* T, Hove\* J; The phase field theory applied to CO<sub>2</sub> and CH<sub>4</sub> hydrate; *J Cryst Growth*; **287**, 486-490, 2006
- E.6. Tegze G, Pusztaí T, Tóth G, Gránásy L, Svandal\* A, Buanes\* T, Kuznetsova\* T, Kvamme\* B; Multi-scale approach to CO<sub>2</sub>-hydrate formation in aqueous solution: Phase field theory and molecular dynamics. Nucleation and growth; *J Chem Phys*; **124**, 234710-1-12, 2006
- E.7. Kamarás K, Thirunavukkuarasu\* K, Kuntscher\* CA, Dressel\* M, Simon\* F, Kuzmany\* H, Walters\* DA, Moss\* DA; Far- and mid-infrared anisotropy of magnetically aligned single-wall carbon nanotubes studied with infrared radiation; *Infrared Physics & Technology*; **49**, 35-38, 2006
- E.8. Klupp G, Kamarás K, Nemes\* NM, Brown\* CM, Leao\* J; Static and dynamic Jahn-Teller effect in the alkali metal fulleride salts A<sub>4</sub>C<sub>60</sub> (A= K, Rb, Cs); *Phys Rev B*; **73**, 085415/1-12, 2006
- E.9. Borondics F, Kamarás K, Nikolou\* M, Tanner\* DB, Chen\* ZH, Rinzler\* AG; Charge dynamics in transparent single-walled carbon nanotube films from optical transmission measurements; *Phys Rev B*; **74**, 045431/1-6, 2006
- E.10. Itkis\* ME, Borondics F, Yu\* A, Haddon\* RC; Bolometric infrared photoresponse of suspended single-walled carbon nanotube films; *Science*; **312**, 413-416, 2006
- E.11. Kuntscher\* CA, Frank\* S, Kamarás K, Klupp G, Kováts É, Pekker S, Bényei\* Gy, Jalsovszky\* I; Pressure-dependent infrared spectroscopy on the fullerene rotor-stator compound C<sub>60</sub>C<sub>8</sub>H<sub>8</sub>; *Phys Stat Sol (b)*; **243**, 2981-2984, 2006
- E.12. Pekker Á, Borondics F, Kamarás K, Rinzler\* AG, Tanner\* DB; Calculation of optical constants from carbon nanotube transmission spectra; *Phys Stat Sol (b)*; **243**, 3485-3488, 2006
- E.13. Kamarás K, Rinzler\* AG, Tanner\* DB, Walters\* DA; Polarization-dependent optical reflectivity in magnetically oriented carbon nanotube networks; *Phys Stat Sol (b)*; **243**, 3126-3129, 2006

- E.14. Klupp G, Matus P, Quintavalle\* D, Kiss LF, Kováts É, Nemes\* NM, Kamarás K, Pekker S, Jánossy\* A; Phase segregation on the nanoscale in Na<sub>2</sub>C<sub>60</sub>; *Phys Rev B*; **74**, 195402/1-7, 2006
- E.15. Oszlányi G., Sütő A., Czugler\* M., Párkányi\* L.; Charge flipping at work: A case of pseudosymmetry; *J Am Chem Soc*; **128**, 8392-8393, 2006
- E.16. Toellner\* TS, Hu\* MY, Bortel G, Sturhahn\* W, Shu\* D; Four-reflection “nested” meV-monochromators for 20-30 keV synchrotron radiation; *Nucl Instr and Meth A*; **557**, 670-675, 2006
- E.17. Bortel G, Faigel G, Kováts E, Oszlányi G, Pekker S; Structural study of C<sub>60</sub> and C<sub>70</sub> cubane; *Phys Stat Sol B*; **243**, 2999-3003, 2006
- E.18. Kováts É, Klupp G, Jakab\* E, Pekker Á, Kamarás K, Jalsovszky\* I, Pekker S; Topochemical copolymerization of fullerenes with cubane in their rotor-stator phases; *Phys Stat Sol (b)*; **243**, 2985-2989, 2006
- E.19. Pekker S, Kováts É, Oszlányi G, Bényei\* Gy, Klupp G, Bortel G, Jalsovszky\* I, Jakab\* E, Borondics F, Kamarás K, Faigel G; Rotor-stator phases of fullerenes with cubane derivatives: A novel family of heteromolecular crystals; *Phys Stat Sol (b)*; **243**, 3032-3036, 2006
- E.20. Tegze M; Effect of low-pass filtering on atomic-resolution x-ray holography; *Phys Rev B*; **73**, 214104/1-6, 2006
- E.21. Todorovic-Markovic\* B, Markovic\* Z, Mohai\* I, Nikolic\* Z, Farkas\* Z, Szépvölgyi\* J, Kováts É, Scheier\* P, Feil\* S; RF thermal plasma processing of fullerenes; *J Phys D, Appl Phys*; **39**, 320-326, 2006
- E.22. Markovic\* Z, Todorovic-Markovic\* B, Mohai\* I, Farkas\* Z, Kováts E, Szépvölgyi\* J, Otasevic\* D, Scheier\* P, Feil\* S, Romcevic\* N; Comparative process analysis of fullerene production by the arc and the radio-frequency discharge methods; *J Nanosci Nanotechnol*; accepted for publication
- E.23. Gránásy L, Pusztai T, Börzsönyi T, Tóth G, Tegze G, Warren\* JA, Douglas\* JF; Nucleation and polycrystalline growth in a phase field theory; A review; *J Mater Res*; accepted for publication as "Outstanding Meeting Paper - Review Article"
- E.24. G. Bortel, G. Faigel; Classification of continuous diffraction patterns: a numerical study; *J Struct Biol*; accepted for publication
- E.25. Faigel G, Bortel G, Fadley\* C, Simionovici\* AS, Tegze M; Ten years of x-ray holography; *X-ray Spectrometry*; accepted for publication

### **Articles in Hungarian**

- E.26. Gránásy L, Pusztai T, Tegze G; Polikristályos megszilárdulás számítógépes modellezése (Numerical modeling of polycrystalline solidification, in Hungarian); *Magyar Tudomány*; **167**, 539-543, 2006

### **Conference proceedings**

- E.27. Gránásy L, Pusztai T, Tegze G, Tóth G, Warren\* JA, Douglas\* JF; From needle crystals to polycrystalline spherulites: a phase field study; In: *Proc. of Modeling of Casting, Welding and Advanced Solidification Processes – XI, Stockholm, Sweden 2005*; eds Gandin Ch A, Bellet M, The Minerals, Metals & Materials So., Warrendale; pp. 15-24, 2006
- E.28. Pusztai T, Bortel G, Gránásy L; Phase field theory of polycrystalline freezing in three dimensions. In: *Proc. of Modeling of Casting, Welding and Advanced Solidification Processes – XI, Stockholm, Sweden 2005*; eds Gandin Ch A, Bellet M, The Minerals, Metals & Materials So., Warrendale; pp. 409-416, 2006
- E.29. Tegze G, Gránásy L; Phase field theory of liquid phase separation and solidification with melt flow. In: *Proc. of Modeling of Casting, Welding and Advanced Solidification Processes - XI, Stockholm, Sweden 2005*, eds Gandin Ch A, Bellet M, The Minerals, Metals & Materials So., Warrendale; pp. 513-520, 2006
- E.30. Oszlányi G, Sütő A; How can we cope with negative scattering density?; *Acta Cryst*; **A62**, s88, 2006
- E.31. Kamarás K, Klupp G; Infrared signatures of the dynamic Jahn-Teller effect in fullerene-based materials; In: *2<sup>nd</sup> International Conference on Low Temperature Physics, Orlando, Florida, USA, 2005*; AIP Conference Proceedings **850**, 1693-1696, 2006
- E.32. Rockenbauer\* A, Csányi\* G, Fülöp\* F, Garaj\* S, Korecz\* L, Lukács\* R, Simon\* F, Forró\* L, Pekker S, Jánossy A; Electron delocalization and dimerization in solid C<sub>59</sub>N doped C<sub>60</sub> fullerene; In: *IWEPNM2005, Kirchberg, Austria, 2005*; CP 786, Eds: Kuzmany H, Fink J, Mehring M, Roth S, AIP Conference Proceedings; pp.41-45, 2005
- E.33. Kováts É, Pekker Á, Pekker S, Borondics F, Kamarás K; Carbon nanotube films for optical absorption; In: *Carbon Nanotubes: From Basic Research to Nanotechnology*; Eds.: V.N. Popov and P. Lambin, NATO Science Series: II Mathematics, Physics and Chemistry, Vol 222, Springer; pp. 169-170, 2006.
- E.34. Faigel G, Bortel G, Tegze M; Hard x-ray holographic methods; In: *NATO Advanced Research Workshop Brilliant Light Facilities and Research in Life and Material Science, Yerevan, Armenia, 2006*; NATO Science Series, accepted for publication

### **Book chapter**

- E.35. Gránásy L, Pusztai T, Börzsönyi T; Phase field theory of nucleation and polycrystalline pattern formation; In: *Handbook of Theoretical and Computational Nanotechnology*; eds Rieth M, Schrommers W, American Sci Publ; 2006

**See also H.1., H.8.**

## F. LIQUID CRYSTALS

*Á. Buka, T. Börzsönyi, N. Éber, K. Fodor-Csorba, A. Jákli, I. Jánossy, T. Tóth-Katona, A. Vajda*

New series of **bent core mesogens** derived either from resorcinol or from 2-methyl-, 2-nitro-, 4-chloro and 4,6-dichloro resorcinol, have been **synthesized**. They differ from the former series by having ethoxycarbonyloxy end groups. Though these compounds are only intermediates of a synthetic pathway, they have mesophases. The 1,3-phenylene-bis[4-(ethoxycarbonyloxy-biphenyl) carboxylate] (I) has an intercalated smectic A phase, while the 4-chloro and 4,6-dichloro substituted compounds exhibit nematic phases. These results have been published in ChemPhysChem and invited to the cover page of the issue.

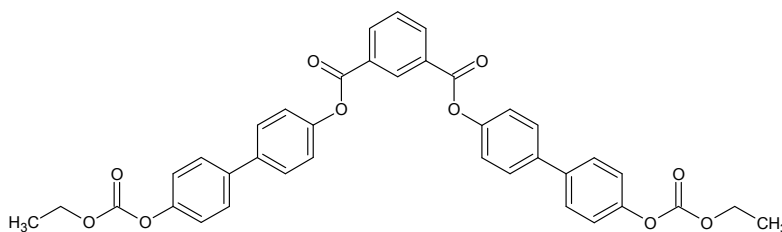


**Figure 1.** 1,3-phenylene-bis[4-(ethoxycarbonyloxy-biphenyl) carboxylate] (I)

A new synthetic pathway has been developed for the **deuteration** of 1,3-phenylene-bis-4-[(10-undecenyloxy)benzoyloxy]benzoate (II), and 4-chloro-1,3-phenylene-bis-4-[(9-decenyloxy)-benzoyloxy]benzoate (III) at different positions. The isotopic labeling has been introduced either to the central ring (II-d4 and III-d3), or to the outer rings (II-d4' and III-d4')

A very sensitive method has been worked out for the measurement of the **surface rotation** of the liquid crystal director **on polymeric orienting layers**. The main part of the set-up is a photoelastic modulator (PEM), which allows for the precise analysis of the polarization state of the transmitted light. We have shown that the second harmonic component of the light beam intensity becomes zero when the major axis of the PEM is parallel to the director at the exit face of the liquid crystalline cell. With the help of the set-up we have investigated reorientation by polarized light in planar cells at normal incidence of the light beam. In undoped samples we could not observe any reorientation in spite of the high sensitivity of the detecting method. On the other hand, in azo-dye doped samples polarizing the light beam by 45° with respect to the surface orientation, we could observe director reorientation. The effect has been found independently whether the orienting layer was polyimide or a polymer with low glass transition temperature. In the latter case gliding-like kinetics has been found. According to our interpretation, the effect is due to the photo-orientation of azo dyes adsorbed at the surface.

The role of the initial conditions in the **decay of periodic roll patterns** in a planarly aligned nematic liquid crystal has been theoretically explored. The decay is characterized by a manifold of modes from which a dominant one is selected depending on the wave number of the pattern. It has been shown by a physical optical description that diffraction optics enhances this selection mechanism. The relaxation time measured as a function of the wave number using a light diffraction technique has provided excellent agreement. It has also been proven experimentally that controlled modifications of the initial conditions allow assessing different decay modes.

A new measurement technique has been introduced to detect the *flexoelectric response* of nematic liquid crystals (NLC) via the electric current produced by periodic mechanical flexing of the NLC's bounding surfaces. This method has been applied to a bent-core NLC synthesized in our laboratory as well as to a rod-shaped NLC. Experimental results have revealed that the bent-core NLC has a giant bend flexoelectric coefficient (three orders of magnitude larger than that of rod-shaped NLC).

*Electroconvection* (EC) has been studied in a homeotropically aligned nematic where a supercritical bifurcation has been found; either stationary or of Hopf type depending on the conductivity. Experimental results of the onset voltage, the critical wave-vector and the traveling-wave frequency measured over a broad range of the driving frequency and the sample conductivity, have been compared with theoretical predictions. For the most part a good agreement has been found.

A systematic study of the onset characteristics of *electric field induced instabilities* in nematic liquid crystals has been carried out. The threshold voltage and the critical wavenumber of the resulting patterns have been calculated using a linear stability analysis. The influence of the anisotropies of the dielectric permittivity and the electrical conductivity is discussed both for planar and homeotropic initial director orientation. It has been demonstrated that the standard model of electroconvection predicts structures in five different wavenumber ranges. Experiments have revealed two more pattern morphologies which are not captured by this model and still need an explanation.

A low molecular weight nematic liquid crystal has been embedded into a relatively loose ( $\approx 15$  wt%) polymer network (*liquid crystal dispersed polymer* – LCDP) cross-linked by photo-polymerization in order to form a self-standing film. A significant thermo-optical and electro-optical response has been detected in a  $340\mu\text{m}$  thick LCDP film.

The overall phase diagram of the *flow of granular materials* on an incline has been explored with emphasis on high inclination angles where the mean layer velocity approaches the terminal velocity of a single particle free falling in air. The granular flow has been characterized by measurements of the surface velocity and the average layer height as a function of the hopper opening, the plane inclination angle and the downstream distance of the flow. Also, we have developed a method to measure the density of the flowing granular material on a rough inclined plane. For low volume flow rates a transition between dense and very dilute (gas) flow regimes has been detected. At high inclination angles the flow does not reach a steady state over the length of the inclined plane. We have shown that air did not qualitatively change the phase diagram and did not quantitatively modify the mean flow velocities of the granular layer except for small changes in the very dilute gas-like phase.

## **E-Mail:**

Tamás Börzsönyi	btamas@szfki.hu
Ágnes Buka	ab@szfki.hu
Nándor Éber	eber@szfki.hu
Katalin Fodor-Csorba	fodor@szfki.hu
Antal Jákli	jakli@szfki.hu
István Janossy	janossy@szfki.hu
Tibor Tóth-Katona	katona@szfki.hu
Anikó Vajda	vajda@szfki.hu

## Grants and international cooperations

- OTKA T037275 Interaction of liquid crystals and polymer films (I. Jánossy, 2002-2006)
- OTKA T-037336 Flow phenomena in liquid crystals (N. Éber, 2002-2006)
- OTKA K 061075 Mesogens with polar ordering of non-chiral building blocks (Á. Buka, 2006-2009)
- OTKA F-060157 Experimental studies of dynamical processes in granular materials (T. Börzsönyi 2006-2008)
- EU-HPRN-CT-2002-00312 Nonequilibrium physics from complex fluids to biological systems (Á. Buka, 2002-2006)
- EU-MSCF-CT-2004-013119 Interactive training and research in nonlinear science from physics to biology (Á. Buka, 2004-2008)
- NATO CRG.LG.973103 Linkage grant Patterns and chaos in electroconvection of liquid crystals (Á. Buka, 2000 -2006)
- COST D35 WG 13-05. Molecular switches based on liquid crystalline materials (K. Fodor-Csorba, 2005-2008)
- 63ÖU4 Hungarian Action Foundation: Advanced liquid crystals with unique architecture (K. Fodor-Csorba, 2006)
- MTA-WATWAW (Hungarian-Polish bilateral) Study of liquid crystals (K. Fodor-Csorba, 2004-2006)
- MTA-ASCR (Hungarian-Czech bilateral) Synthesis and study of ferroelectric liquid crystals leading to preparation of mixtures with defined properties (K. Fodor-Csorba, 2004-2006)
- MTA-CNR (Hungarian-Italian bilateral) New banana-shaped monomers and their polymer derivatives (K. Fodor-Csorba, 2004-2006)
- MTA-INSA (Hungarian-Indian bilateral) Experimental and theoretical studies on liquid crystals. (N. Éber, 2004-2006)
- MTA-CAS (Hungarian-Chinese bilateral) Physical and chemical study of liquid crystals. (N. Éber, 2003-2006)
- MTA-SASA (Hungarian-Serbian bilateral) Structure and physical study of liquid crystals. (N. Éber, 2003-2006)

## Long term visitors

- Dr. Ekrem Cicek: Suleyman Demirel University, Medicine Faculty, Isparta, Turkey, 6 January-31 August, 2006, (EU-RTN grant, host: Á.Buka).
- Ömer Polat: Mugla University, Faculty of Science and Letters, Department of Physics, Kötekli-Muğla, Turkey, 19 February-29 August, 2006, (EU-RTN grant, host: Á.Buka).
- Kinga Gomola: University of Warsaw, Poland, 1 April - 30 June, 2006 (EU-RTN grant, host: Á. Buka)
- Prof. David Statman, Department of Physics, Allegheny College, Meadville, USA, June 2006 (host: I. Jánossy)
- V. Basore, Department of Physics, Allegheny College, Meadville, USA, June 2006 (host: I. Jánossy)
- Michal Kohut: University of Prague, Prague, Czech Republic, 15 October- 15 December, 2006 (COST D35 WG 13/05, host: K. Fodor-Csorba)

## Publications

### Articles

- F.1. Obadović\* DZ, Vajda A, Garić\* M, Bubnov\* A, Hamplová\* V, Kašpar\* M, Fodor-Csorba K; Thermal analysis and X-ray studies of chiral ferroelectric liquid crystalline materials and their binary mixtures; *J Thermal Analysis and Calorimetry*; **82**, 519-523, 2005
- F.2. Otowski\* W, Biernat\* A, Fodor-Csorba K, Witko\* W; Spectroscopic investigation of ferroelectric liquid crystals composed of banana-shaped achiral molecules; *Mol Cryst Liq Cryst*; **450**, 29[229]-37[237], 2006
- F.3. Harden\* J, Mbanga\* B, Éber N, Fodor-Csorba K, Sprunt\* S, Gleeson\* J T, Jákli A; Giant flexoelectricity of bent-core nematic liquid crystals; *Phys Rev Lett*; **97**, 157802/1-4, 2006
- F.4. Wiant\* D, Stojadinovic\* S, Neupane\* K, Sharma\* S, Fodor-Csorba K, Jákli A, Gleeson\* J T, Sprunt\* S; Critical behavior at the isotropic-to-nematic phase transition in a bent-core liquid crystal; *Phys Rev E*; **73**, 030703/1-4, 2006
- F.5. Manzo\* C, Paparo\* D, Marrucci\* L, Jánossy I; Light-induced rotation of dye-doped liquid crystal droplets; *Phys Rev E*; **73**, 051707/1-14, 2006
- F.6. Pesch\* W, Kramer\* L, Éber N, Buka Á; The role of initial conditions in the decay of spatially periodic patterns in a nematic liquid crystal; *Phys Rev E*; **73**, 061705/1-10, 2006
- F.7. Zhou\* S Q, Éber N, Buka Á, Pesch\* W, Ahlers\* G; Onset of electro-convection in homeotropically aligned nematic liquid crystal; *Phys Rev E*; **74**, 046211/1-14, 2006
- F.8. Bényei\* Gy, Jalsovsky\* I, Vajda A, Jákli A, Demus\* D, Shankar Rao\*, Krishna Prasad\* S, Fodor-Csorba K; First liquid crystalline cuneane-caged derivatives. Structure property relationship study; *Liquid Crystals*; **33**, 689-696, 2006
- F.9. Eremin\* A, Naji\* L, Nemes\* A, Stannarius\* R, Schultz\* M, Fodor-Csorba K; Microscopic structures of the B7 phase: AFM and electron-microscopy studies; *Liquid Crystals*; **33**, 789-794, 2006
- F.10. Xu\* J, Dong\* R Y, Domenici\* V, Fodor-Csorba K, Veracini\* C A; <sup>13</sup>C and <sup>2</sup>H NMR study of structure and dynamics in banana B2 phase of a bent-core mesogen; *J Phys Chem B*; **110**, 9434-9441, 2006
- F.11. Dong\* R Y, Zhang\* J, Fodor-Csorba K; On the carbon-13 chemical shift tensors of bent-core mesogens; *Chem Phys Lett*; **417**, 475-479, 2006
- F.12. Fodor-Csorba K, Jákli A, Vajda A, Gács-Baitz\* E, Krishna Prasad\* S, Shankar Rao\* D S, Dong\* R Y, Xu\* J, Galli\* G; Intercalated smectic A phase in banana-shaped liquid crystals with carbonate end groups; *Chem Phys Chem*; **7**, 2184-2188, 2006

- F.13. Manzo\* C, Paparo\* D, Marrucci\* L, Jánossy I; Total optical torque and angular momentum conservation in dye-doped liquid crystal droplets spun by circularly polarized light; *Mol Cryst Liq Cryst*; **454**, 101-110, 2006
- F.14. Obadović\* D Z, Stojanović\* M, Jovanović–Šanta\* S, Lazar\* D, Vajda A, Éber N; The influence of new d-seco-estrone derivatives on the behaviour of the cholesteric liquid crystals binary mixtures; *Int J Mod Phys B*; **20**, 2999–3013, 2006
- F.15. Obadović\* D Z, Garić\* M, Jovanović–Šanta\* S, Lazar\* D, Vajda A, Éber N; the influence of some d-seco-estrone derivatives onto the phase transitions of binary mixtures of cholesteric liquid crystals; *Journal of Research in Physics*; **30**, 131-137, 2006
- F.16. Börzsönyi T, Ecke\* R E; Rapid granular flows on a rough incline: phase diagram, gas transition, and effects of air drag; *Phys Rev E*; accepted for publication
- F.17. Calucci\* L, Forte\* C, Fodor-Csorba K, Menucci\* B, Pizzanelli\* S; Conformations of banana shaped molecules studied by <sup>2</sup>H NMR spectroscopy in liquid crystalline solvents; *J Phys Chem*; **74**, 061301/1-9, 2006
- F.18. Domenici\* V, Fodor-Csorba K, Frezzato\* D, Moro\* G, Veracini\* C A; Deuterium NMR evidences of slow dynamics in the nematic phase of a banana-shaped liquid crystal; *Ferroelectrics*; accepted for publication
- F.19. Jánossy I, Vajda A, Statman\* D; Influence of the molecular weight of a polymer on the gliding of nematic liquid crystals; *Mol Cryst Liq Cryst*; accepted for publication

#### **Article in Hungarian**

- F.20. Éber N; Folyadékkristály televíziók – a XXI. század képernyői (Liquid crystal televisions – displays of the XXI century, in Hungarian); *Fizikai Szemle*; **LVI**, 119-123, 2006

#### **Conference proceedings**

- F.21. Buka Á, Éber N, Pesch\* W, Kramer\* L; Convective patterns in liquid crystals driven by electric field; In: *Self-Assembly, Pattern Formation and Growth Phenomena in Nano-Systems*; Eds.: A. A. Golovin, A. A. Nepomnyashchy, NATO Science Series II, Mathematica, Physics and Chemistry, Vol. 218, Springer, Dordrecht; pp. 55-82, 2006
- F.22. Jánossy I, Sandhya\* K L; Azimuthal anchoring and gliding of liquid crystals on polymer surfaces; In: *XVI. CLC Conference, 18-21 September 2005, Stare Jablonki, Poland*; Ed.: J. Zmija, Proc. SPIE; accepted for publication

**See also: E.4., E.23., E.35.**

## G. ELECTRON CRYSTALS

*G. Kriza, P. Matus<sup>#</sup>, Gy. Mihály<sup>+</sup>, L. Németh<sup>#</sup>, Á. Pallinger<sup>#</sup>, B. Sas, F.I.B. Williams*

**Dissipation in high- $T_c$  superconductors.** — The dynamics of Abrikosov vortices in high- $T_c$  superconductors is a formidable problem of both theoretical and practical interest. Dynamical properties result from the interplay of vortex-vortex repulsion due to overlapping flow fields, interplane magnetic and Josephson coupling, quenched disorder manifested in vortex pinning, thermal excitations, and force exerted on the vortices by an external transport current. Vortex dynamics, in turn, is the main factor in low-energy dissipation in superconductors.

To investigate the vortex dynamics in single crystals of the high-temperature superconductor  $\text{Bi}_2\text{Sr}_2\text{CaCu}_2\text{O}_8$  (BSCCO), we have conducted extensive magnetization and high-current transport measurements in the superconducting phase as a function of temperature, magnetic field, and electron doping of the superconducting planes. From the shape of the magnetic hysteresis loops and voltage–current characteristics, we infer the temperature–magnetic field phase diagram of the vortex system. We have established the existence of a metastability line both in optimally doped and underdoped samples. At temperatures below this line, field-cooled and zero-field-cooled sample preparations yield different voltage–current characteristics. We have shown that, somewhat counterintuitively, field-cooled samples are metastable and after applying a high current or a small magnetic field excursion, their behavior becomes identical to that of zero-field-cooled samples. We have also described how the temperature of vortex lattice melting changes with charge carrier concentration. These results enable us to analyze the factors contributing to vortex lattice melting.

**Nuclear magnetic resonance in superconducting fullerenes.** — Buckminsterfullerenes intercalated with alkali atoms represent, with no doubts, the most investigated class of  $\text{C}_{60}$  materials. The main source of interest is the superconductivity with unusually high critical temperature in  $A_3\text{C}_{60}$  compounds ( $A$  stands for an alkali metal). The relative orientation and the dynamic variation of the orientation of the fullerene molecules have profound effect on the electronic properties of these materials. As a probe of electronic excitations, we have investigated the  $^{23}\text{Na}$  nuclear magnetic resonance (NMR) in the superconducting fulleride  $\text{Na}_2\text{CsC}_{60}$ . We have shown that the phonons involving the librational motion of the  $\text{C}_{60}$  molecules influence the electronic properties down to at least 10 K. We have interpreted this surprising result with the highly oriented nature of the carbon orbitals forming the conduction band.

### E-Mail:

György Kriza	kriza@szfki.hu
László Németh	lnemeth@szfki.hu
Péter Matus	matus@szfki.hu
György Mihály	mihaly@phy.bme.hu
Ágnes Pallinger	pagnes@szfki.hu
Bernadette Sas	sas@szfki.hu
F.I.B. Williams	willia@szfki.hu

---

<sup>#</sup> *Ph.D. student*

<sup>+</sup> Permanent position: Budapest University of Technology and Economics

## Grants and international cooperations

- OTKA K 62866 Collective dynamics of elastic lattices in disorder potential (F.I.B. Williams, 2006-2009)
- SPEC – Saclay Collaboration agreement with Service de Physique de L'Etat Condense (SPEC) CEA-Saclay, France on electron crystals and nano-electronics (2005-2008)

## Publications

### Articles

- G.1. Németh L, Kriza G, Matus P, Alavi\* B; NMR evidence of hidden order in the high-temperature phase of  $(\text{TaSe}_4)_2\text{I}$ ; *J. Phys. IV (France)*; **131**, 357-358, 2005
- G.2. Vad\* K, Mészáros\* S, Nándori\* I, Sas B; Length-scale-dependent phase transition in  $\text{Bi}_2\text{Sr}_2\text{CaCu}_2\text{O}_8$  single crystals; *Philos Mag*; **86**, 2115-2123, 2006
- G.3. Matus P, Alloul\* H, Kriza G, Brouet\* V, Singer\* PM; S. Garaj\* S; Forró\* L; Influence on local  $\text{C}_{60}$  orientation on the electronic properties of  $\text{A}_3\text{C}_{60}$  compounds; *Phys. Rev. B*; accepted for publication

*See also: D.3., E.14.*

## H. METAL PHYSICS

*K. Tompa, I. Bakonyi, P. Bánki, M. Bokor, Cs. Hargitai, Gy. Lasanda, L. Péter, E. Tóth-Kádár*

**Metal-hydrogen systems.** — In-situ hydrogen charging (discharging) process was realized in  $\text{Pd}_{0.90}\text{Ag}_{0.10}\text{-H}$  and  $\text{Pd}_{0.80}\text{Ag}_{0.20}\text{-H}$  alloys on which simultaneous hydrogen concentration and nuclear spin-spin relaxation time measurements were performed. Concentration-gradient driven diffusion coefficient was estimated from the hydrogen concentration-charging (discharging) time curve and data for the intrinsic diffusivity were deduced from the spin-spin relaxation time. Two-component spin-spin relaxation behaviour was found in the whole hydrogen concentration range. One of these components is attributed to hydrogen atoms embedded in the  $\alpha$ -phase (low H-content) and the other one to hydrogen atoms in the  $\beta$ -phase (high H-content). The diffusional motion is localized up to  $10^5$ - $10^6$  intrinsic steps and there is no hydrogen atom exchange between the  $\alpha$ - and  $\beta$ -phases on the time scale of spin-spin relaxation.

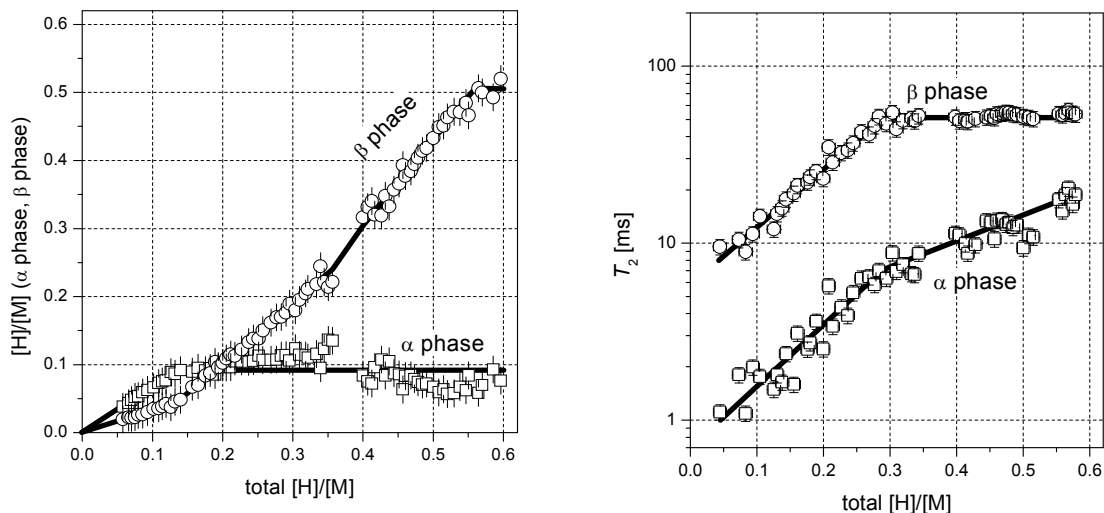


**Figure 1.** In-situ hydrogen charging process in  $\text{Pd}_{0.90}\text{Ag}_{0.10}\text{-H}$  alloy: Hydrogen concentrations  $[\text{H}]/[\text{M}]$  in the  $\alpha$  and the  $\beta$  phase (left graph).  $^1\text{H}$  spin-spin relaxation times characteristic to intrinsic diffusivity (right graph).

**Hydration of semi-structured proteins.** —  $^1\text{H}$  NMR signals of physiological solutions of proteins were investigated (in cooperation with the Institute of Enzymology, Biological Research Center, HAS). We developed a novel approach based on the simultaneous measurements of different NMR characteristics in a wide temperature range that gives a more detailed picture on the protein-water interface than what was known by measuring and interpreting a single quantity at ambient temperature. The main results are the quantitative determination of the number of hydration water molecules, the elements of hydration water dynamics (activation energy and correlation times) and the differences in dynamics as seen by the different time windows provided by the different types of relaxation rates ( $R_1$ ,  $R_{1\rho}$  and  $R_2$ ). We found significant differences between globular proteins and intrinsically unstructured proteins (IUPs). Understanding the functioning of IUPs demands a thorough characterization of their surface properties with particular reference to their water interface. The main conclusions of our studies are that the larger is

the size of their hydration shell, the stronger is the spin diffusion interaction between protein and bound water protons in low-temperature ranges and the higher are the relaxation rates and activation energies in the high-temperature range. All these specific features add up to characterize the unique surface properties of IUP-s. Due to their unfolded and largely exposed nature and their frequent functioning in molecular recognition, such a detailed description of the structure and dynamics of their water interface will advance our understanding of the atomic-level mechanism of their function.

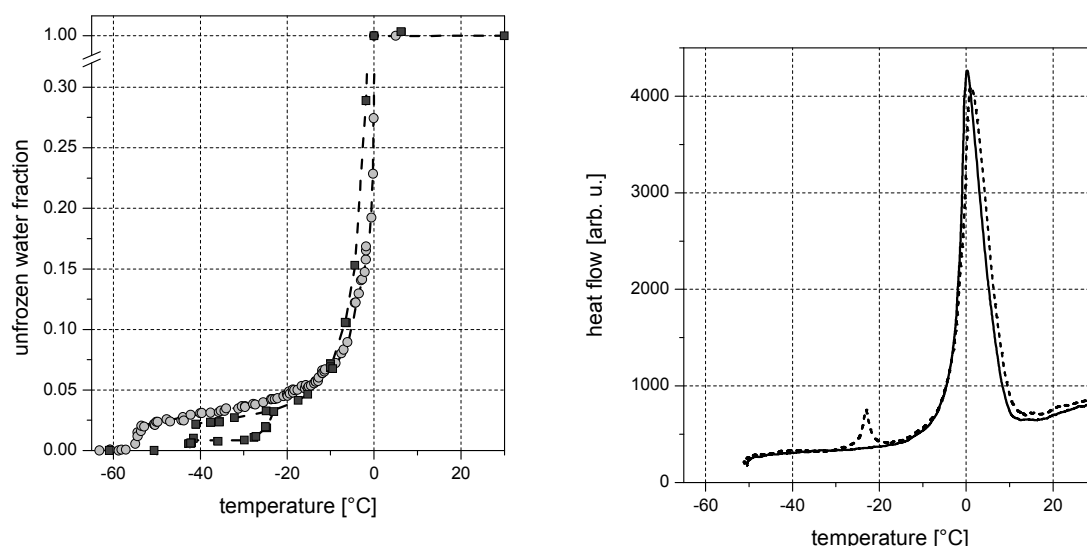
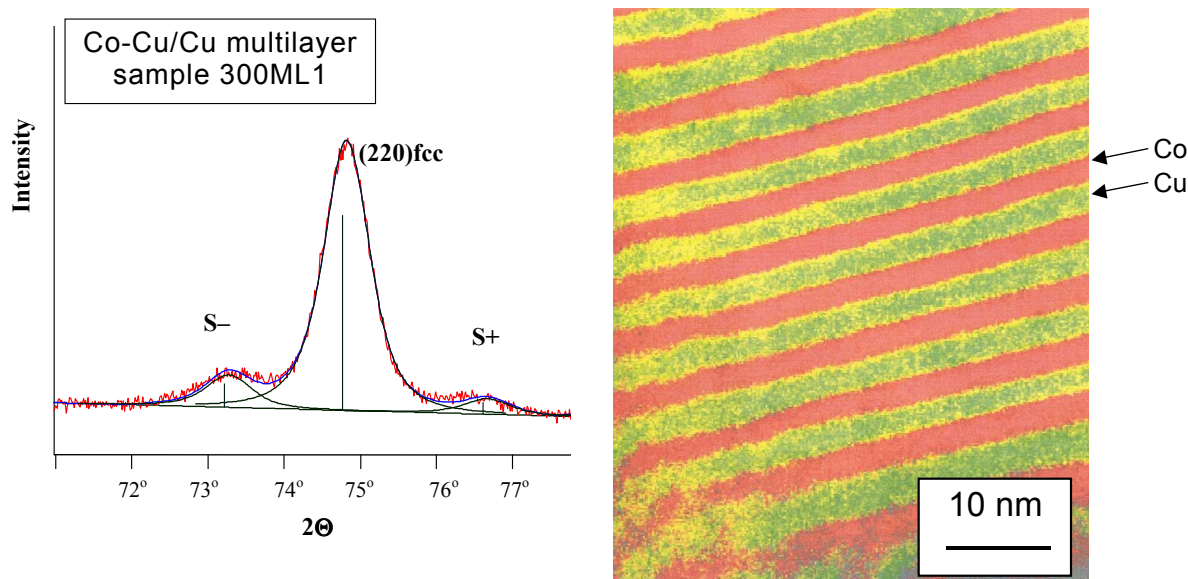


**Figure 2.** Illustrative examples on the interaction of the globular protein bovine serum albumin (BSA) and the buffered aqueous solvent as reflected by the hydration properties.

Left graph: Unfrozen water fraction for BSA solution (circles) and for buffer solution (squares). Right graph: Heat flow DSC curves for BSA solution (solid line) and for buffer solution (dashed line). The interaction of the protein and the NaCl content of the solvent results in the disappearance of the hysteresis in the unfrozen water fraction and the small endothermic peak of the DSC curve.

**Structure and giant magnetoresistance (GMR) of electrodeposited multilayers.** – Electrodeposited Co-Cu/Cu multilayers were prepared under a variety of deposition conditions on either a polycrystalline Ti foil or on a silicon wafer covered by a Ta buffer and a Cu seed layer. X-ray diffraction (XRD) revealed a strong (111) texture for all multilayers with clear satellite peaks for the multilayers on Si/Ta/Cu substrates, in some cases for up to the third reflection (Fig. 3a). Cross-sectional transmission electron microscopy investigations indicated a much more uniform multilayer structure on the Si/Ta/Cu substrates. The bilayer periods from XRD satellite reflections were in reasonable agreement with nominal values. An analysis of the overall chemical composition of the multilayers gave estimates of the sublayer thickness changes due to the Co-dissolution process during the Cu deposition pulse. The actual layer thickness changes derived in this manner were well justified by the elemental map recorded on a cross-sectional TEM sample (Fig. 3b).



(a) (b)

**Figure 3.** (a) The vicinity of the (220) reflection in the XRD pattern of the electrodeposited multilayer Si/Ta/Cu(20nm)/[Co(3.4nm)/Cu(2.5nm)] ×300 (layer thicknesses are nominal). The satellite peaks are labelled by S. (b) EDX elemental map taken by cross-sectional TEM analysis on the electrodeposited multilayer Si/Ta/Cu(20nm)/[Co(3.4nm)/Cu(1.0nm)] ×300 (layer thicknesses are nominal). The actual layer thicknesses derived from an overall chemical analysis of the multilayer were Co(2.0nm)/Cu(2.4nm) corresponding very well to the layer thicknesses seen in the elemental map.

In agreement with the structural studies, magnetoresistance data also indicated the formation of more perfect multilayers on the smooth Si/Ta/Cu substrates. An analysis of the magnetoresistance behaviour revealed the presence of superparamagnetic (SPM) regions in the magnetic layers. The contribution of these SPM regions to the total observed giant magnetoresistance was found to be dominating under certain deposition conditions, e.g., for magnetic layer thicknesses less than 1 nm (about 5 monolayers).

### E-Mail:

Imre Bakonyi	bakonyi@szfki.hu
Péter Bánki	banki@szfki.hu
Mónika Bokor	mbokor@szfki.hu
Csaba Hargitai	hacsa@szfki.hu
György Lasanda	lasi@szfki.hu
László Péter	lpeter@szfki.hu
Kálmán Tompa	tompa@szfki.hu
Enikő Tóth-Kádár	tke@szfki.hu

### Grants and international cooperations

OTKA K 060 821 Investigation of deposits and nanostructures prepared by controlled precisional electrodeposition (L. Péter, 2006-2008)

Wellcome Trust ISRF GR067595MA Study of partially structured protein solutions (2005-2007). The RISSPO is subcontractor (project leader: K. Tompa) in this research grant for the Institute of Enzimology of HAS.

TÉT RO-22/05 Hungarian-Romanian Bilateral Collaboration : GMR multilayer structures (I. Bakonyi, 2006-2007)

## Publications

### Articles

- H.1 Mitróová\* Z, Mihalik\* M, Zentko\* A, Bokor M, Kamarás K, Kavečanský\* V, Kováč\* J, Csach\* K, Trpčevská\* J; Synthesis, structural and magnetic properties of  $TM^{2+}_2 [MoIV(CN)_8] \cdot nH_2O$ ; *Ceramics - Silikaty*; **49**, 181-187, 2005
- H.2 Bakonyi I; Metastable phases and nanocrystalline forming ability (NFA) of melt-quenched Ni-rich (Zr,Hf)-Ni alloys; *Int J Mater Res*; **97**, 471-474, 2006
- H.3 Cziráki\* Á, Péter L, Weihnacht\* V, Tóth J, Simon\* E, Pádár J, Pogány L, Schneider\* CM, Gemming\* T, Wetzig\* K, Tichy\* G, Bakonyi I; Structure and giant magnetoresistance behaviour of Co-Cu/Cu multilayers electrodeposited under various deposition conditions; *J Nanosci Nanotechnol*; **6**, 2000-2012, 2006
- H.4 Kováč\* J, Zentková\* M, Bokor M, Mihalik\* M, Kavečanský\* V, Mitróová\* Z, Zentko\* A, Pekker Á, Kamarás K; Magnetic properties and  $^1H$  NMR spectroscopy of  $TM_2^{2+} [W^{IV}(CN)_8] \cdot nH_2O$ ; *physica status solidi (c)*; **3**, 130-133, 2006
- H.5 Péter L, Rolik\* Z, Kiss LF, Tóth J, Weihnacht\* V, Schneider\* CM, Bakonyi I; Temperature dependence of the giant magnetoresistance and magnetic properties in electrodeposited Co-Cu/Cu multilayers: the role of superparamagnetic regions; *Phys Rev B*; **73**, 174410/1-10, 2006
- H.6 Tompa\* P, Bánki P, Bokor M, Kamasa P, Kovács\* D, Lasanda G, Tompa K; Protein-water and protein-buffer interactions in the aqueous solution of an intrinsically unstructured plant dehydrin: NMR intensity and DSC aspects; *Biophysical Journal*; **91**, 2243-2249, 2006
- H.7 Lasanda G, Bánki P, Bokor M, Tompa K;  $^1H$  NMR spectra and echoes in Pd-H and Pd-Ag-H alloys; *J All Comp*; accepted for publication
- H.8 Mitróová\* Z, Mihalik\* M, Zentko\* A, Bokor M, Kamarás K, Kavečanský\* V, Kováč\* J, Csach\* K, Trpčevská\* J; Synthesis and physical properties of octacyanometallates; *J Solid State Electrochem*; accepted for publication
- H.9 Péter L, Pádár J, Tóth-Kádár E, Cziráki\* Á, Sóki\* P, Pogány L, Bakonyi I; Electrodeposition of Co-Ni-Cu/Cu multilayers. Part 1: Composition, structure and magnetotransport properties; *Electrochim Acta*; accepted for publication
- H.10 Péter L, Weihnacht\* V, Tóth J, Pádár J, Pogány L, Schneider\* CM, Bakonyi I; Influence of superparamagnetic regions on the giant magnetoresistance of electrodeposited Co-Cu/Cu multilayers; *J Magn Magn Mater*; accepted for publication

### **Conference proceeding**

- H.11 Bakonyi I, Péter L; Progress on electrodeposited multilayer films with giant magnetoresistance (GMR) behaviour: 1993-2004. In: *Proc. 8th Int Symp. on Magnetic Materials, Processes and Devices, 206th Electrochemical Society Meeting, Honolulu, Hawaii, U.S.A., 2004*; Eds. S. Krongelb et al., The Electrochemical Society, Pennington, New Jersey, U.S.A., ECS PV 2004-23; pp. 227-244, 2006
- H.12 Bakonyi I, Péter L; Electrodeposited multilayer films with giant magnetoresistance (GMR) behaviour. In: *Proc. Int. Workshop on Nanostructured Materials in Electroplating, Sandanski, Bulgaria, 2006*; Eds. D. Stoychev, E. Valova, I. Krastev and N. Atanassov, St. Kliment Ohridski University Press, Sofia; pp. 75-80, 2006

### **Book chapter**

- H.13 Péter L, Bakonyi I; Electrodeposition and properties of nanoscale magnetic/non-magnetic metallic multilayer films (Chapter 12); In: *Electrocrystallization in Nanotechnology*; Ed. G. Staikov, Wiley-VCH, Weinheim, Germany; pp. 242-260, 2006

### **Other**

- H.14 Hatvani\* I, Rác\* P, Bánki P, Bokor M, Tompa K; NMR-spektroszkópiával nyert kísérletes és műtéti adatok a vitrectomiát követő gyors cataractaképződés magyarázatához – I. Az üvegtesti teret kitöltő anyagok NMR-vizsgálata széles hőmérséklet tartományban (Experimental and surgical data obtained by NMR spectroscopy related to accelerated cataract development following vitrectomy – I. NMR investigation of vitreous body and various biomaterials filled in the vitreous cavity in a wide temperature range, in Hungarian); *Szemészet*; **143**, 7-11, 2006

**See also: I.9., I.13.**

# I. METALLURGY AND MAGNETISM

*L.K. Varga, I. Balogh, É. Fazakas<sup>#</sup>, A. Kákay<sup>#</sup>, P. Kamasa, G. Konczos, Gy. Kovács<sup>+</sup>, J. Pádár, L. Pogány, F.I. Tóth*

**Metallurgy.** — In order to investigate the bulk glass forming ability, Al and Cu based alloys have been prepared beside the Fe based alloys. Various Al-U based amorphous alloys have been prepared for the first time in the literature such as

- $\text{Al}_{100-x}\text{U}_x$  where  $x = 8, 10, 12, 14$ ,
- $\text{Al}_{90}\text{Ni}_8\text{U}_2$ ,  $\text{Al}_{90}\text{Ni}_5\text{U}_5$ ,  $\text{Al}_{88}\text{Ni}_{10}\text{U}_2$
- $\text{Al}_{85}\text{Ni}_8\text{U}_5\text{Co}_2$ ,  $\text{Al}_{85}\text{Ni}_5\text{U}_8\text{Co}_2$

The thermal stability of them was similar or better than the corresponding amorphous alloys where mischmetal replaces U.

The stability of Cu-Zr-Ti bulk amorphous alloys could be further improved by partial replacement of Cu by Ag.

**Soft magnetic nanocrystalline alloys.** — A new quasi-DC hystero-graph was developed based on the best measuring devices available on the market. Toroidal samples can be measured in the field of a linear conductor placed in the axes of the toroid applying 1 turn for the secondary winding. A Helmholtz coil ( $H_{\max} \sim 600$  Oe) was built for measuring ferromagnetic amorphous ribbon pieces of at least 10 milligram. Softwares have been developed to control the measurements both under triangular H (t) and triangular B(t) excitation fields.

The new quasi-DC hystero-graph enabled us to study the dependence of the coercive field ( $H_c$ ) as a function of the rate of triangular magnetizing field for the ultrasoft nanocrystalline alloys with a static  $H_c$  of about 1 A/m. It turned out that the static  $H_c$  for the square loop of FINEMET could not be determined even at the lowest available rate of magnetizing field (see Fig.1). For such low coercivities (below 1 A/m) a new method was developed based on differential permeability measurements as a function of a DC bias field, where the cycle time can be as large as 3 hours. The static coercive field can be obtained from the distance between the permeability maxima (see Fig. 2).

The so far elusive inverse hysteresis transformation,  $H(t) = H^{-1} \{M(t)\}$ , has been given in closed form by using the hyperbolic T(x) model of hysteresis. In this way it is possible to calculate the magnetizing field waveform required to obtain any magnetization waveform (typically sinusoidal and triangular) for a given hysteresis loop.

Softwares have been developed to measure the anhysteretic magnetization curve, the virgin curve (Fig. 3) and the first-order reversed curves (FORC's, Fig. 4). Data processing of these curves will enable us to obtain the fingerprint characteristics of the hysteresis processes for ultrasoft magnetic materials.

---

<sup>#</sup> *Ph.D. student*

<sup>+</sup> Permanent position: Loránd Eötvös University, Budapest

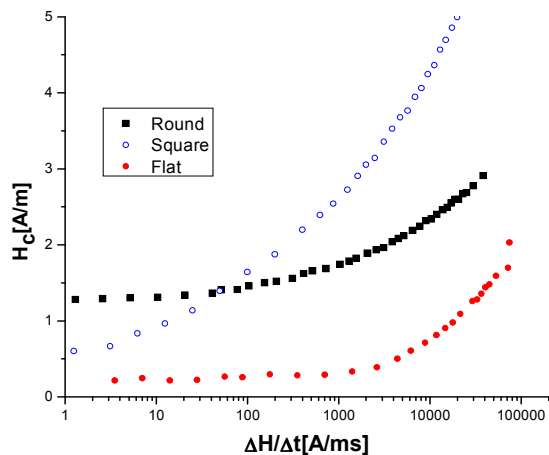


**Figure 1.** Coercivity as a function of the rate of the triangular saturating field for a FINEMET nanocrystalline alloy annealed at 540 °C for 1 h : without (round loop) and with DC magnetic field applied longitudinal (square loop) and transversal (flat loop).

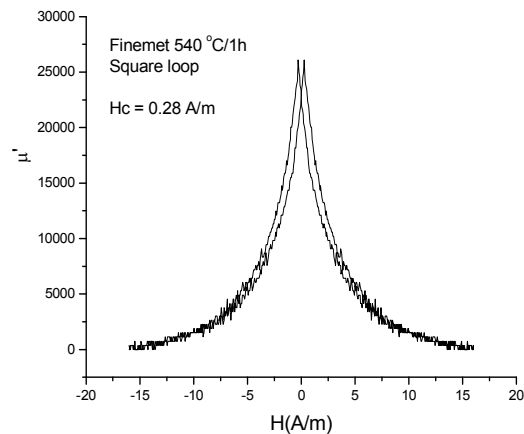


**Figure 2.** Differential permeability measured at 400 Hz as a function of the biasing DC field.

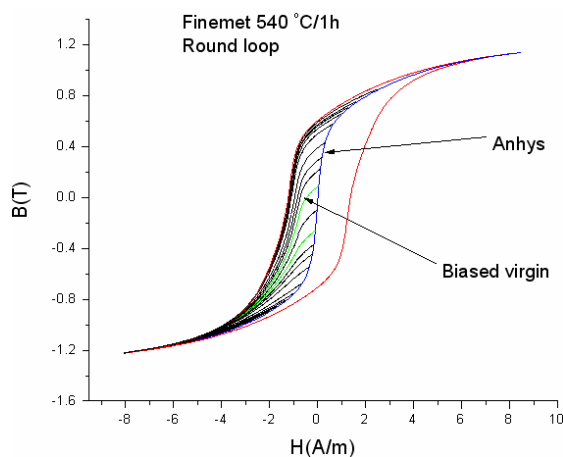


**Figure 3.** Anhysteresis curve and a set of biased virgin curves starting from a demagnetized state at a given DC bias field

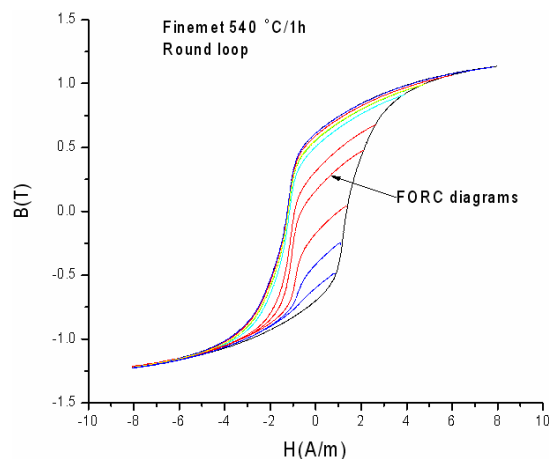


**Figure 4.** First order reversal curves (FORC's) starting from negative saturation and reversing back from a point of the major loop.

**SEM magnetic domain studies.** — The magnetic properties of FINEMET type  $\text{Fe}_{75}\text{Si}_{15}(\text{NbBCu})$  ribbons were investigated during and after special heat treatments. Materials with the highest standard technical magnetic parameters were prepared in collaboration with an industrial partner. Extremely large and stable permeability (over 750000 at 50Hz and over 100000 at 10kHz exciting field) was reached. The same heat treatments resulted in the most stable product for 10kHz use. Wide domains (of 0.01mm characteristic size), deeply piercing into ribbons, were observed. On the other hand, near the surface, closure domains and branches of domains were also detected. Shapes of domain walls in this surface region were smoothly curved and zigzag type. All of the observed types of domain structure were weakly sensitive to the surface roughness. The distribution of the above three types of domain areas substantially changed after special heat treatments during which the initial industrial magnetic parameters have been changed.

**Fast heating rate DTA.** — A differential thermal analysis (DTA) experimental setup enabling a controlled heating rate of  $2500 \text{ K min}^{-1}$  in the temperature range up to  $1200 \text{ K}$  was developed to investigate the crystallization kinetics of amorphous alloys. When ferromagnetic materials are investigated, the simultaneously recorded magnetic susceptibility complements the thermal measurements. Except some “quench-up” experiments with effective heating rates of about  $10^4$ - $10^6 \text{ K/s}$  carried out on amorphous ribbons, there are no reported thermal analysis experiments using controlled high heating rate above  $500 \text{ K/min}$  in this temperature range.

In Fig. 5, the DTA and TMAG (thermomagnetic measurement) traces are plotted as obtained on a  $\text{Fe}_{85}\text{B}_{15}$  amorphous sample by applying high heating rate. As shown, for a binary Fe-B alloy (and also modified with a small amount of Cr or Zr), the formation of the  $\text{Fe}_3\text{B(II)}$  phase is completely suppressed at the high heating rate applied.

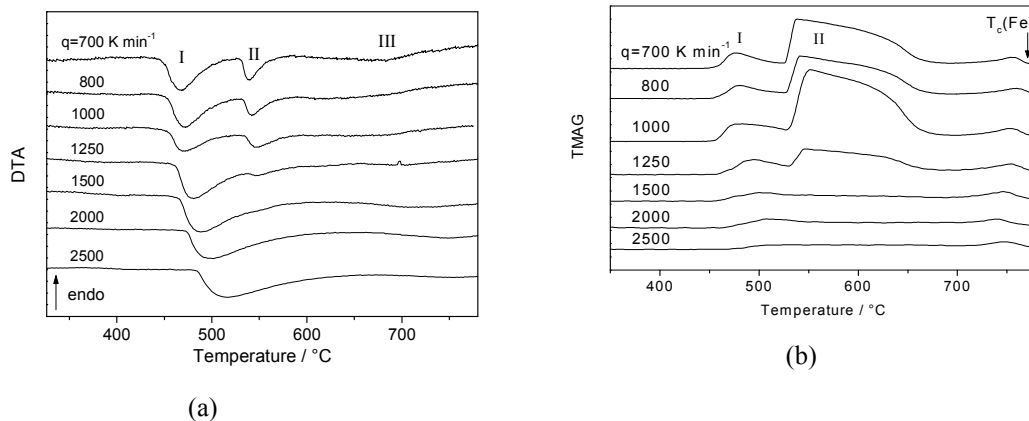


**Figure 5.** Devitrification process of an amorphous  $\text{Fe}_{85}\text{B}_{15}$  alloy obtained with different heating rates: **(a)** DTA curves from the crystallization region, and **(b)** corresponding TMAG curves.

The DTA traces for amorphous  $\text{Al}_{85}\text{Y}_8\text{Ni}_5\text{Co}_2$  are plotted in Fig. 6a. The activation energy together with the devitrification temperature is the two main characteristics of the thermal stability for the glassy alloys obtained by rapidly quenching of the melt.

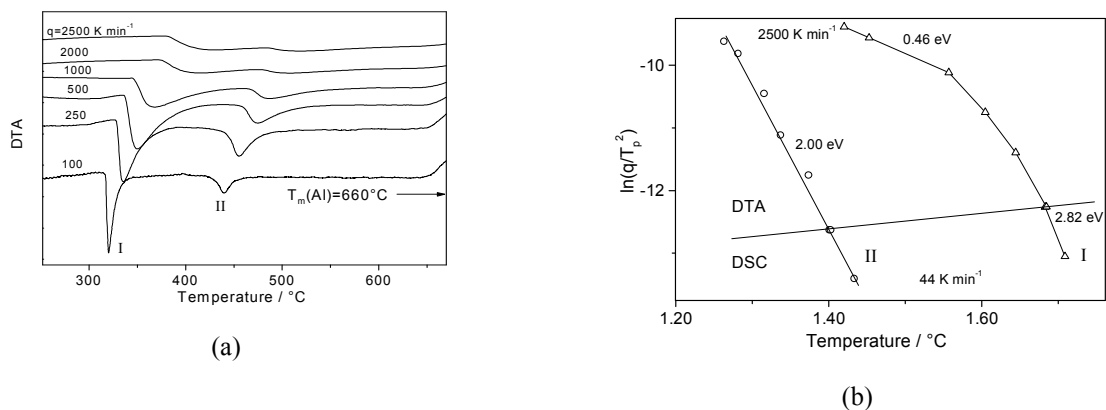


**Figure 6.** **(a)** DTA scans for  $\text{Al}_{85}\text{Y}_8\text{Ni}_5\text{Co}_2$  with increasing heating rate; **(b)** Kissinger plots for both crystallization steps (low heating rate data from DSC). For the first stage (I) of nanocrystallization, the plot deviates from a linear behaviour.

The shift of the peak temperatures versus heating rate is represented in Kissinger’s plot in Fig. 6b. With increasing heating rate, the effect of decreasing the activation energy of first stage of crystallization is observed, an effect never observed by conventional DSC.

## E-Mail

István Balogh	ibalogh@szfki.hu
Éva Fazakas	efazakas@szfki.hu
Attila Kákay	attilak@szfki.hu
Pawel Kamasa	kamasa@szfki.hu
Géza Konczos	konczos@szfki.hu
György Kovács	kovacsgy@ludens.elte.hu
József Pádár	padar@szfki.hu
Lajos Pogány	pogany@szfki.hu
Ferenc I. Tóth	ftoth@szfki.hu
Lajos K. Varga	varga@szfki.hu

## Grants and international cooperations

- OTKA K62466 Investigation of the deterioration of power plant construction materials by magnetic methods (Project leader: J. Ginsztler, BME, SZFKI participant: L.K. Varga, 2006-2009)
- GVOP-3.2.1.-2004-04-0281/3.0): High-frequency and high-temperature magnetic study of nanocrystalline and bulk amorphous materials (L.K. Varga, 2005-2006)
- HAS-SAS Hungarian-Slovakian Academy Exchange Programme: Study of physical properties of special magnetic materials (L.K. Varga, 2005-2007)
- HAS-PAS Hungarian-Polish Academy Exchange Programme: Investigation of thermophysical properties of coatings (P. Kamasa, 2005-2007)

## Publications

### Articles

- I.1 Szabó\* S, Juhász\* R, Pogány L, Daróczy\* L, Beke\* DL; Excellent magnetic properties, domain and atomic structure of specially heat treated Finemet type materials; *Mater Sci Forum*; **473-474**, 477-482, 2005
- I.2 Gercsi Zs, Mazaleyrat\* F, Varga LK; High temperature soft magnetic properties of Co-doped nanocrystalline alloys; *J Magn Magn Mater*; **302**, 454-458, 2006
- I.3 Gutowski\* MW, Varga LK, Kákay A; Fast, Preisach-like characterization of hysteretic systems; *Physica B*; **372**, 76-78, 2006
- I.4 Kákay A, Szabó\* Zs, Kovács Gy, Varga LK; Temperature dependence of the Preisach function for ultrasoft nanocrystalline alloys; *Physica B*; **372**, 401-405, 2006
- I.5 Kamasa P, Myslinski\* P; Changes of thermal, mechanical and magnetic properties of an amorphous Fe<sub>80</sub>Cr<sub>5</sub>B<sub>15</sub> alloy during magnetic and structural phase transitions; *Centr Eur J Phys*; **4**, 178-186, 2006
- I.6 Kamasa P, Myslinski\* P, Pyda\* M; Experimental aspects of temperature-modulated dilatometry of polymers; *Thermochim Acta*; **442**, 48-51, 2006

- I.7 Kane\* SN, F. Alves\* F, Gercsi Zs, Mazaleyra\* F, Gupte\* S, Chiriac\* H, Vázquez\* M; Study of magnetoimpedance effect in Co–Fe–Si–B glass-covered microwires; *Sensors and Actuators A*; **129**, 216-219, 2006
- I.8 Lovas\* A, Bárdos\* A, Kamasa P, Kovác\* J, Bán\* K; Annealing experiments on bulk amorphous alloys around the glass transition temperature; *J Magn Magn Mater*; **304**, e657-e659, 2006
- I.9 Varga I, Pogány L, Hargitai C, Bakonyi I; Extracting domain wall patterns from SEM magnetic contrast images; *J Magn Magn Mater*; **302**, 405-412, 2006
- I.10 Varga LK, Gercsi Zs, Kovács Gy, Mazaleyra F; The influence of size on coercive field of ultra soft magnetic materials; *J Magn Magn Mater*; **301**, 527-531, 2006
- I.11 Mikó\* A, Takács\* M, Lakatos-Varsányi\* M, Varga LK; Pulse plated amorphous Fe-P thin layers for high frequency applications; *Mater Sci Froum*; accepted for publication
- I.12 Mikó\* A, Kuzmann\* E, Lakatos-Varsányi\* M, Kákay A, Nagy\* F, Varga LK; Mössbauer and XRD study of pulse-plated Fe-P and Fe-Ni thin layers; *Hyperf Int*; accepted for publication

#### ***Conference proceedings***

- I.13 Dyakova\* V, Kamenova\* Tz, Varga LK, Bakonyi I, Stojanova\* L, Russev\* K, Yankova\* S; Structural features, thermal and mechanical properties of rapidly solidified amorphous and nanocrystalline cobalt-zirconium alloys of high cobalt content; In: *Proc. 20<sup>th</sup> Natl. Conf. on Non-Destructive Testing (Sozopol, Bulgaria, 2005)*; Nauchn. Izv. na NTS po Mashinostroeniya, Bulgaria, **12**; pp. 299-302, 2005

#### ***Other***

- I.14 Konczos G.: Korszerű anyagok és technológiák, jegyzet BME fizikushallgatók részére (Advanced Materials and Technologies, Textbook of the Budapest University of Technology and Economics for Students in Physics, in Hungarian); pp. 1-140, 2006; Available at <http://www.szfki.hu/~konczos/tanfolyamok/>

***See also: H.3., H.6., H.9., H.10., O.25.***

## J. NEUTRON SPECTROSCOPY IN CONDENSED MATTER

*L. Rosta, L. Almásy, L. Cser, I. Gladkih, I. Füzesy, J. Füzi, Gy. Káli, T. Kun, A. Len, M. Markó<sup>#</sup>, G. Nagy<sup>#</sup>, J. Orbán, E. Rétfalvi<sup>#</sup>, Zs. Sánta<sup>#</sup>, N.K. Székely<sup>#</sup>, Gy. Török, T. Veres<sup>#</sup>*

**Structure of soft condensed matter – starch.** — Over two thirds of the global starch industry is directed towards the exploitation of starch for non-food applications, the remaining third represents billions of tonnes per year used for obtaining food products. A key issue in the development of modern processed foods is to be able to specify the rate and extent of starch digestion that will be of benefit to human health and fitness. To characterize the physical and chemical properties and structure of starch solutions between different experimental conditions three type of starches have been studied by small-angle neutron scattering (SANS): potato, wheat and maize starch. The samples were produced by different techniques; different temperature and pressure values were used for obtaining solutions, suspensions and gels. The starch granule structure is modelled as a finite number of lamellae: crystalline regions and amorphous regions, embedded in a background region (Fig. 1). By treating the results obtained from SANS measurements the structure of granules could be compared within the three type of starches. The most pronounced change was observed in case of suspensions which were produced at ambient temperature and measured in-situ at different concentrations and temperatures. The wheat starch granules broke, while in the wheat suspension considerable lamellae structured fragments were present. The wheat starch gels showed different lamellae thickness at different temperatures. While the 0.2-2% concentrated wheat and maize samples showed no temperature and concentration dependence, the potato starch solutions structure changes significantly with the concentration.

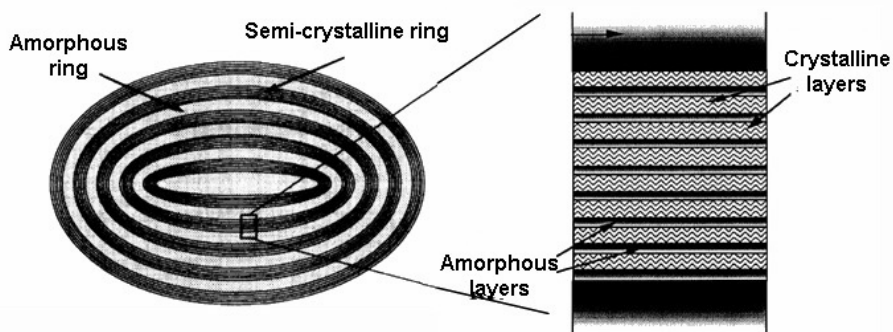


**Figure 1.** Model of starch granule lamellar structure: crystalline and amorphous regions

**Structure of biological matter – model membranes.** — In collaboration with a German group (Dresden), lipid vesicles in dilute dispersion of model lipid POPC (1-palmitoyl-2-oleoyl-*sn*-glycero-3-phosphocholine) have been studied by small-angle neutron scattering. The dispersions were prepared by extrusion through filters of different pore sizes. The experimental data were treated by a newly developed model, which allowed us to determine the proportions of different sorts of vesicles (unilamellar and multilamellar) and to determine their structural and hydration parameters, for vesicles of different radii and multilamellarity. In Fig. 2 the schematic cross section of a unilamellar vesicle is shown, together with the model profile of the neutron scattering length density across the bilayers (for a vesicle consisting of three bilayers).

---

<sup>#</sup> Ph.D. student

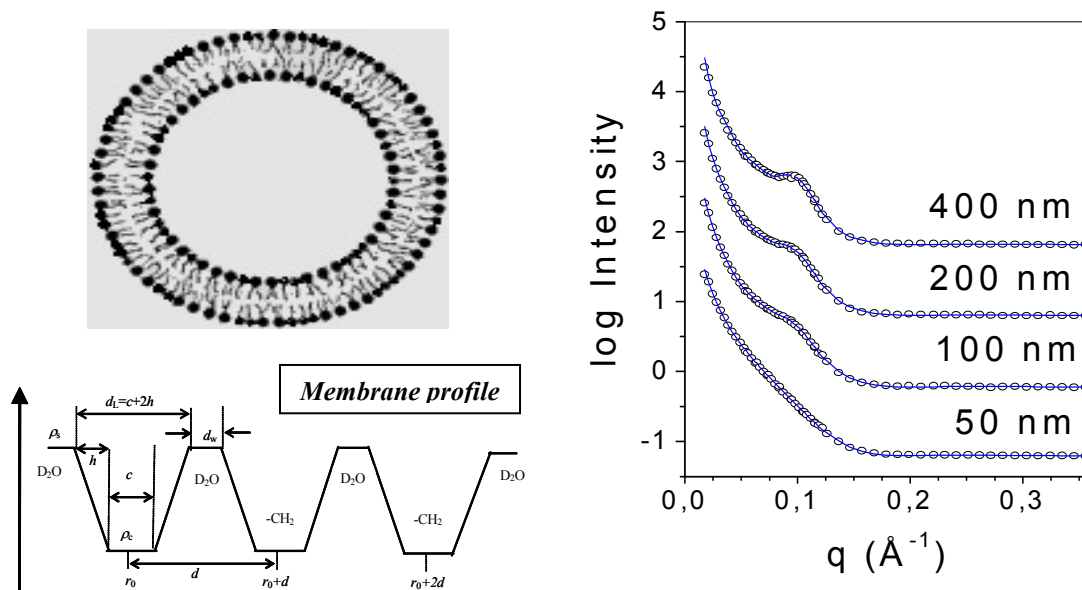


**Figure 2.** Left panel: Schematic structure and the scattering length profile of the vesicles. Right panel: Small angle scattering curves for POPC vesicle suspensions prepared using filters of different diameters.

**Neutron optics.** — 1. A new mathematical method was applied to the neutron holography data obtained on the PbCd alloy. This method allowed the direct observation of the distance between the Cd nucleus and the Pb nuclei occupying the surrounding first four neighboring shell. The inter-atomic distances were determined with picometer accuracy. They show a non-monotonic shift of the atomic positions due to the Cd atom. In order to interpret the data obtained the Friedel oscillation model was involved. The result is shown on Fig. 3.

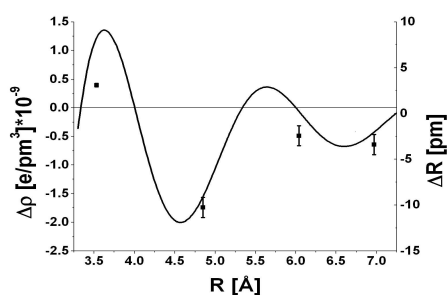


**Figure 3.** The electron density oscillation  $\Delta\rho$  calculated from the Friedel theory (solid line) and the shift of the inter-atomic distance  $\Delta R$  (black points) as the function of the distance from the Cd atom.

2. The first neutron holographic image was obtained by the use of the dedicated instrument installed at the 8th horizontal channel of the Budapest Research Reactor. For the sample an  $\text{NH}_4\text{Cl}$  single crystal was chosen. The results prove that the internal source approach according to our expectation is feasible even at the medium power reactor.

**Neutron instrumentation.** The 10 MW Budapest Research Reactor (BRR) and its experimental facilities on the KFKI site is a unique large-scale facility in the Central European region. The Neutron Spectroscopy Department is one of the Laboratories of the associate Institutes forming the Budapest Neutron Centre, which is open for the domestic and international user community and serves for basic and applied research, commercial utilisation and education. Experiments performed by the local staff and in collaboration with national or foreign users coming from universities, industrial or other research laboratories. We operate several cold and thermal neutron beam instruments: a small angle

scattering (SANS) spectrometer, a reflectometer (REFL), a three axis spectrometer (TASC) and a cold neutron beam test facility as well as a thermal beam three axis spectrometer (TAST) and time-of-flight diffractometer (TOFD). This latter TOF project was started in 2000 in collaboration with the Hahn-Meitner-Institut. The spectrometer - previously tested on a cold beam - has been reinstalled on a radial thermal neutron beam. The TOF monochromator system consists of a double chopper with maximum rotation speed of 12000 rpm and two single with 6000 rpm. The total flight path is 25m. The instrument will operate with a 60x100 cm<sup>2</sup> 2-dimensional position sensitive detector in back scattering geometry. At our first neutron tests we confirmed the excellent – 1x10<sup>-3</sup> – resolution in  $\Delta d/d$  at good intensity. It shows that the expected value 4x10<sup>-4</sup> can be achieved. The first real experiments have started this year, too: archaeological bronze objects and nanosized ceramic powders were studied.

### **E-Mail:**

László Rosta	rosta@szfki.hu
László Almásy	almasy@sunserv.kfki.hu
László Cser	cser@sunserv.kfki.hu
Irina Gladkih	gladkih@sunserv.kfki.hu
István Füzesy	fuzesy@szfki.hu
János Füzi	fuzi@sunserv.kfki.hu
György Káli	kali@szfki.hu
Tibor Kun	kunt@szfki.hu
Adél Len	lenadel@sunserv.kfki.hu
Márton Markó	marko@szfki.hu
Gergely Nagy	nature.elatus@gmail.com
János Orbán	orban@szfki.hu
Eszter Rétfalvi	retfalvi@sunserv.kfki.hu
Zsombor Sánta	santa@szfki.hu
Noémi Kinga Székely	szekely@szfki.hu
Gyula Török	torok@szfki.hu
Tamás Veres	vertam@freemail.hu

### **Grants and international cooperations**

EU HII3-CT-2003-505925 Access to Research Infrastructure (BNC, L. Rosta, 2004-2007)

EU HII3-CT-2003-505925 JRA2 Detector Development project (L. Rosta, 2004-2007)

EU HII3-CT-2003-505925 JRA3 Focusing Neutron Optics project (J. Füzi, 2004-2007)

EU HII3-CT-2003-505925 JRA2 Polarised Neutron Techniques (Gy.Török, 2004-2007)

NAÜ- 13507 Improvement of Neutron beam performance and sample environment in residual stress (Gy. Török, 2006-2007)

NAP VENEUS-2005 OMFB-00648/2005 Visegrad Cooperation for Development and Application of Neutron Spectroscopy Techniques in Multidisciplinary Research (L. Rosta, 2005-2008)

TÉT RUS 13-2004 Nanoparticle (Gy. Török, 2005-2006)

TÉT RUS 14-2004 Neuholo (L. Cser, 2005-2006)

Study of nanostructures in functional materials by means of neutron scattering at the Frank Laboratory of Neutron Physics (FLNP) of the Joint Institute for Nuclear Research (JINR), Dubna (L.Rosta, 2005- 2007.)

Introduction of young scientists and researches working at the BNC into the use of time-of-flight method realized by the experimental trainings and courses at the IBR-2 Pulsed Reactor at the Frank Laboratory of Neutron Physics (FLNP) of the Joint Institute for Nuclear Research (JINR), Dubna (L.Rosta, 2006 - 2007.)

## Publications

### Articles

- J.1. Almásy L, Len A, Markó M, Rétfalvi E; The effective wavelength in SANS experiment using mechanical velocity selector; *Zeitschrift für Kristallographie*; **S23**, 211-216, 2006
- J.2. Avdeev\* MV, Aksenov\* VL, Balasoiu\* M, Garamus\* VM, Schreyer\* A, Török Gy, Rosta L, Bica\* D, Vékás\* L; Comparative analysis of the structure of sterically stabilized ferrofluids on polar carriers by small-angle neutron scattering; *Journal of Colloid and Interface Science*; **295**, 100-107, 2006
- J.3. Cser L, Krexner\* G, Markó M, Prem\* M, Sharkov\* I, Török Gy; Atomic resolution neutron holography (Present status and future prospects); *Physica B*; **385-386**, 1197-1199, 2006
- J.4. Cser L, Krexner\* G, Markó M, Sharkov\* I, Török Gy; Instrumental distortion effects in atomic resolution neutron holography; *Physica B*; **385-386**, 1200-1202, 2006
- J.5. Füzi J; Dynamic vector hysteresis modeling; *Physica B*; **372**, 396-400, 2006
- J.6. Füzi J; Analytical hysteresis model; *Physica B*; **372**, 393-395, 2006
- J.7. Füzi J; Magnetic characteristics of dipole clusters; *Physica B*; **372**, 239-242, 2006
- J.8. Füzi J; Neutron beam phase space mapping; *Physica B*; **385-386**, 1253-1255, 2006
- J.9. Knaapila\* M, Almásy L, Garamus\* VM, Pearson\* C, Pradhan\* S, Petty\* MC, Scherf\* U, Burrows\* HD, Monkman\* AP; Solubilization of polyelectrolytic hairy-rod polyfluorene in aqueous solutions of nonionic surfactant; *J Phys Chem B*; **110**, 10248-10257, 2006
- J.10. Knaapila\* M, Garamus\* VM, Dias\* FB, Almásy L, Galbrecht\* F, Charas\* A, Morgado\* J, Burrows\* HD, Scherf\* U, Monkman\* AP; Influence of solvent quality on the self-organization of archetypical hairy-rods - branched and linear side chain polyfluorenes: Rigid rods versus "beta sheets" in solution; *Macromolecules*; **39**, 6505-6512, 2006
- J.11. Krakovsky\* I, Almásy L, J Pleštil\* J; Structure and swelling behaviour of hydrophilic epoxy networks investigated by SANS; *Polymer*; **47**, 218-226, 2006
- J.12. Lebedev\* VT, Török Gy; Effect of anomalous particles diffusion damping in ferrofluid near Curie temperature; *Romanian Reports in Physics*; **58**, 249-254, 2006

- J.13. Lebedev\* VT, Török Gy, Nazarova\* OV, Panarin\* EF, Orlova\* DN, Pavlov\* GM; Hierarchy of structural organization of fullerene-containing polyvinylformamide in solutions; *Fullerenes, Nanotubes and Carbon Nanostructures*; **14**, 321-326, 2006
- J.14. Perera\* A, Sokolić\* F, Almásy L, Koga\* Y; Kirkwood-Buff integrals of aqueous alcohol binary mixtures; *J of Chemical Physics*; **124**, 124515/1-9, 2006
- J.15. Peters\* J, Bleif\* HJ, Káli Gy, Rosta L, Mezei\* F; Performance of TOF powder diffractometers on reactor sources; *Physica B*; **385-386**, 1019-1021, 2006
- J.16. Rogante\* M, Lebedev\* VT, Kralj\* S, Rosta L, Török Gy; Neutron techniques for welding project methods development in nuclear/traditional industrial application; *Multidiscipline Modeling in Materials and Structures*; **2**, 419-433, 2006
- J.17. Rosta L, Füzi J, Hományi\* L; Benchmark testing of a multiblade neutron velocity selector; *Physica B*; **385-386**, 1283-1286, 2006
- J.18. Schmiedel\* H, Almásy L, Klose\* G; Multilamellarity, structure and hydration of extruded POPC vesicles by SANS; *European Biophysics Journal with Biophysics Letters*; **35**, 181-189, 2006
- J.19. Török Gy, Lebedev\* VT, Bica\* D, Vékás\* L, Avdeev\* MV; Concentration and temperature effect in microstructure of ferrofluids; *Journal of Magnetism and Magnetic Materials*; **300**, e221-e224, 2006
- J.20. Török Gy, Lebedev\* VT, Bica\* D, Vékás\* L, Avdeev\* MV; Concentration and temperature effect in microstructure of ferrofluids; *Romanian Reports in Physics*; **58**, 279-285, 2006
- J.21. Török Gy, Len A, Rosta L, Balasoiu\* M, Avdeev\* MV, Aksenov\* VL, Ghenescu\* I, Hasegan\* D, Bica\* D, Vékás\* L; Interaction effects in non-polar and polar ferrofluids by small-angle neutron scattering; *Romanian Reports in Physics*, **58**, 255-261, 2006
- J.22. Zamponi\* M, Wischnewski\* A, Monkenbusch\* M, Willner\* L, Richter\* D, Likhtman\* AE, Kali G, Farago\* B; Molecular observation of constraint release in polymer melts; *Phys Rev Letters*; **96**, 238302/1-4, 2006
- J.23. Trounov\* VA, Sokolov\* AE, Lebedev\* VT, Smirnov\* OP, Kurbakov\* AI, Van den Heuvel\* J, Batyrev\* E, Yuryeva\* TM, Plyasova\* IM, Török Gy; Detection of hydrogen-copper clustering in  $Zn_1Cu_xO$  compounds using neutron scattering methods; *Physics of the Solid State*; **48**, 1291-1297, 2006
- J.24. Zemlyanaya\* EV, Kiselev\* MA, Zbytovska\* J, Almásy L, Aswal\* VK, Strunz\* P, Wartewig\* S, Neubert\* RHH; Numerical analyses of the structure of unilamellar vesicles based on small angle scattering data; *Crystallography Reports*; **51**, S1, 22-26, 2006
- J.25. Füzi J, Dávid\* E, Kozłowski\* T, Lewis\* P, Messing\* G, Mezei\* F, Penttilä\* S, Rosta L, Russina\* M, Török Gy; Neutron optical imaging study of neutron moderator and beam extraction system; *Physica B*; **385-386**, 1315-1317, 2006

- J.26. Cser L, Krexner\* G, Markó M, Sharkov\* I, Török Gy; Neutron holography; *Acta Physica Hungarica*; accepted for publication
- J.27. Cser L, Török Gy, Krexner\* G, Markó M, Sharkov\* I; Direct observation of local distortion of crystal lattice with picometer accuracy using atomic resolution neutron holography; *Phy Rev Letters*; accepted for publication
- J.28. Káli Gy, Sánta Zs, Bleif\* HJ, Mezei\* F, Rosta L, Szalók\* M; Commissioning of the high resolution TOF diffractometer at the Budapest Research Reactor; *Zeitschrift für Kristallographie*; accepted for publication
- J.29. Len A, Pépy\* G, Rosta L, Harmat\* P; Two-dimensional data treatment on anisotropical SANS and USANS small-angle neutron scattering patterns of doped tungsten wires; *J of Applied Crystallography*; accepted for publication
- J.30. Trounov\* VA, Lebedev\* VT, Grushko\* YS, Sokolov\* AE, Ivanova\* II, Rybakov\* VB, Yuryeva\* TM, Ivanchev\* SS, Török Gy; Several neutron scattering methods in the investigation of materials and components of equipments (in Russian); *Kristallografija*; accepted for publication
- J.31. Trounov\* VA, Lebedev\* VT, Sokolov\* AE, Grushko\* YS, Török Gy, Van den Heuvel\* J, Batyrev\* E, Yuryeva\* TM, Plyasova\* IM; Investigation of Hydrogen storage of composites on the base of ZnOCu (in Russian); *Kristallografija*; accepted for publication
- J.32. Székely NK, Almásy L, Radulescu\* A, Rosta L; SANS study of aqueous solutions of pentanediol and hexanediol; *J Appl Cryst*; accepted for publication

#### ***Articles in Hungarian***

- J.33. Len A; A kisszögű neutronszórás archeometriai alkalmazási lehetőségei (Applications of small angle neutron scattering in archaeometry, in Hungarian); *Archeometriai Műhely* - e-journal published by the Hungarian National Museum; ([www.ace.hu/am/index.html](http://www.ace.hu/am/index.html)), accepted for publication
- J.34. Sánta Zs; Nagyfelbontású repülési idő diffraktométer a Budapesti Neutron Központban (High Resolution Time of Flight Diffractometer at the Budapest Neutron Centre, in Hungarian); *Archeometriai Műhely* - e-journal published by the Hungarian National Museum; ([www.ace.hu/am/index.html](http://www.ace.hu/am/index.html)), accepted for publication

#### ***Conference proceedings***

- J.35. Füzi J; Vector hysteresis model for magnetic field computation; In: *Proceedings CD, 12<sup>th</sup> IGTE Symposium on Numerical Field Calculation in Electrical Engineering, Graz, Austria*; Ed: Bíró O; 513-518, 2006
- J.36. Füzi J; Ferroresonant circuit simulation with dynamic hysteresis model; In: *Proceedings CD, 12<sup>th</sup> IGTE Symposium on Numerical Field Calculation in Electrical Engineering, Graz, Austria*; Ed: Bíró O; 75-78, 2006

- J.37 Fűzi J; Vector Hysteresis model based on micromagnetic analogy; In: *Proceedings CD, 12<sup>th</sup> IGTE Symposium on Numerical Field Calculation in Electrical Engineering, Graz, Austria*; Ed: Bíró O; 69-74, 2006
- J.38 Heaton\* ME, Rogante\* M, Len A; A feasibility study for a SANS investigation of a heat cured and laser machined organic resin microturbine as used for airflow sensing; In: *Proceedings of the International Conference on Materials-Energy-Design, MED06 Dublin*; Institute of Technology, Ireland, 2006

#### **Book chapter**

- J.39. Fűzi J; Dynamic and vector preisach models for engineering applications; In: *Preisach Memorial Book, Hysteresis Models in Mathematics, Physics and Engineering*; Ed: Iványi A, Akadémiai Kiadó, Budapest; pp. 51-64, 2005

#### **Others**

- J.40. Lepekhin\* AV, Lebedev\* VT, Trounov\* VA, Török Gy, Lebedev\* VM; Small angle diffractometer “membrane” for high flux reactor; *PNPI Report*; **2604**, 18 pages, 2005
- J.41. Cser L, Study of upgrading of the small angle neutron scattering device at the research reactor of the ITN nuclear and technological institute, *IAEA-TECDOC*; **1486**, 39-52, 2006

## K. NEUTRON SCATTERING

*E. Sváb, M. Fábán<sup>#</sup>, I. Harsányi, P. Jóvári, L. Kőszegi, Gy. Mészáros, Sz. Pothoczki<sup>#</sup>,  
L. Pusztai, L. Temleitner<sup>#</sup>*

**Covalent glasses.** — The structure of  $0.7\text{SiO}_2\text{-}0.3\text{Na}_2\text{O}$  glass was investigated by means of neutron- and high-energy X-ray diffraction. The maximum momentum transfer was  $35 \text{ \AA}^{-1}$  and  $23.5 \text{ \AA}^{-1}$  for the two experiments. The two datasets were modelled simultaneously by the Reverse Monte Carlo (RMC) simulation technique. By using reasonable constraints it was possible to separate the 6 partial pair correlation functions (see Fig. 1). Nearest neighbour distances, coordination numbers and bond angle distributions have been revealed. It was found that 63% of the O atoms is in bridging position. The Na-O distance is  $2.29 \text{ \AA}$  and the coordination number is 2.5. The Na-Na nearest neighbour distance is  $2.6 \text{ \AA}$ , a value significantly smaller than previously reported. Neighbouring sodium ions tend to be located at the same oxygen atom.

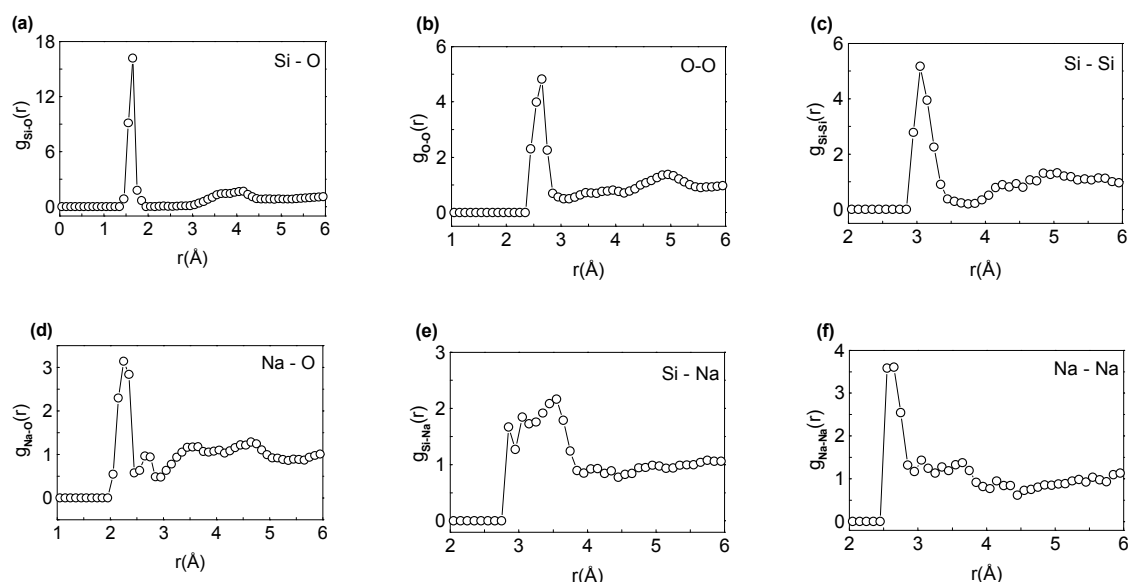


**Figure 1.** The partial pair distribution functions obtained by the simultaneous RMC fit of the two measurements (a) Si-O pair; (b) O-O pair; (c) Si-Si pair; (d) Na-O pair, (e) Si-Na pair; (f) Na-Na pair.

The structure of amorphous  $\text{Ge}_{15}\text{Te}_{85}$  has been investigated by X-ray and neutron diffraction and Ge K-edge EXAFS (Extended X-ray Absorption Fine Structure) measurements. The three datasets have been modelled simultaneously in the framework of the RMC simulation technique. Due to the high contribution of  $g_{\text{TeTe}}(r)$ , the Te-Te partial pair correlation function, and the small difference between the equilibrium Ge-Te and Te-Te distances ( $\sim 2.61 \text{ \AA}$  and  $2.76\text{-}2.80 \text{ \AA}$ , respectively) diffraction techniques are not able to separate the first peaks of  $g_{\text{TeTe}}(r)$  and  $g_{\text{GeTe}}(r)$ . This problem has been circumvented by using Ge K-edge EXAFS data, which are not sensitive to Te-Te correlations.

**Metallic glasses.** — Amorphous  $\text{Al}_{89}\text{La}_6\text{Ni}_5$  has been studied by X-ray diffraction (XRD), Ni K-edge and La L-edge EXAFS measurements. XRD is sensitive mostly to Al-Al correlations, Ni K-edge data are determined by Ni-Al correlations while the La L-edge

<sup>#</sup> Ph.D. student

measurement gives information on the environment of La atoms. Thus the combination of the three techniques can provide us with a detailed description of the structure of a ternary system. It has been found that the nearest Ni-Al and Al-Al distances are  $2.38 \pm 0.02$  Å and  $2.73 \pm 0.02$  Å, respectively. Both values are considerably shorter than the sum of corresponding atomic radii (2.67 Å and 2.86 Å). The Ni-Al coordination number calculated from the model is  $6.2 \pm 0.3$ . It is remarkable that a good quality fit could be obtained by a configuration in which 98% of Ni atoms have exactly 6 neighbours. This value would suggest the presence of well defined atomic motifs (e.g. NiAl<sub>6</sub> octahedra or trigonal prisms). A thorough investigation of the atomic configuration does not reveal any special local ordering around Ni.

**Liquids** – The structure of *liquid antimony pentachloride* SbCl<sub>5</sub> and *tungsten hexachloride* WCl<sub>6</sub> has been studied by neutron diffraction and subsequent RMC modelling. As the two liquids have not been studied before, basic information like the liquid state molecular geometry was missing. In liquid antimony-pentachloride we find that molecules take the shape of a trigonal bipyramid, with strictly straight axial Cl-Sb-Cl bond angles. It is now proven that liquid WCl<sub>6</sub> can be considered as a real molecular liquid, consisting of molecules of octahedral shape. It may be concluded on the basis of our long-term systematic studies on molecular liquids that as the size of individual molecules increases (and for 'centre-ligands' types, like the two liquids in question, this means also the sphericity), the importance of intermolecular (orientational) correlations seems to decrease compared to the intramolecular contributions, as exemplified by the cases of liquid antimony-pentachloride and tungsten-hexachloride.

**Disorder in ice** – Studying the structure of hexagonal (Ih) ice we showed that both the Bragg and the diffuse scattering parts of neutron powder diffraction data can be interpreted simultaneously by constructing large models of the structure that are consistent with the measured total scattering functions within errors (see Figure 2, part a). The RMCPOW (Reverse Monte Carlo for POWders) algorithm proved to be readily applicable for the purpose. It is found that proton disorder on its own cannot be responsible for the measured level and shape of diffuse scattering. The present results, particularly the O-H and O-O partial radial distribution functions (see Figure 2, part b) and the distribution of the O-H...O hydrogen bond angles suggest that small changes of the hydrogen bonded network are most probably responsible for the slightly different shape of the diffuse scattering signal at 120 and 200 K.

**Incommensurate antiferromagnetism in FeAl<sub>2</sub>**. — We have performed a neutron diffraction (ND) study on *FeAl<sub>2</sub>* below the magnetic phase transition temperature (~30 K) with the aim of obtaining information on the character of the magnetic structure. The ND pattern at 1.5 K and the temperature dependence of the weak magnetic satellite reflections have been determined (see Fig. 3). The position of, and the area under these peaks are temperature dependent. As the peaks are rather narrow, though slightly broadened compared to the nuclear reflections, a long-range ordering of the moments can be stated. We have established the incommensurate nature of the magnetic structure with a period length of 1.1 nm. The magnetic moments are in the range of 0.3-0.5 μ<sub>B</sub>.

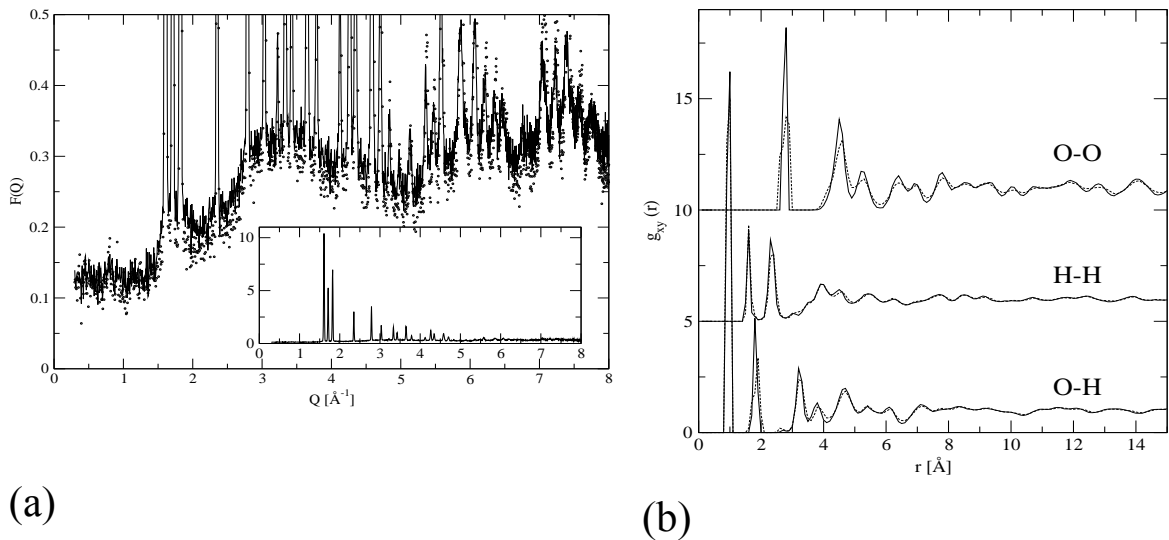


**Figure 2.** (a) Large panel: measured powder diffraction pattern of  $(D_2O)$  ice Ih at 120 K (symbols) and 200 K (solid line); the focus is on the diffuse scattering part. Inset: powder diffraction pattern of ice Ih at 200 K. (b) Comparison of the partial pair correlation functions for the 120 K (solid lines) and 200 K (dashed lines) states. In both cases, systems of  $8^3$  unit cells were applied.

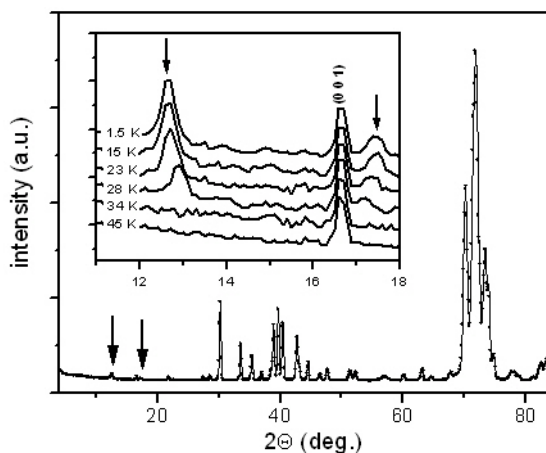


**Figure 3.** Neutron diffraction pattern of  $FeAl_2$  at 1.5 K ( $\lambda=2.4266 \text{ \AA}$ ). The insert shows the low angle part taken at different temperatures between 1.5-45 K. Arrows indicate the temperature dependent weak magnetic satellite reflections, showing the formation of long-range ordered incommensurate magnetic structure.

**Non-destructive materials testing on archeological objects.** — Restorers of the Hungarian National Museum appealed to us during their recent restoration work on a *helmet*, found at the beginning of the 20<sup>th</sup> century, which belongs to the Déri endowment. Our contribution was the non-destructive structure determination on a given part of the helmet. Parallel neutron diffraction measurements were also made on different iron oxides to compare the spectrum obtained from the heavily rusted object. In spite of the off stoichiometric composition and the large amount of hydrogen it is reasonable to assume that, apart from the presence of iron, the second phase is most probably hematite.

#### E-Mail:

Margit Fábíán	fabian@szfki.hu
Ildikó Harsányi	harsanyi@szfki.hu
Pál Jóvári	jovari@szfki.hu
László Kószegi	koszegi@szfki.hu

György Mészáros	meszaros@szfki.hu
Szilvia Pothoczki	pszszse@freemail.hu
László Pusztai	lp@szfki.hu
Erzsébet Sváb	svab@szfki.hu
László Temleitner	temla@szfki.hu

## Grants and international cooperations

- OTKA T 042495 Neutron diffraction study of atomic and magnetic structures (E. Sváb, 2003-2006)
- OTKA T 048580 Structural studies of liquids and amorphous materials by diffraction and computer modelling (L. Pusztai, 2005-2008)
- MTA-BAS (Hungarian-Bulgarian bilateral): Neutron scattering investigation of the structure of ordered and disordered magnetic and non magnetic materials (E. Sváb, 2004-2006)

## Publications

### Articles

- K.1. Pusztai L, McGreevy\* RL; On the structure of simple molecular liquids  $\text{SbCl}_5$  and  $\text{WCl}_6$ ; *J Chem Phys*; **125**, 044508/1-7, 2006
- K.2. Jóvári P, Pusztai L; Structural changes in liquid selenium with increasing temperature; *J Mol Liq*; **129**, 115-119, 2006
- K.3. Harsányi I, Pusztai L, Soetens\* JC, Bopp\* PhA; Molecular dynamics simulations of aqueous RbBr-solutions over the entire solubility range at room temperature; *J Mol Liq*; **129**, 80-85, 2006
- K.4. Saksl\* K, Jóvári P, Franz\* H, Zeng\* QS, Liu\* JF, Jiang\* JZ; Atomic structure of  $\text{Al}_{89}\text{La}_6\text{Ni}_5$  metallic glass; *J Phys: Condens Matter*; **18**, 7579-7592, 2006
- K.5. Kaban\* I, Jóvári P, Hoyer\* W, Delaplane\* RG, Wannberg\* A; Structural studies on Te-rich Ge-Te melts; *J Phys: Condens Matter*; **18**, 2749-2760, 2006
- K.6. Hoppe\* U, Brow\* RK, Tischendorf\* BC, Jóvári P, Hannon\* AC; Structure of  $\text{GeO}_2$ - $\text{P}_2\text{O}_5$  glasses studied by X-ray and neutron diffraction; *J Phys: Condens Matter*; **18**, 1847-1860, 2006
- K.7. Somogyvári\* Z, Sváb E, Krezhov\* K, Kiss LF, Kaptás D, Vincze I, Beregi E, Bourée\* F; Non-collinear magnetic order in a Sc-substituted barium-hexaferrite; *J Magn Magn Mat*; **304**, e775-e777, 2006
- K.8. Fábrián M, Sváb E, Mészáros Gy, Kőszegi L, Temleitner L, Veress\* E; Structure study of borosilicate matrix glasses; *Zeitschrift für Kristallographie*; **Suppl.23**, 461-466, 2006
- K.9. Harsányi I, Jóvári P, Mészáros Gy, Pusztai L, Bopp\* PhA; Neutron and X-ray diffraction studies of aqueous rubidium bromide solutions; *J Mol Liq*; accepted for publication

- K.10. Kaban\* I, Jóvári P, Hoyer\* W, Welter\* E; Determination of partial pair distribution functions in amorphous Ge<sub>15</sub>Te<sub>85</sub> by simultaneous RMC simulation of diffraction and EXAFS data; *J Non-Cryst Solids*; accepted for publication
- K.11. Fábrián M, Sváb E, Mészáros Gy, Révay\* Zs, Proffen\* Th, Veress\* E; Network structure of multi-component sodium borosilicate glasses by neutron diffraction; *J Non-Cryst Solids*; accepted for publication
- K.12. Fábrián M, Sváb E, Mészáros Gy, Révay\* Zs, Veress\* E; Neutron diffraction study of sodium borosilicate waste glasses containing uranium; *J Non-Cryst Solids*; accepted for publication

***Book chapter***

- K.13. Temleitner L, Pusztai L; Investigation of the structural disorder in ice Ih using neutron diffraction and Reverse Monte Carlo modeling; In: *Physics and Chemistry of Ice*; Ed. W.F. Kuhs, Royal Society of Chemistry, Cambridge, UK; accepted for publication

***See also: D.2.***

## L. INTERACTIONS OF INTENSE LASER FIELDS WITH MATTER

*Gy. Farkas, P. Dombi, S. Varró, N. Kroó, Á. Hoffmann, Zs. Lenkefi*

**Theoretical research.** — We proposed a novel way of tailoring electron pulses with the help of ultrashort, carrier-envelope phase controlled laser pulses and surface plasmons. The new scheme allows for controlling photoelectron emission from metals surfaces spatially, spectrally and temporally thus providing a unique tool for time-resolved pump-probe-type studies with an electron beam. These results can have significant impact on the currently developing ultrafast electron diffraction method which promises the unification of atomic resolution in space and attosecond resolution in time in material science. We are also investigating new ways of generating attosecond pulses with surface harmonics which has the advantage that already moderately energetic femtosecond pulses can be converted to attosecond oscillations than before.

Based on our previous experimental low order perturbative surface harmonic generation, calculations showed that by Fourier-synthetising these harmonics 500 attosecond light pulses can be obtained in the free air, using a simple laser and a metallic surface.

We revealed by a model calculation that the efficiency of the Sommerfeld-precursor strongly depends on the beginning sharp discontinuity (created by the plasma-mirror) of the initiating laser pulse which fact offers a method to determine the absolute phase of the laser pulse.

We have analysed the reflection and transmission of a few-cycle femtosecond Ti:Sa laser pulse impinging on a metal nano-layer. It has been shown that in general a non-oscillatory frozen-in wake-field appears following the main pulse with an exponential decay and with a definite sign of the electric field. The scattering of a laser pulse impinging on a thin plasma layer has also been analysed at relativistic intensities (Fig. 1). The plasma electrons were represented by a surface current density along the layer. The nonlinearities stemming from the relativistic kinematics of the free electrons lead to the appearance of higher-order harmonics in the scattered spectra. We have found that e.g. the fourth harmonic peak strongly depends on the carrier-envelope phase difference with a modulation being almost 25 percent. The above phenomena can perhaps serve a basis for the construction of a robust linear carrier-envelope phase difference meter.

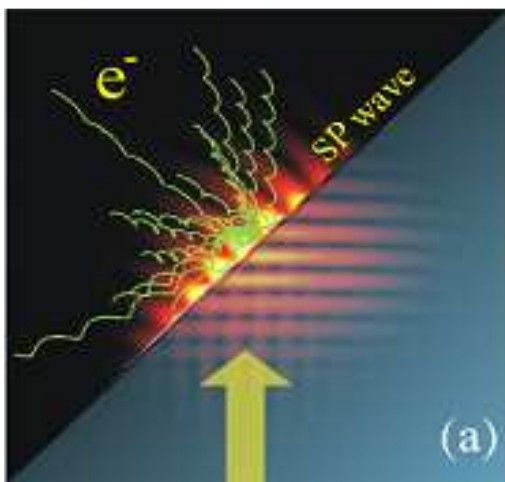


**Figure 1.** Surface plasmon-enhanced electron emission induced by an ultrashort laser pulse

We have worked out the theory of high-density black-body radiation on the basis of a new concept of binary photo-multiplets which satisfy the exclusion principle, thus they behave like fermions.

**Experimental research.** — In collaboration with the Max Planck Institute of Quantum Optics a so-called long-cavity Ti:sapphire oscillator that delivers femtosecond pulses with 250 nJ and 3 MHz repetition rate was set up in Budapest. This unique light source delivers ideal driving pulses for several applications, the above mentioned ultrafast electron diffraction being just one of them. These types of high-

energy, high repetition rate ultrafast lasers also pose some laser technological challenges (e.g. how to compress them below 10 fs) which have also been investigated. During these tests a new type of backscattering mechanism from optical fibres was found that seems to be unique in this parameter regime. We have also done preparations for setting up a simple vacuum chamber combined with an electron spectrometer that will be able to characterize surface-plasmon-enhanced photoelectron emission.

## E-Mail

Győző Farkas	farkas@szfki.hu
Péter Dombi	dombi@szfki.hu
Sándor Varró	vs@szfki.hu
Norbert Kroó	kroo@office.mta.hu
Ákos Hoffmann	hoffmann@szfki.hu, ahoffmann@physyk.uni-bonn.de
Zsolt Lenkefi	lenkefi@szfki.hu

## Grants and international cooperations

- OTKA T048324 Theoretical and experimental study of the newest nonlinear processes of ‘attophysics’ generated by superintense laser fields within the light wavelength and oscillation period scales (S. Varró, 2005-2007)
- OTKA IN 64303 Investigation of laser-induced ultrafast processes on metal surfaces”, Bilateral cooperation with the Max Planck Institute for Quantum Optics, Garching, Germany (S. Varró, 2006-2007)
- OTKA F60256 Investigation of femto- and attosecond light-solid interactions with controlled-waveform laser pulses”, individual young scientist grant of the Hungarian Scientific Research Fund (P. Dombi, 2006-2009)
- ÖVEGES József Grant of the National Office for Research and Technology (P. Dombi, 2007-2008)
- COST Action P 14 “*ULTRA*” Laser-matter physics with ultra-short pulses, high-frequency pulses and ultra-intense pulses. (Gy. Farkas, 2004-2008)
- Max Planck Institute for Quantum Optics (Garching, Germany), Surface plasmon research using STM (N. Kroó)
- Physical Institute of University of Bonn (Germany), Charge density waves in photorefractive materials (A. Hoffmann)

## Publications

### Articles

- L.1. Dombi P, Krausz\* F, Farkas Gy; Ultrafast dynamics and carrier-envelope phase sensitivity of multiphoton photoemission from metals; *J Mod Opt*; **53**, 163, 2006
- L.2. Irvine\* SE, Dombi P, Farkas Gy, Elezzabi\* AY; Influence of the carrier-envelope phase of few-cycle pulses on ponderomotive surface-plasmon electron acceleration; *Phys Rev Lett*; **97**, 146801, 2006
- L.3. Varró S; Einstein’s fluctuation formula. A historical overview; *Fluctuation and Noise Letters*; **6**, R11-R46, 2006

- L.4. Kroó N, Czitrovszky A, Nagy A, Oszetzky D, Walther\* H; Surface plasmons and photon statistics; *J Modern Optics*; **53**, 2309, 2006
- L.5. Varró S; Reflection of a few-cycle laser pulse on a metal nano-layer: generation of phase dependent wake-fields; *Laser Physics Letters*; accepted for publication
- L.6. Varró S; Scattering of a few-cycle laser pulse by a plasma layer : the role of the carrier-envelope phase difference at relativistic intensities; *Laser Physics Letters*; accepted for publication
- L.7. Varró S; Irreducible decomposition of Gaussian distributions and the spectrum of black-body radiation; *Physica Scripta*; accepted for publication

### **Articles in Hungarian**

- L.8. Dombi P; Optikai frekvenciametrológia, avagy mire jók a frekvenciafésűk? (Optical frequency metrology – what are frequency combs for? in Hungarian); *Fizikai Szemle*; **LVI**, 91-94, 2006
- L.9. Farkas Gy; Attoszekundumos ( $10^{-18}$  sec) fényimpulzusok (Attosecond ( $10^{-18}$  sec) light pulses, in Hungarian); *Fizikai Szemle*; accepted for publication

### **Book chapters**

- L.10. Varró S; A foton 100 éve (The 100 years of the photon, in Hungarian); In: *A kvantumoptika és –elektronika legújabb eredményei (The latest results in quantum optics and quantum electronics)*; eds.: Heiner Zs, Osvay K, SZTE, Szeged, Hungary; pp. 9-35, 2006
- L.11. Dombi P; Femtoszekundumos oszcillátorok és fázis-stabilizálás (Femtosecond oscillators and phase stabilization, in Hungarian); In: *A kvantumoptika és –elektronika legújabb eredményei (The latest results in quantum optics and quantum electronics)*; eds.: Heiner Zs, Osvay K, SZTE, Szeged, Hungary; pp. 66-73, 2006
- L.12. Farkas Gy; Többfotonos folyamatok és attoszekundumos jelenségek (Multiphoton processes and attosecond phenomena, in Hungarian); In: *A kvantumoptika és –elektronika legújabb eredményei (The latest results in quantum optics and quantum electronics)*; eds.: Heiner Zs, Osvay K, SZTE, Szeged, Hungary; pp. 208-227, 2006

### **Others**

- L.13. Varró S; Einstein's fluctuation formula. A historical overview; *Fluctuation and Noise Letters, a topical review*; **6**, R11-R46, 2006
- L.14. Varró S, A fény kettős természete. Einstein és a fotonok (The dual nature of light. Einstein and the photons, in Hungarian); *Természet Világa, 2006. I. Különszám : A fizika százada*; **137**, 38-43, 2006
- L.15. Varró S, Dombi P; A 2005. évi fizikai Nobel-díj. Kvantumoptika és szivárványfésű (The Nobel prize in physics 2005, in Hungarian); *Élet és Tudomány*; **LXI**, 560-563, 2006

- L.16. Varró S Dombi P; Optikusok elismerése. A 2005. évi fizikai Nobel-díj (The Nobel Prize in Physics 2005, in Hungarian); *Természet Világa*, **137**, 560-563, 2006
- L.17. Kroó N; Néhány gondolat a matematikáról (Several thoughts on mathematics, in Hungarian); *Magyar Tudomány*; 610-613, 2006
- L.18. Kroó N; Az alapkutatások jövője, különös tekintettel Európára (The future of fundamental research, with special regard of Europe, in Hungarian); *Fizikai Szemle*; **LVI**, 37-42, 2006

## M. LASER PHYSICS

*K. Rózsa, G. Bánó, L. Csillag, Z. Donkó, P. Hartmann, P. Horváth<sup>#</sup>, Z.Gy. Horváth, K. Kutasi, P. Mezei*

**Computational plasma studies.** — We have developed a particle-in-cell simulation code to investigate the characteristics of carbon tetrafluoride (CF<sub>4</sub>) radiofrequency-excited discharges, which are of primary importance in the etching of silicon and silicon-dioxide in microelectronic industry. It has been found that in the case of dual-frequency (e.g. by 100 MHz / 1 MHz) excitation, at low pressures the flux-energy distribution of CF<sub>3</sub><sup>+</sup> ions hitting the powered electrode can be tuned by the voltage of the low-frequency source, while the high-frequency voltage can be used to set the plasma density and thereby the flux of the ions to the electrode. This independent control of the ion flux and ion energy makes dual-frequency RF discharges an attractive plasma source for microelectronics applications.

In the field of strongly coupled plasma physics we have performed extensive molecular dynamics (MD) simulations and investigated thermodynamic and collective properties of two dimensional and bilayered many-particle systems. We have demonstrated that 2D Yukawa systems exhibit non-Newtonian shear viscosity. We have investigated the ground state configurations of magnetic particles confined into a 2D lattice. A lattice parameter dependent phase boundary between ferromagnetic and anti-ferromagnetic states has been found. Our MD simulations on strongly interacting quark-gluon plasmas we have shown a resonant-like energy transfer from the background gluon field to the massive quarks near the hadronization temperature.

**Electrolyte cathode atmospheric pressure glow discharge (ELCAD).** — The abnormal characteristics of a capillary ELCAD plasma were investigated. The cathode fall obtained from the measured discharge voltage as a function of the electrode distance was found to be higher than that of a normal ELCAD and increases with increasing current. Since the physical dimensions of this discharge are small, the length of the cathode dark space (LCDS) and the diameter of the cathode spot were determined through the intensity distribution received by applying of a CCD camera and the FITSVIEW astronomical image processing software. In the determination of LCDS, the change of the electrolyte surface caused by the discharge was taken into account. The current density was much higher than that measured in a normal ELCAD plasma and increased linearly with increasing discharge current corresponding to an abnormal glow. The LCDS value was calculated by the similarity law for the ELCAD. The LCDS value obtained from the experiments and the calculation agree well and both are smaller compared with that obtained in a normal ELCAD. The agreement of the measured LCDS with the calculated one supports the validity of the similarity law for the ELCAD. In the cathode surface-cathode dark space, the gas temperature was estimated considering that the H<sub>2</sub>O<sup>+</sup> molecular ions, generated in the cathode dark space, reach the cathode through symmetrical charge transfer collisions. In accordance with our measured results, a higher gas temperature was estimated than that calculated in a normal ELCAD. These results indicate that the significantly enhanced current density of the capillary ELCAD decreases the LCDS and increases the gas temperature in the boundary layer compared with the case of a normal ELCAD.

---

<sup>#</sup> Ph.D. student

**Multispectral imaging reflectometer.** — The development of a pinhole based imaging system, - in cooperation with the Research Institute for Technical Physics and Materials Sciences - is in progress. High power, multi-laser (multispectral) and incoherent (LED) light sources enabled us to record, store and analyse incident angle and spectral dependent reflectivity data of the test surfaces.

**Hollow cathode lasers.** — Near 200 nm deep ultraviolet hollow-cathode metal ion lasers can be used as light sources for UV Raman and laser-induced fluorescent spectroscopy. These lasers are usually excited by charge transfer reactions between noble gas ions and metal atoms. High density of noble gas ions is created in hollow-cathode discharges while the necessary metal atom density can be produced either by thermal evaporation or utilizing the cathode sputtering effect of the discharge. Our recent investigation is focused on the development of a sputtered 224 nm segmented hollow-cathode silver ion laser. The lifetime of the laser is limited by the impurities present in the helium-argon buffer gas and also by the metal atoms deposited onto the anode electrodes. These metal atoms have a tendency to create a non-homogenous layer, which may block the propagation of the light or can create shortcuts between the neighboring anode and cathode electrodes. A novel discharge arrangement has been developed in order to prolong the lifetime of the laser tube. The basic idea is to have ground-independent electrical connections for both the anode and the cathode electrodes. This way the ‘anodes’ can be occasionally sputtered by the discharge connecting them to a negative bias voltage. This process results in a smooth anode surface for an extended time period. 220 mW peak power has been achieved using our latest model.

### **E-Mail:**

Károly Rózsa	karcsi@sunserv.kfki.hu
Gergely Bánó	bano@sunserv.kfki.hu
László Csillag	csillag@szfki.hu
Zoltán Donkó	donko@sunserv.kfki.hu
Péter Hartmann	hartmann@sunserv.kfki.hu
Péter Horváth	phorvath@sunserv.kfki.hu
Zoltán Gy. Horváth	horvath@szfki.hu
Kinga Kutasi	kutasi@sunserv.kfki.hu
Pál Mezei	mezeipal@szfki.hu

### **Grants and international cooperations**

OTKA T-48389 Modern plasma simulation techniques (Z. Donkó, 2005–2008)  
OTKA PD-049991 Post-doc position (P. Hartmann, 2005–2008)  
OTKA T-042493 The role of the ions of the basic electrolyte solution in the electrolyte cathode atmospheric glow discharge ( P. Mezei, 2003-2006)  
MTA-OTKA-NSF 90/46140 Strongly coupled Coulomb systems (Z. Donkó, 2005-2007)  
GVOP-3.1.1.-2004-05-0435/3.0 Multispectral imaging reflectometer (M.Fried and Z.Gy. Horváth, 2005-2007)  
OMFB-00184/2005 (Hungarian-Czech bilateral project) Plasmadiagnostics (G. Bánó, 2005-2006)

## Publications

### Articles

- M.1. Donkó Z, Petrović\* ZLj; Analysis of a capacitively coupled dual-frequency CF<sub>4</sub> discharge; *Jpn J Appl Phys*; **45**, 8151-8156, 2006
- M.2. Donkó Z, Hartmann P, Kutasi K; On the reliability of low-pressure dc glow discharge modelling; *Plasma Sources Sci Technol*; **15**, 178–186, 2006
- M.3. Hartmann P, Kalman\* GJ, Donkó Z; Two-dimensional Yukawa liquids: structure and collective excitations; *J Phys A: Math Gen*; **39**, 4485-4491, 2006
- M.4. Hartmann P, Donkó Z, Kalman\* GJ, Lévai\* P; Molecular dynamics simulation of strongly coupled QCD plasmas; *Nucl Phys A*; **774**, 881-884, 2006
- M.5. Donkó Z, Goree\* J, Hartmann P, Kutasi K; Shear viscosity and shear thinning in two-dimensional Yukawa liquids; *Phys Rev Lett*; **96**, 145003/1-4, 2006
- M.6. Mahassen\* H, Kutasi K, Golden\* KI, Kalman\* GJ, Donkó Z; Longitudinal collective modes in asymmetric charged-particle bilayers; *J Phys A: Math Gen*; **39**, 4601-4605, 2006
- M.7. Sullivan\* T, Kalman\* GJ, Kyrkos\* S, Bakshi\* P, Rosenberg\* M, Donkó Z; Phonons in Yukawa lattices and liquids; *J Phys A: Math Gen*; **39**, 4607-4611, 2006
- M.8. Rosenberg\* M, Kalman\* GJ, Kyrkos\* S, Donkó Z; Beam-plasma interaction in strongly coupled plasmas; *J Phys A: Math Gen*; **39**, 4613-4618, 2006
- M.9. Dimitrijevic\* MS, Csillag L; Spectral line broadening influence on the mode structure of the He-Kr and He-Ar gas lasers; *J Appl Spectr*; **73**, 405-407, 2006
- M.10. Mezei P, Cserfalvi\* T; The investigation of an abnormal electrolyte cathode atmospheric glow discharge (ELCAD); *J Phys D: Appl Phys*; **39**, 1-6, 2006
- M.11. Hlavenka\* P, Plašil\* R, Bánó G, Korolov\* I, Gerlich\* D, Ramanlal\* J, Tennyson\* J, Glosík\* J; Near infrared second overtone cw-cavity ringdown spectroscopy of D<sub>2</sub>H<sup>+</sup> ions; *Int J Mass Spectr*; **255-256**, 170-176, 2006
- M.12. Hartmann P, Donkó Z, Bakshi\* P, Kalman\* GJ, Kyrkos\* S; Molecular dynamics studies of the solid-liquid phase transition in 2D Yukawa systems; *IEEE Trans Plasma Sci*; accepted for publication
- M.13. Hartmann P, Donkó Z, Kalman\* GJ, Kyrkos\* S, Rosenberg\* M, Bakshi\* P; Collective modes in 2D Yukawa solids and liquids; *IEEE Trans. Plasma Sci*; accepted for publication
- M.14. Feldmann\* J, Kalman\* GJ, Hartmann P, Rosenberg\* M; Ground state and collective modes of magnetic dipoles on a two-dimensional lattice; *IEEE Trans Plasma Sci*; accepted for publication

### ***Article in Hungarian***

- M.15. Mezei P, Cserfalvi\* T; Gázkisülései analízis a környezetvédelemben (Gas discharge analysis in the environmental protection, in Hungarian); *Fizikai Szemle*; **LVI**, 217-221, 2006

### ***Conference proceedings***

- M.16. Donkó Z, Petrović\* ZLj; Analysis of a capacitively coupled dual-frequency CF<sub>4</sub> discharge; In: *Proc. of 6<sup>th</sup> International Conference on Reactive Plasmas and 23<sup>rd</sup> Symposium on Plasma Processing, January 24-27, Sendai, Japan, 2006*; Eds.: Hatakeyama R and Samukawa S, The Japan Society of Physics; pp. 99-100, 2006
- M.17. Donkó Z, Petrović\* ZLj; Control of ion properties in dual-frequency capacitively coupled CF<sub>4</sub> / Ar discharges; In: *Proc. of 18<sup>th</sup> International Conference on the Atomic and Molecular Physics of Ionised Gases, July 12-16, Lecce, Italy 2006*; Eds.: Cacciatore M et al, European Physical Society; pp. 213-214, 2006

### ***Book chapter in Hungarian***

- M.18. Bánó G, Kutasi K; Rezonátor-lecsengési spektroszkópia (Cavity ring-down spectroscopy, in Hungarian); In: *A kvantumoptika és -elektronika legújabb eredményei*; Eds.: Heiner Zs, Osvay K, University of Szeged, Szeged; pp. 190-195, 2006

## O. LASER APPLICATION

*A. Czitrowszky, M. Füle<sup>#</sup>, P. Gál<sup>#</sup>, P. Jani, Á. Kiss, M. Koós, S. Lakó, A. Nagy, T. Nemes, D. Oszetzky<sup>#</sup>, S. Tóth<sup>#</sup>, L. Vámos<sup>#</sup>, M. Veres*

**Optical measuring techniques.** — A dual wavelength optical particle spectrometer with a new data acquisition system and electronics with increased sensitivity was developed. This new instrument was calibrated in the aerosol laboratory which was further developed for extending the calibration aerosol spectrum and generation of different kinds of calibrating particles in a wide size range. A new software package was developed to control the generation of specific aerosols and calibration procedure of aerosol measuring instruments. This software package contains parameter control, data acquisition, and data evaluation.

A size measuring accuracy algorithm was developed for the case of coated nanospheres. Limits of resolution were established in comparison with water droplet particles. Optimization algorithm was developed for the size determination in photon correlation experiments. The 25 ps channel width photon correlator using TDC technology is under construction.

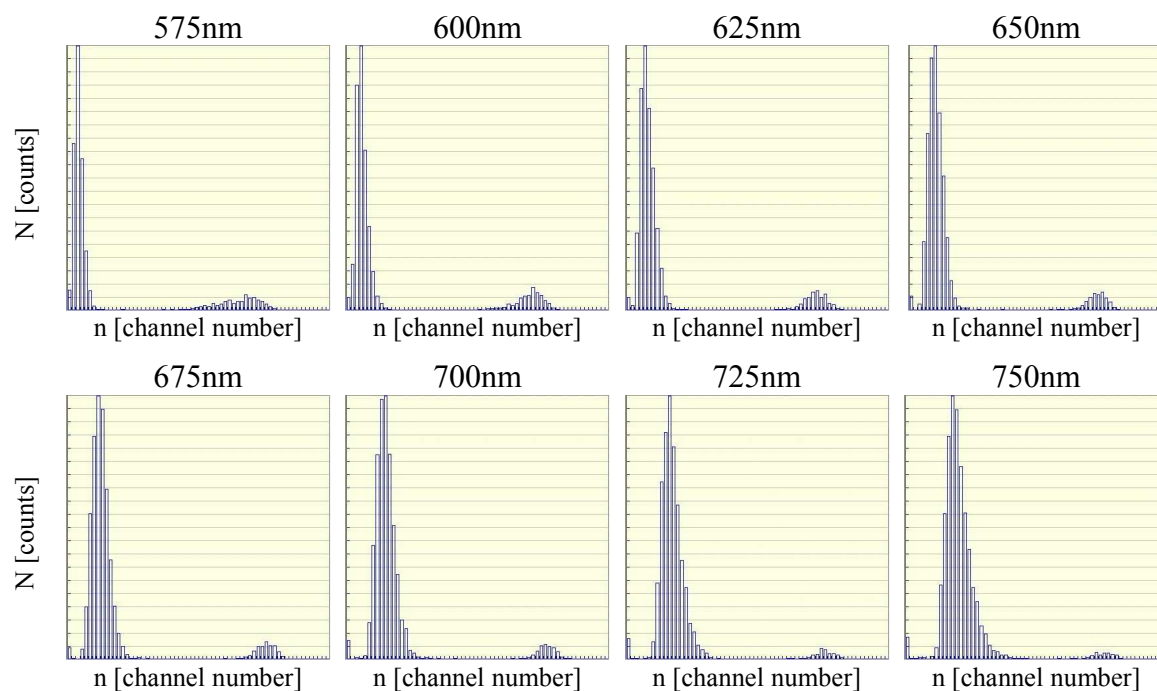


**Figure 1.** Size distribution of calibrating aerosol particles scanned from 575 to 750 nm, obtained by a differential mobility analyzer measured by newly developed dual wavelength optical particle spectrometer (DWOPS). The measurements show the unique size resolution of the developed system.

Using high time resolution, low noise Peltier cooled detectors with high quantum efficiency a high quality photon counting system was developed for studying of the statistical properties of classical- and non-classical light.

Measurement of the statistics of photons generated in nonlinear optical processes were performed in the case of surface plasmons, parametric deconversion etc. The statistics of

---

<sup>#</sup> Ph.D. student

the excitation light and the light generated by surface plasmons was compared. The results show the coincidence in these two statistics within the error of measurement ( $\sim 3\%$ ).

**Atmospheric Pollution.** — A mobile laboratory for environmental monitoring of atmospheric pollution was equipped with a number of new instruments elaborated for the determination of the concentration, chemical composition and physical characteristics of the atmospheric pollution. Air contamination maps were composed in several districts within the city of Budapest and its surrounding. Databases containing all collected results were analyzed. The collected data were compared with the statistics of the adverse health effects to the pregnancy, where significant negative influence was determined. The aerosol particle deposition in human breathing passages was modelled and specific deposition parameters were determined in case of respiratory diseases. (The work was done in the frame of the National Research and Development Programme NKFP-3A/089.)

**Nanotechnology.** — A high resolution interferometric surface testing system was elaborated for measurement of thermal and elastic dilatations. A new electronic system enables to increase the data evaluation rate ( $\sim 5$  times) and the resolution ( $\sim 2$  times). The new system is available for investigation of aerosol particles sedimented on different surfaces – e.g. for testing of the purity of microelectronic wafers.

In the frame of this project a new measurement setup was proposed for the measurement of timing resolution of single photon detectors. The proposed measurements were carried out for some commercially available avalanche photodiodes and modules. It was established that the timing resolution (FWHM) is in the range of 30 ps. The measurement system using digital signal processing (DSP) technology is under construction. (The work was done in the frame of the National Research and Development programme NKFP-3A/071.)

A new PC controlled detector system with a submicron resolution X-Y positioning mechanics was developed for registration of digital holograms. The stepping/scanning mode of the image registration with a pre-programmed trajectory and stitching of 64 (8x8) images enables to increase the virtual resolution and the quality of the holograms. A patent for this new technique was elaborated and applied. (This work was done in the frame of the Research Programme GVOP-3.1.1-0403/3.0.)

**Amorphous carbon thin layers.** — Despite the intensive investigation performed in the last decade, the scientific interest to hydrogenated amorphous carbon (a-C:H) thin films is still growing. The main reason for this is the possibility of their application in different fields of modern technology due to a wide variety of promising properties. Besides the diamond-like coatings, an increasing interest has evolved devoted to layers prepared at low ion energies, where polymer-like a-C:H films form. These films seem to be good candidates for active materials in optoelectronic devices. Incorporation of different foreign atoms into the carbon based amorphous matrix provides additional possibility for the tuning of macroscopic features of a-C:H thin layers and for their technological applications.

Our research work was focused on the polymeric thin films prepared from benzene, especially on the influence of layer thickness on some optical and luminescence properties as well as on the atomic bonding structure of a-C:H. Incorporation of silicon atoms in amorphous carbon matrix was also examined. As an application of diamond-like carbon (DLC) layers we have investigated the coronary stent coating with it.

A detailed study of steady state photoluminescence (PL) properties of polymer-like a-C:H samples of different thickness (60-2249 nm) provides experimental evidence for a

remarkable change of these properties when the layer thickness increases. Photon energy of PL and PLE (PL excitation spectrum) peak position exhibits red shift of 0.22 eV and 0.25 eV respectively as the thickness increases from 60 nm up to 1025 nm followed by a gradual decrease of the light emission in the ultraviolet region. The optical absorption edge shifts also to lower photon energy and the optical gap decreases by  $\sim 0.5$  eV when the thickness increases in the above mentioned range. Fig.2 shows the dependence of PL peak energy and optical gap on the sample thickness prepared from benzene at -30 V self bias and 18.5 Pa process pressure. Influence of layer thickness on the refractive index we have also investigated. Spectral dependence of refractive index remained similar when the layer thickness increases, though its value is enhanced in the case of thicker samples.

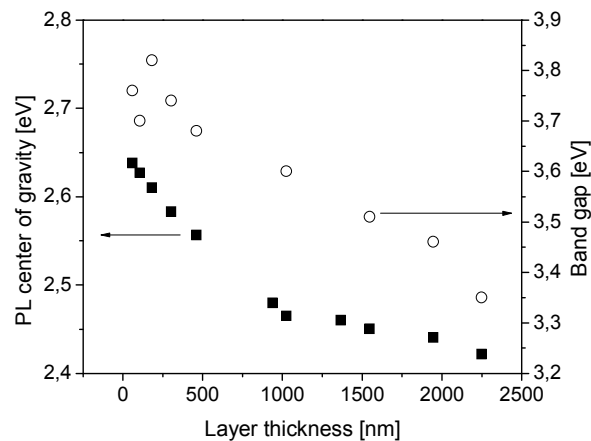
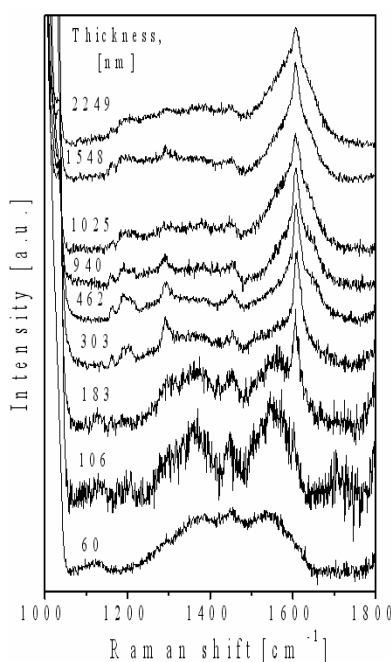


**Figure 2:** Thickness dependence of the optical band gap and the center of gravity of the PL emission on samples prepared at -30 V self bias and 18.5 Pa process pressure

The evolution of the structure with increase of layer thickness of a-C:H samples prepared from benzene was monitored by Raman scattering study. Fig. 3 shows Raman spectra for a thickness series of polymer-like a-C:H samples prepared at -30V self bias and 18.5 Pa process pressure. Broad scattering bands are characteristic feature of Raman spectra below 183 nm sample thickness above which very narrow bands typical for a molecule scattering is developing as the thickness increases. At the same time the intensity of this narrow band decreases for thickness > 462 nm and parallel a broad scattering band in the G peak region ( $\sim 1600$   $\text{cm}^{-1}$ ) develops. These Raman scattering results indicate a significant structural changes with increase of layer thickness. While the layer of 60 nm contains of  $\text{sp}^2$  clusters built mainly of chains, the increase of thickness up to 500 nm results in the development of an amorphous matrix formed by distorted or partially destroyed benzene rings as well as in the appearance of intact substituted benzene rings in the structure. The observed changes of PL and optical properties corroborate very well with the evolution of the structure with increase of layer thickness as it was concluded from Raman spectra.



is developing as the thickness increases. At the same time the intensity of this narrow band decreases for thickness > 462 nm and parallel a broad scattering band in the G peak region ( $\sim 1600$   $\text{cm}^{-1}$ ) develops. These Raman scattering results indicate a significant structural changes with increase of layer thickness. While the layer of 60 nm contains of  $\text{sp}^2$  clusters built mainly of chains, the increase of thickness up to 500 nm results in the development of an amorphous matrix formed by distorted or partially destroyed benzene rings as well as in the appearance of intact substituted benzene rings in the structure. The observed changes of PL and optical properties corroborate very well with the evolution of the structure with increase of layer thickness as it was concluded from Raman spectra.

**Figure 3.** Thickness dependence of Raman scattering spectra excited by 785 nm of a-C:H layers prepared at -30 V self bias and 18.5 Pa process pressure

We have continued the research work aimed the

development of bio-, and haemocompatible coating of cardiovascular stents. In this stage of work a technological arrangement was constructed for the preparation of diamond-like (DLC) coating onto the surface of cardiovascular stents in the plasma enhanced chemical vapor deposition process. This arrangement makes it possible to cover 15 stents simultaneously. Different experiments were performed to test homogeneity, compactness, ageing behavior of covering layer. Fig 4. shows SEM image of DLC coated stent before and after crimping and expansion. This scan shows an excellent adherence of covering layer to the surface of stent. The enlarged image of the surface area (Fig. 4c) also supports the good quality of the layer.

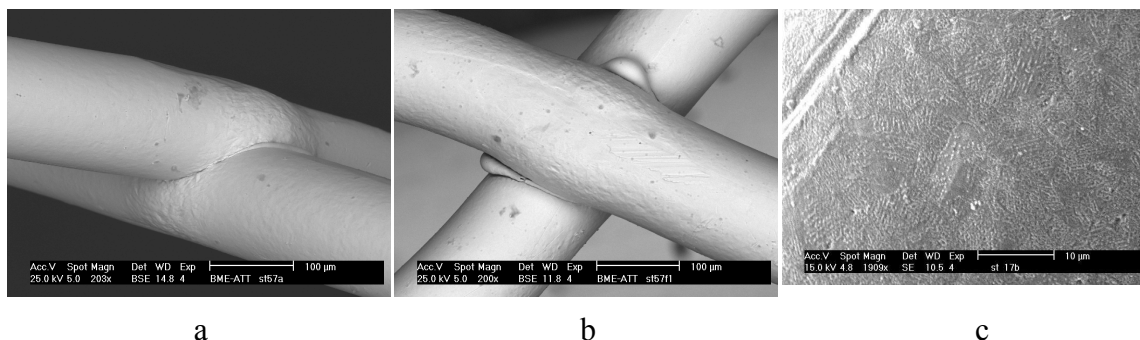


**Figure 4.** SEM micrograph of the a-C:H thin film deposited onto the stent surface before (a) and after (b) crimping and expansion. Enlarged film surface (c).

## E-Mail:

Aladár Czitrovszky	<a href="mailto:czi@szfki.hu">czi@szfki.hu</a> , <a href="mailto:czitrovszky@sunserv.kfki.hu">czitrovszky@sunserv.kfki.hu</a>
Miklós Füle	<a href="mailto:fule@szfki.hu">fule@szfki.hu</a>
Péter Gál	<a href="mailto:gal@szfki.hu">gal@szfki.hu</a>
Péter Jani	<a href="mailto:pjani@sunserv.kfki.hu">pjani@sunserv.kfki.hu</a>
Árpád Kiss	<a href="mailto:kissa@szfki.hu">kissa@szfki.hu</a>
Margit Koós	<a href="mailto:koos@szfki.hu">koos@szfki.hu</a>
Sándor Lakó	<a href="mailto:lako@szfki.hu">lako@szfki.hu</a>
Attila Nagy	<a href="mailto:anagy@szfki.hu">anagy@szfki.hu</a>
Tibor Nemes	<a href="mailto:nemes@szfki.hu">nemes@szfki.hu</a>
Dániel Oszetzky	<a href="mailto:odani@szfki.hu">odani@szfki.hu</a>
Sára Tóth	<a href="mailto:tothsara@szfki.hu">tothsara@szfki.hu</a>
Lénárd Vámos	<a href="mailto:vamos@szfki.hu">vamos@szfki.hu</a>
Miklós Veres	<a href="mailto:vm@szfki.hu">vm@szfki.hu</a>

## Grants and international cooperations

NKFP-3A/089	National Research and Development Program, Environmental pollution of the atmosphere (A. Czitrovszky, 2004-2007)
NKFP- 3A/071	National Research and Development Program, Nanotechnology II (Sub-coordinator: A. Czitrovszky, 2004-2007)
NKFP-3A/042/04	National Research and Development Program – Development of new generation coronary stents on the base of clinical experiences from haemocompatible materials coated by nanostructured carbon (M. Koós, 2004-2006)
OTKA T-043359	Preparation and complex characterization of carbon based nanocomposites (M. Koós, 2003-2006)

GVOP-3.1.1., No 0403/3.0, DIADEM (in cooperation with Budapest Technical University, coordinator: A. Czitrovsky, 2005-2007)  
 GVOP-3.1.1., No 0259/3.0 Photo-catalytic decomposition of pollutants (in cooperation with the University of Szeged, coordinator: A. Czitrovsky, 2005-2007)  
 Bilateral Austro-Hungarian Cooperation, Contract No A-13/03 (A. Czitrovsky, 2003-2006)  
 HMTH- 686/2005, MITOSZ (A. Czitrovsky, 2005-2006)  
 TÉT Bilateral (Hungarian-Ukrainian) Cooperation, Contract No. UK-12 (M. Koós, 2005-2006)

## Publications

### Articles

- O.1. Farkas\* Á, Balásházy\* I, Czitrovsky A, Nagy A; Simulation of therapeutic and radioaerosol deposition in diseased airways; *J Aerosol Medicine*; **18**, 102-104, 2005
- O.2. Balásházy\* I, Farkas\* Á, Czitrovsky A, Szigethy\* D, Nagy\* J; Modelling local deposition patterns of inhaled aerosols in bronchial human airways; *J Aerosol Medicine*; **18**, 98-99, 2005
- O.3. Rudnai\* P, Virágh\* Z, Varró\* MJ, Vaskövi\* É, Beregszászi\* T, Náráy\* M, Czitrovsky A; Impact of air pollution on the children's health near a communal waste incinerator; *Epidemiology*; **17 S**, 414-415, 2006
- O.4. Vámos L, Jani P; Optimization algorithm of LDA signal processing for nanoparticles; *SPIE Opt Eng*; **6293**, 629303/1-8, 2006
- O.5. Tóth S, Veres M, Füle M, Koós M; Influence of layer thickness on the photoluminescence and Raman scattering of a-C:H prepared from benzene; *Diamond and Related Materials*; **15**, 967-971, 2006
- O.6. Veres M, Koós M, Orsós\* N, Tóth S, Füle M, Mohai\* M, Bertóti\* I; Incorporation of Si in a-C:H films monitored by infrared excited Raman scattering; *Diamond and Related Materials*; **15**, 932-935, 2006
- O.7. Veres M, Tóth S, Füle M, Koós M; Thickness dependence of the structure of a-C:H thin films prepared by rf-CVD evidenced by Raman spectroscopy; *J Non-Cryst Solids*; **352**, 1348-1351, 2006
- O.8. Tóth S, Füle M, Veres M, Pócsik I, Koós M, Tóth\* A, Ujvári\* T, Bertóti\* I; Photoluminescence of ultra-high molecular weight polyethylene modified by fast atom bombardment; *Thin Solid Films*; **497**, 279-283, 2006
- O.9. Tóth S, Veres M, Füle M, Koós M; Fabry-Perot resonance enhancement-inhibition of spontaneous light emission from a-C:H thin films; *J Non-Cryst Solids*; **352**, 1336-1339, 2006

- O.10. Füle M, Tóth S, Veres M, Koós M; Size of spatial confinement at luminescence centers determined from resonant excitation bands of a-C:H photoluminescence; *J Non-Cryst Solids*; **352**, 1340-1343, 2006
- O.11. Holomb\* R, Mateleshko\* N, Mitsa\* V, Johansson\* P, Matic\* A, Veres M; New evidence of light-induced structural changes detected in As-S glasses by photon energy dependent Raman spectroscopy; *J Non-Cryst Solids*; **352**, 1607-1611, 2006
- O.12. Budai\* J, Tóth\* Z, Juhász\* A, Szakács\* G, Szilágyi\* E, Veres M, Koós M; Reactive pulsed laser deposition of hydrogenated carbon thin films: The effect of hydrogen pressure; *J Appl Phys*; **100**, 043501/1-9, 2006
- O. 13. Jani P, Vámos L., Nemes T; Timing resolution (FWHM) of some photon counting detectors and electronic circuitry; *Measurement Science and Technology*; accepted for publication
- O.14. Budai\* J, Tóth S, Tóth\* Z, Koós M; Diamond-like carbon films prepared by reactive pulsed laser deposition in hydrogen and methane ambient; *Thin Solid Films*; accepted for publication

#### **Conference proceedings**

- O.15. Szymanski\* W, Golczewski\* A, Nagy A, Gál P, Czitrovsky A; An innovative approach to optical measurement of atmospheric aerosols – determination of the size and the complex refractive index of single aerosol particles; In: *6th International Symposium on Advanced Environmental Monitoring, June 27-30, 2006. Heidelberg, Germany; I-D03*
- O.16. Oszetzky D, Kiss A, Czitrovsky A, Nagy A, Gál P; 3D measurement of nanoparticles on wafer surface using phase shifted laser interferometry; In: *Proc. 7th International Aerosol Conference, Sept. 10-15, 2006. St. Paul, Minnesota, USA*; Eds.: P. Biswas, D.R. Chen, S. Hering, American Association for Aerosol Research, Mount Laurel, USA; pp.401-402, 2006
- O.17. Golczewski A, Nagy A, Gál P, Czitrovsky A, Szymanski W; Determination of the size and complex refractive index of single aerosol particles using dual wavelength optical particle spectrometer (DWOPS); In: *7th International Aerosol Conference, Sept. 10-15, 2006. St. Paul, Minnesota, USA*; Eds.: P. Biswas, D.R. Chen, S. Hering, American Association for Aerosol Research, Mount Laurel, USA; p.404, 2006
- O.18. Oszetzky D, Nagy A, Czitrovsky A; Controllable photon source; In: *Proc. SPIE Vol. 6372*; 637214, 2006
- O.19. Rudnai\* P, Virágh\* Z, Varró\* MJ, Vaskövi\* É, Beregszászi\* T, Mácsik\* Á, Náray\* M, Czitrovsky A; Air pollution and its impact on the children's health near a communal waste incinerator; In: *International Conference on Child Health and Environment, Brussels, 23-25 November, 2005*; pp. 14-16
- O.20. Jani P, Vámos L; Scattering properties of coated nanoparticles compared to water droplets; In: *7th International Aerosol Conference IAC2006 (St. Paul, Minnesota,*

USA, 10-15 Sept., 2006; Eds.: P. Biswas, D.R. Chen, S. Hering, American Association for Aerosol Research, Mount Laurel, USA; p. 490

- O.21. Vámos L, Jani P; Törésmutató és hullámhossz független részecskeszám meghatározási algoritmus (Wavelength and refractive index independent particle number algorithm, in Hungarian); In: *VIII. National Aerosol Conference, Siófok-Szabadifürdő, 25-26 May 2006*; ed.: Salma J, ELTE, Budapest; pp. 57-58, 2006
- O.22. Veres M, Tóth S, Füle M, Koós M; Formation of amorphous carbon nanoparticles in plasma discharge; In: *VIII. National Aerosol Conference, Siófok-Szabadifürdő, 2006. 05 25-26*; ed.: Salma J, ELTE, Budapest; pp. 19-20, 2006
- O.23. Czitrovsky A, Kiss Á, Oszetzky D, Nagy A, Gál P, Pogány L; 3D measurement of geometrical parameters of nanoparticles using laser interferometry; In: *National Aerosol Conference, Szabadifürdő, May 25-26 2006*; ed.: Salma J, ELTE, Budapest; pp. 15-16, 2006
- O.24. Veres M, Tóth S, Füle M, Dobránszky\* J, Major\* L, Koós M; Protective coating on coronary stents with functionalizable surface; In: *Proc. 20th European Conference on Biomaterials 27 September - 1 October 2006, Nantes, France (available on CD)*

**Book chapter:**

- O.25. Koós M, Veres M, Tóth S, Füle M; Raman spectroscopy of CVD carbon thin films excited by near-infrared light; In: *Carbon: The Future Material for Advanced Technology Applications*; Eds.: G. Messina and S. Santangelo., Springer' series Topics in Applied Physics Vol. 100, pp. 423–444, 2006

**Patent:**

- O.26. Gyimesi\* F, Füzessy\* Z, Czitrovsky A, Nagy A, Molnárka\* Gy, Szigethy\* D; Processing of digital holograms; Hungarian patent, pending

**See also L.4.**

## P. FEMTOSECOND LASERS

*R. Szipőcs, Á. Bányász<sup>#</sup>, J. Fekete<sup>#</sup>*

**Distortion free delivery and dispersion control of high intensity femtosecond laser pulses by means of hollow core photonic bandgap optical fibers.** — Hollow core photonic bandgap (HCPBG) fibers form a special class of photonic crystal fibers, which are often referred to as hollow core photonics crystal fibers (HCPCF-s). In HCPCF-s, most of the optical power is guided in the air core, which allows delivery of femtosecond laser pulses with energies in the 1 to 10 nJ regime without considerable nonlinear distortion. This feature makes them attractive for applications that require single mode delivery of relatively high intensity ultrashort pulses, such as miniaturized multiphoton microscopes. In case of optical pulses with energy values as high as 700 nJ, generation of megawatt optical solitons have been demonstrated at around 1.4 micron in HCPCF-s due to the fact that these special fibers exhibit anomalous dispersion over most of their bandwidth. This attractive feature is demonstrated in Fig. 1a, where the attenuation and the dispersion of a commercially available HCPCF designed for 1060 nm is shown. For comparative purposes, computed transmission loss and group delay dispersion of a quarterwave dielectric mirror stack centered at 1060 nm is shown in Fig. 1b.

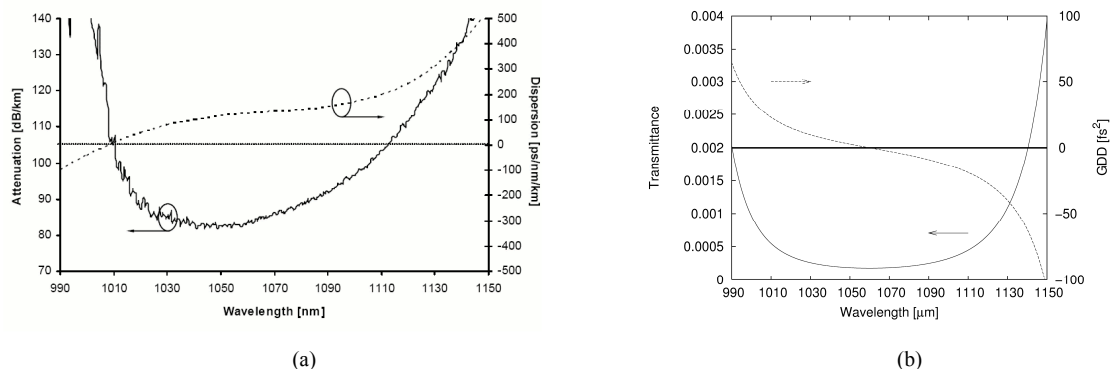


**Figure 1. (a)** Typical attenuation spectrum (solid line) and chromatic dispersion (dotted line) of a commercial HC-1060-2 HCPCF. **(b)** Computed transmission loss and group delay dispersion of a quarterwave dielectric mirror stack having the structure of substrate |  $(HL)^{15} H$  | air,  $n_H = 2.0$ ,  $n_L = 1.48$ , where  $H$  and  $L$  denote high and low refractive index, quarterwave layers at 1060 nm, respectively.

One can observe that compared to solid core photonic crystal fibers, the spectral bandwidth is relatively small, approximately 15% of the central wavelength in HCPCF-s. This is a common feature of quarterwave (i.e., not chirped) dielectric mirror stacks as well (see Fig. 1b). Regarding dispersion, one can say the following: in HCPCF-s, the fiber exhibits normal dispersion on the short wavelength side, which corresponds to negative dispersion values when the dispersion is given in  $ps/nm/km$  units, while over the central part and on the long wavelength side of the photonic bandgap, the dispersion is anomalous (positive dispersion values in Fig. 1a). The wavelength range over which the dispersion is close to zero is very narrow, which limits both the spectral bandwidth and tuneability of femtosecond laser sources for dispersion free delivery through such HCPCF-s. Additionally, the dispersion changes rapidly as the function of wavelength in the

<sup>#</sup> Ph.D. student

anomalous dispersion regime, which limits their use for dispersion compensation of heavily chirped, broadband, high energy femtosecond laser pulses as well. Regarding dispersion of quarterwave dielectric mirrors stacks, we find the same behaviour (see Fig. 1b): on the short wavelength side, they exhibit normal dispersion (positive values when the dispersion is measured in  $fs^2/reflection$  units), while on the long wavelength side, they have anomalous dispersion (negative group delay dispersion, GDD values). Accordingly, both HCPCF-s and quarterwave mirror stacks exhibit positive (normal) third-order dispersion (TOD) values, which originates from the *wavelength dependent penetration depth* of the electromagnetic field in both cases. The only difference between their dispersive properties is that dispersion of HCPCF-s is superimposed by the (anomalous) waveguide dispersion, which shifts the zero dispersion wavelength to the short wavelength side of the bandgap.

The problem of limited bandwidth of hollow-core PBG fibers seems to be solved by the introduction of ultra-large bandwidth hollow-core all-silica Bragg PBG fibers with nano-supports. These fibers have not been commercialized and their dispersion properties have not been discussed in the literature yet.

In collaboration with researchers at Furukawa Electric Institute of Technology Ltd. and R&D Ultrafast Lasers Ltd., dispersion and loss properties of all-silica hollow core Bragg photonic bandgap fibers were investigated by the vector finite element method. As a first step, we investigated dispersive and loss properties of quarterwave, ultra-large bandwidth HC all-silica Bragg PBG fibers as a function of core diameter. One would expect that changing the core size affects both the bandwidth and dispersion of a Bragg fiber, since this parameter changes the effective “angle of incidence” of the fundamental mode. Computation of the dispersion profile was performed by using the Vector Finite Element Method (V-FEM) for solving the Helmholtz eigenvalue equation for the electric and magnetic field distributions on a HC Bragg PBG fiber cross section (see Fig. 2a). The dispersion was derived from the real part of the effective refractive indices ( $n_{eff}$ ) for a certain mode, which values correspond to the eigenvalues of the Helmholtz equation at a given wavelength. The confinement loss was obtained from the imaginary part of the propagation constant ( $\beta = (2\pi/\lambda) n_{eff}$ ). The effect of support bridges were not considered in our calculations (in practice, they increase the effective indices of the air layers by a value of 0.01-0.02).

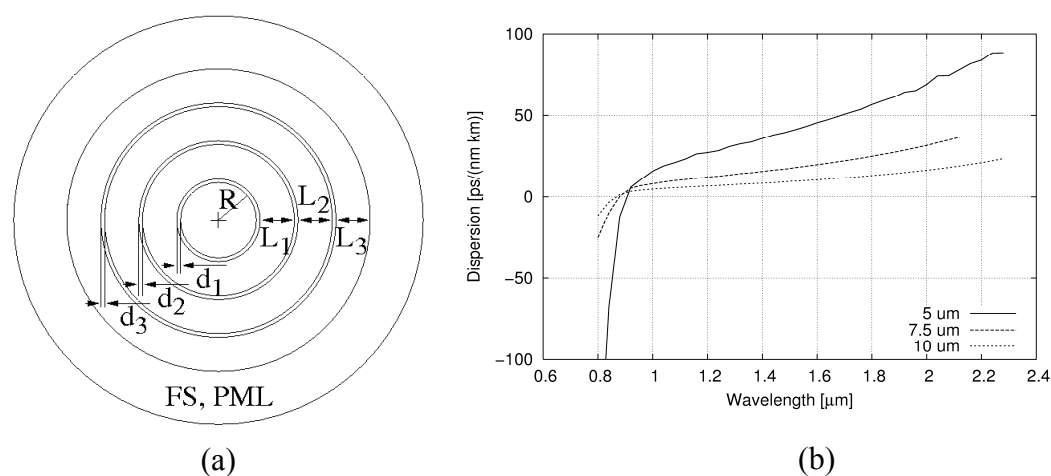


**Figure 2.** (a) Scheme of ultra-large bandwidth hollow-core all-silica Bragg fibers with nano-supports.  $d_1 = d_2 = d_3 = 370$  nm thick fused silica cladding layers,  $L_1 = L_2 = L_3 = 410$  nm thick air spacer cladding layers. (b) Computed dispersion of for different core diameters.  $R$  takes values of  $5 \mu m$ ,  $7.5 \mu m$  and  $10 \mu m$ .

In Fig. 2b, computed dispersion of ultra-large bandwidth HC Bragg PBG fibers of different core radii are plotted as the function of wavelength. The presented structures were designed for obtaining a bandgap around one micron. Based on the analogy between 1D and 2D PBG structures, physical thicknesses of the (high index) fused silica cladding layers and the (low index) air spacer layers we derived from the quarterwave condition at one micron.

As one would expect, each structure exhibits anomalous dispersion over most of the bandgap. We found that a higher core radius results in a broader photonic bandgap, a lower confinement loss and a lower dispersion slope, which can be explained by the increasing “angle of incidence” in case of an increasing core radius. Compared to standard HC PBG structures, these HC Bragg PBG fibers exhibit a considerably increased spectral bandwidth and lower dispersion slope, that could be well suited for broadband delivery and second order dispersion (GDD) control of femtosecond pulses. However, the designs presented in Fig. 2 do not allow cubic phase (third-order dispersion, TOD) control, which becomes very important in applications aiming for sub-50 fs performance.

Our recent studies show that the dispersion slope of the presented design can be varied by some structural modification, which in longer term offers a new alternative for distortion free delivery or dispersion control of ultra-broadband, or broadly tunable ( $\Delta\lambda > 200$  nm) high intensity optical pulses by means of pure microstructured optical fiber technology.

### **E-Mail:**

Ákos Bányász	banyasza@szfki.hu
Julia Fekete	feketej@sunserv.kfki.hu
Róbert Szipőcs	szipoecs@sunserv.kfki.hu

### **Grants and international cooperations**

- OTKA T-049296 Propagation of ultrashort laser pulses in photonic crystal fibers and fiber amplifiers (R. Szipőcs, 2005-2007)
- OTKA T-048725 Ultrafast linear and nonlinear processes in macromolecules (R. Szipőcs, 2005-2008)
- NKFP 0394/2004 National Research and Development Program – New, low dispersion acousto- and electrooptic devices for femtosecond pulse lasers (Sub-coordinator: R. Szipőcs, 2005-2006)
- NKFP1-00007/2005 National Research and Development Program – Femtobiology (Coordinator: R. Szipőcs, 2006-2008)

### **Contract**

- SZFKI-R&D Ultrafast Lasers Ltd contract on „Research and development of femtosecond pulse pump-probe spectroscopic system, (Coordinator: R. Szipőcs, 2006-2007)

### **Publications**

#### *Articles*

- P.1. Bányász Á, Keszei\* E; Nonparametric deconvolution of femtosecond kinetic data; *J Phys Chem A*; **110**, 6192-6207, 2006

- P.2. Gustavsson\* T, Bányász Á, Lazzarotto\* E, Markovitsi\* D, Scalmani\* G, Frisch\* MJ, Barone\* V, Improta\* R; Singlet excited-state behavior of uracil and thymine in aqueous solution: A combined experimental and computational study of 11 uracil derivatives; *J Am Chem. Soc*; **128**, 607-619, 2006
- P.3. Várallyay\* Z, Fekete J, Bányász Á, Szipőcs R; Optimizing input and output chirps up to the third order for sub-nanojoule, ultra-short pulse compression in small core area PCF; *Appl Phys B*; accepted for publication; available online, DOI: 10.1007/S00340-006-2484-7

#### ***Articles in Hungarian***

- P.4. Szipőcs R; Femtoszekundumos lézer- és parametrikus oszcillátorok femtobiológiai alkalmazásokhoz (Femtosecond pulse laser and parametric oscillators for applications in femtobiology, in Hungarian); *Magyar Tudomány*; **166**, 1535, 2005

#### ***Book chapter in Hungarian***

- P.5. Szipőcs R, Fekete J, Katona\* G, Rózsa\* B; Nemlineáris mikroszkópia és biológiai-orvosi alkalmazásai (Nonlinear microscopy and its application for biology and medicine, in Hungarian); In: *A kvantumoptikai és -elektronika legújabb eredményei*; ISBN 963 482 779 9, Eds. Heiner Zs., Osvay K, SZTE, pp. 166-174, 2006

#### ***Other***

- P.6. Rózsa\* B, Katona\* G, Vizi\* ES, Lukács\* A, Várallyay\* Z, Ságghy\* A, Valenta\* L, Maák\* P, Fekete J, Bányász Á, Szipőcs R; Real time 3D two-photon microscopy for neurology; *Technical Digest of Biomedical Optics Topical Meeting*, ISBN 1-55752-807-1, Paper TuI67, © Optical Society of America, 2006

## Q. OPTICAL THIN FILMS

*K. Ferencz*

**Optical thin film structures consisting of nanoscale laminated layers.** — We have continued our research concerning the development of optical thin film structures containing of nanooptically thick layers for advanced applications in laser physics and information technology. We have refined our new electron-beam deposition technology for producing of optical coatings containing nanooptically thick titania, silica, tantala, alumina, hafnia layers. Using needle-like optimization thin film design method, we have continued our research concerning the development of many kinds of ultrafast nanooptical coating systems – ultra-wide-band, low dispersion antireflection coatings, low dispersion beamsplitter coatings, ultrafast dichroic mirrors, wide-band output coupler mirrors, spectral shape filters for amplifiers, for example. Using the „OPTIMAC” optimization thin film design method, we have developed new type interference filter layer structures consisting of nanooptically thin metallic layers useful in the UV, VIS and IR spectral ranges. We have developed a reactive e-beam evaporation technology for producing electrically conductive and optically transparent oxide semiconductor layers, especially indium-tin-oxide (ITO) layers. Using our new deposition technology we have developed special type visible antireflection coatings having high reflectance for infrared radiation and microwaves.

**Other developments on optical coatings.** — Our work on ultrafast optical coatings is still in progress cooperating with the Max-Planck-Institute for Quantum Optics, Garching, Germany for many types of advanced applications in laser oscillators, amplifiers, autocorrelators, coherent X-ray generation, etc. We have developed small-scale optical manufacturing technology for producing of large size fused silica compensating wedges having a few tenths of millimeter minimal thicknesses. We have arranged a new optical coating laboratory infrastructure financed by company Optilab Ltd. in our campus, where a new optical coating machine type INTEGRITY 36, manufactured by the US company DENTON VACUUM will start its operation in the near future. Our new coating machine manifests the state-of-the-art optical coating technology, the combination of ion-assisted deposition technology, oil-free cryopumping and a sophisticated computer control system.

We have continued the development of integrated optical grating couplers for biotechnological application as a switching or sensing element using bacteriorhodopsin as nonlinear optical material. Using our microstructured coating samples new types of biologically active nanotechnological devices were developed in cooperation with the Biophysics Institute at the Szeged Biological Research Centre. Our work on interference filters is still in progress for high sensitivity detection of protein molecules elaborated by gene manipulation methods.

Based on our standard multiple-beam interference method for analysing optical coatings we have developed a new fast quantitative technique for analysing thin mineral oil films on water surfaces (project „Aquanal”). Using our CCD array spectrometer we have investigated the spreading phenomena of different kind of oil materials on water surfaces, and we have found that the equilibrium thicknesses of the oil films in many cases are much more thicker than the monolayer thicknesses are. We plan to continue our research in this field using new type oil samples to understand the details of the interaction between mineral oils and water surface. Based on our investigations we have developed optical multilayers useful as cheap sensors in oil contamination detection tasks.

These results were obtained in the frame of the scientific cooperation with the Optilab Ltd.

**E-Mail:**

Kárpát Ferencz      optilab@t-online.hu

**Contract**

OPTILAB-SZFKI No. 1908/2006

**Grants and international cooperations**

- NATO SfP 974262 Optoelectronic devices based on the protein bacteriorhodopsin (Coordinator: C.E. Wolf, Germany, participant: K. Ferencz, 2000-2006)
- NKFP3A/0005/2002 Nanobiotechnology: Elaborate a method to build nanotechnological devices for use in biology (Coordinator: P. Ormos, Szeged, participant: K. Ferencz, 2002-2007)
- NKFP3A/071/2004 Nanotechnological material modifications and their metrology (Coordinator: J. Gyulai, MTA MFA, participant: K. Ferencz, 2004-2007)
- NKFP3A/079/2004 On-site analysis of natural waters, geological media by micro- and nano-sensation methods („Aquanal”) (Coordinator: I. Bársony, MTA MFA, participant: K. Ferencz, 2004-2007)

## R. GROWTH AND CHARACTERIZATION OF OPTICAL CRYSTALS

*I. Földvári, L. Bencs, E. Beregi, G. Dravec<sup>#</sup>, V. Horváth, Á. Péter, K. Polgár, Zs. Szaller*

**Growth and study of nonlinear borate crystals.** — Ho-doped YAB single crystals were grown by the top-seeded flux method, and their high resolution absorption spectra were determined by Fourier Transform (FT) spectroscopy in the 4000-25000 $\text{cm}^{-1}$  spectral and 9-300K temperature ranges. The  $\text{Ho}^{3+}$  transitions from the  $^5\text{I}_8$  ground state, to the excited  $^5\text{I}_7$ ,  $^5\text{I}_6$ ,  $^5\text{I}_5$ ,  $^5\text{I}_4$ ,  $^5\text{F}_5$ ,  $^5\text{S}_2$ ,  $^5\text{F}_4$ ,  $^5\text{F}_3$ ,  $^5\text{F}_2$ ,  $^3\text{K}_8$ ,  $^5\text{F}_1+^5\text{G}_6$ , and  $^5\text{G}_5$  manifolds were identified. The unique feature of the 9 K spectra was the presence and resolution of the optical hyperfine structures of several electronic transitions related to the nuclear magnetic moment ( $I=7/2$ ) of the  $^{165}\text{Ho}$  isotope (example in Fig.1). This was due to the favorable combination of high crystal quality, homogeneous, tension free, single site lattice positions of the  $\text{Ho}^{3+}$  ions in YAB, and the extreme resolution ( $0.01\text{cm}^{-1}$ ) of the FT equipment.

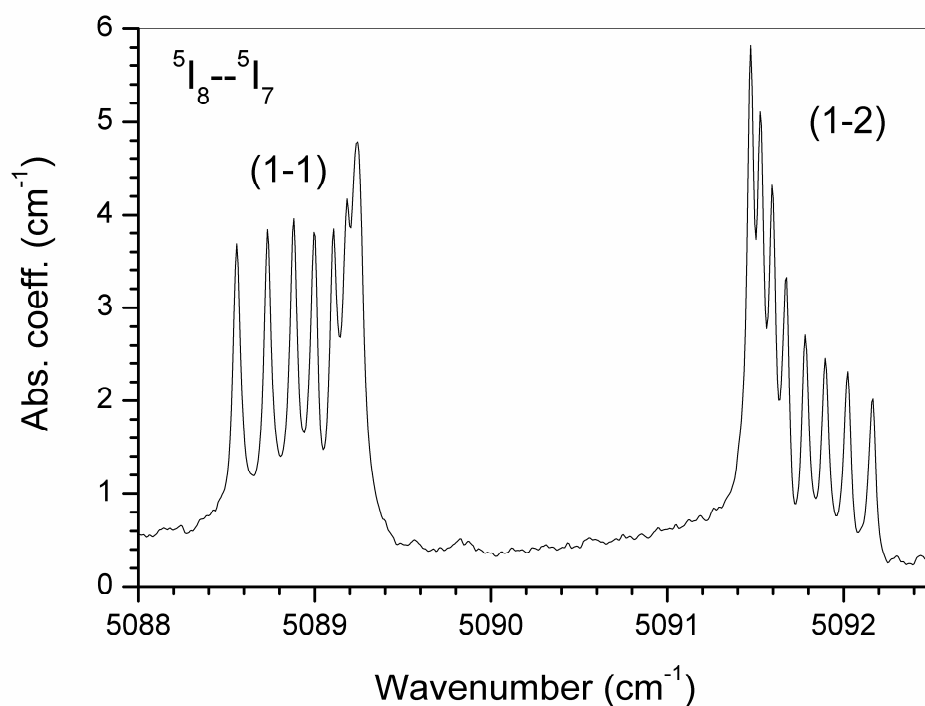


**Figure 1.** Optical hyperfine structure in selected range of the high resolution, low temperature spectra of YAB:Ho single crystal.

Luminescence spectra of YAB:Er crystals were determined in the ultraviolet-visible spectral and 10-300K temperature ranges. The dominant  $\text{Er}^{3+}$ -emission belonged to the  $^4\text{S}_{3/2} \rightarrow ^4\text{I}_{15/2}$  transition ( $\sim 18000\text{cm}^{-1}$ ). Its Stark components were assigned and found to be consistent with those derived from the absorption spectra and crystal field calculations. The temperature dependence and decay kinetics of the luminescence were in accordance with a phonon-assisted non-radiative energy loss model. After excitations to selected  $\text{Er}^{3+}$  levels other luminescence transitions were also detected. Among them the  $^4\text{F}_{7/2} \rightarrow ^4\text{I}_{13/2}$  and  $^2\text{H}_{11/2} \rightarrow ^4\text{I}_{13/2}$  transitions looked interesting since they terminated to an excited state.

<sup>#</sup> Ph.D. student

High resolution FT spectroscopy was applied to monitor the electron-phonon interaction in YAB single crystals doped with  $\text{Er}^{3+}$  and  $\text{Dy}^{3+}$  ions. The weak vibronic transition spectra were replicas of the rare-earth related zero phonon line series shifted by vibrational frequencies. The position, width and temperature dependence of the vibronic transitions could be described by two phonon Raman scattering model for both YAB:Er and YAB:Dy crystals. The electron-phonon interaction in this boron-oxygen structure was relatively strong, permitting to identify boron isotopic effects too.

**Growth and study of  $\text{LiNbO}_3$  single crystals with different compositions and doping.**

— Alkali metal oxide solvents (10mol% of  $\text{Na}_2\text{O}$ ,  $\text{K}_2\text{O}$ ,  $\text{Rb}_2\text{O}$  and  $\text{Cs}_2\text{O}$  with Li/Nb=1 host component ratio) were applied for the flux growth of stoichiometric  $\text{LiNbO}_3$  (sLN) single crystals. The crystallization temperature ranges were determined from differential scanning calorimetry measurements.  $\text{K}_2\text{O}$ ,  $\text{Rb}_2\text{O}$  and  $\text{Cs}_2\text{O}$  behaved as ideal solvents for  $\text{LiNbO}_3$ , and they did not enter into the lattice. The crystallization temperatures were nearly the same for  $\text{Rb}_2\text{O}$  and  $\text{Cs}_2\text{O}$  containing flux, and this resulted in similar composition and yield of the growing crystals.  $\text{K}_2\text{O}$  proved to be the best flux component providing the lowest crystallization temperature, the largest yield of sLN crystal, and  $\text{K}_2\text{O}$  was the only solvent, from which crystals of constant stoichiometric composition could be grown. The  $\text{Na}_2\text{O}$ -based flux behaved differently, incorporation of Na ions was detected in the crystal by chemical analysis, and the properties of these crystals were different. The crystallization temperature was higher for  $\text{Na}_2\text{O}$  based flux than for the others.

The  $\text{LiNbO}_3$  crystals grown from  $\text{Na}_2\text{O}$ ,  $\text{Rb}_2\text{O}$ , and  $\text{Cs}_2\text{O}$  containing fluxes were characterized by infrared and Raman spectroscopic methods, using the intensity ratio of two OH<sup>-</sup> absorption peaks at 3480 and 3465 $\text{cm}^{-1}$  in thermal equilibrium. This non-destructive method was accurate enough for the determination of the lithium content of pure  $\text{LiNbO}_3$  crystals grown from  $\text{Rb}_2\text{O}$  and  $\text{Cs}_2\text{O}$  containing flux, close to the stoichiometric composition (49.7–50.0mol%  $\text{Li}_2\text{O}$ ). From the remarkable differences of both infrared and Raman spectra of  $\text{LiNbO}_3$  crystals grown from  $\text{Na}_2\text{O}$  solvent, the incorporation of Na to Li sites was concluded.

The spectral width of Raman lines in lithium niobate was measured as a function of the cationic molar ratio, in a wide range from stoichiometric to sub-congruent (from 48.6 to 47 mol% Li) compositions. The broadening observed on the sub-congruent side followed the slopes of the congruent-to-stoichiometric range. The micro-Raman analysis permitted to characterize short-range heterogeneities ( $\mu\text{m}$  scale), such as growth striations in bulk crystals, or lithium out-diffusion in the surroundings of titanium-diffused waveguides, with a typical accuracy of 0.04 mol%.

Excitation and emission spectra at 4,2 K in the  $^5\text{D}_0 \rightarrow ^7\text{F}_0$ ,  $^7\text{F}_1$  spectral range were applied to monitor the  $\text{Eu}^{3+}$  sites in stoichiometric  $\text{LiNbO}_3$ :Eu crystals. 14 different  $\text{Eu}^{3+}$  centers were identified from the position of the Stark multiplets. These centers represented different lattice sites and related charge compensations. Excitation and emission spectra of Tb and Eu double doped congruent  $\text{LiNbO}_3$  crystals were determined in the 200-700nm range, at room temperature (RT) and 12K. The 12K emission from the  $\text{LiNbO}_3$ :Tb,Eu crystal under light excitation at 485nm ( $^7\text{F}_6 \rightarrow ^5\text{D}_4$  Tb-absorption), besides the Tb-related lines, contained also the  $^5\text{D}_0 \rightarrow ^7\text{F}_4$  (705nm) and  $^5\text{D}_0 \rightarrow ^7\text{F}_1$  (625m) Eu-emissions. The 12K excitation spectra clearly indicated that the  $^5\text{D}_0 \rightarrow ^7\text{F}_4$  emission could be excited at both Tb and Eu absorption lines. Tb  $\rightarrow$  Eu energy transfer occurred in this material since the  $^5\text{D}_4 \rightarrow ^7\text{F}_4$  terbium emission overlaps the  $^7\text{F}_0 \rightarrow ^5\text{D}_0$  absorption of the europium ions.

**Growth and study of bismuth tellurite ( $\text{Bi}_2\text{TeO}_5$ ) and bismuth germanate crystals.** — Optical absorption spectra of  $\text{Ho}^{3+}$  in Czochralski grown  $\text{Bi}_2\text{TeO}_5$ :Ho single crystals were

monitored in the 4500-25000cm<sup>-1</sup> spectral and 9-300K temperature ranges by FT spectroscopy. In the spectra thirteen manifolds were identified with their Stark components from the <sup>5</sup>I<sub>8</sub> ground to the excited <sup>5</sup>I<sub>7</sub>, <sup>5</sup>I<sub>6</sub>, <sup>5</sup>I<sub>5</sub>, <sup>5</sup>I<sub>4</sub>, <sup>5</sup>F<sub>5</sub>, <sup>5</sup>S<sub>2</sub>+<sup>5</sup>F<sub>4</sub>, <sup>5</sup>F<sub>3</sub>, <sup>5</sup>F<sub>2</sub>, <sup>3</sup>K<sub>8</sub>, <sup>5</sup>F<sub>1</sub>+<sup>5</sup>G<sub>6</sub>, and <sup>5</sup>G<sub>5</sub> levels. Crystal field calculations indicated that the Ho-Bi substitution takes place mostly at the Bi(1) site. The strong anisotropy of the polarized absorption spectra was consistent with the low symmetry of these lattice sites. Three characteristic emissions were observed in the room temperature luminescence spectra corresponding to the <sup>5</sup>F<sub>3</sub>→<sup>5</sup>I<sub>8</sub>, <sup>5</sup>F<sub>5</sub>→<sup>5</sup>I<sub>8</sub>, and <sup>5</sup>I<sub>4</sub>→<sup>5</sup>I<sub>8</sub> transitions, after any excitation to higher energy Ho<sup>3+</sup> levels. The Judd-Ofelt calculations provided similar oscillator strength values to those obtained from the polarized absorption spectra. The Judd-Ofelt parameters were used for calculating the spontaneous emission probabilities. The <sup>5</sup>I<sub>7</sub>→<sup>5</sup>I<sub>8</sub> and <sup>5</sup>F<sub>4</sub>→<sup>5</sup>I<sub>8</sub> transitions have high branching ratios and emission probabilities allowing the possibility of laser action in the Bi<sub>2</sub>TeO<sub>5</sub>:Ho single crystal.

Bi<sub>4</sub>Ge<sub>3</sub>O<sub>12</sub> (eulytine) and Bi<sub>12</sub>GeO<sub>20</sub> (sillenite) single crystals were irradiated with various fluencies of high energy (1.7 and 0.35MeV) O, Ne, Ar, Kr, Xe and Pb ions originated from cyclotron. The ion-induced tracks were monitored by Rutherford backscattering method in channeling geometry. The track sizes were systematically smaller for the 1.7MeV than for 0.35MeV irradiation in both crystals. The experimental threshold electronic stopping power values were in good agreements with the model predictions using the basic material parameters.

**Application of analytical methods for optical crystals and other media.** — Simultaneous, multi-element graphite furnace atomic absorption spectrometry (GFAAS) method was developed for the determination of As, Cd, Cr, Cu and Pb content in honey samples. Using the best chemical modifier (Pd(NO<sub>3</sub>)<sub>2</sub>-Mg(NO<sub>3</sub>)<sub>2</sub>), the matrix effect of honey could strongly be suppressed for Cr and Pb, and reduced for As, Cd and Cu.

The influence of heating systems on the transport and deposition of particulate pollution was investigated in churches located in cold climate by energy dispersive X-ray fluorescence and electron probe X-ray microanalysis. The hot-air blow heating was found to be the most dangerous for the art works and plaster, while the use of electrically heated pews and electrical heaters was less problematic.

Low-pressure gas chromatography - ion trap mass spectrometry (LPGC-ITMS) method was developed to shorten the analysis time for 18 US Environmental Protection Agency priority listed polycyclic aromatic hydrocarbons (PAHs). The method was applied to monitor these PAHs in gas and aerosol samples collected in the ambient air during different seasons at six different locations in Northern Belgium. The PAH concentrations varied significantly, from 17 ng/m<sup>3</sup> at a rural site to 114 ng/m<sup>3</sup> near a petroleum harbour and industry, and showed relation to anthropogenic activities. The results showed that the vehicular emission was a major source of PAHs in Flanders.

## E-Mail

László Bencs	bencs@szfki.hu
Elena Beregi	beregi@szfki.hu
Gabriella Dravecz	dravecz@szfki.hu
István Földvári	foldvari@szfki.hu
Valentina Horváth	hvalen@szfki.hu
Ágnes Péter	apeter@szfki.hu
Katalin Polgár	polgar@szfki.hu

## Grants and international cooperations

- OTKA T-046481 Growth and spectroscopic investigation of self-frequency-doubling laser crystals (I. Földvári, 2004-2007)
- OTKA T-046667 Materials and systems for high density data recording (E. Lőrincz (BME) and I. Földvári, 2004-2006)
- COST Action P8 Materials and Systems for Optical Data Storage and Processing (H.-J. Eichler, Hungarian leader I. Földvári, 2002-2006). Multinational EC program
- HAS-DFG bilateral project. Multiplexed volume holographic data storage in bismuth tellurite crystals ( $\text{Bi}_2\text{TeO}_5$ ) using nanosecond laser pulses (I. Földvári, 2005 – 2007). Partner: Westfälische Wilhelms-Universität, Münster
- HAS-Polish Academy bilateral cooperation program. Growth and spectroscopic investigation of rare-earth-doped nonlinear optical crystals (I. Földvári, 2005-2007). Partner: Institute of Low Temperature and Structure Research, PAS, Wrocław
- HAS - CNR Bilateral Cooperation Program. Growth and spectroscopic investigation of self-frequency-doubling laser crystals (I. Földvári, 2004-2006). Partner: Università di Parma
- Hungarian - Italian Intergovernmental S & T Cooperation Programme. Growth and FTIR spectroscopy of optical crystals (L. Kovács, contributor I. Földvári, 2004-2007). Partner: Università di Parma.
- HAS-Russian Academy of Sciences Project No. 26. Materials for solid state lasers and stimulated Raman emission (K. Polgár, 2005-2007). Partner: General Physics Institute, RAS, Moscow.
- HAS-Russian Academy Project 25. Investigation of crystal defects in broad forbidden band crystals (J. Janszky, contributor K. Polgár, 2005-2007). Partner: Joffe Phys. Techn. Institute, RAS, St.Petersburg.
- Bilateral cooperation with University of Metz, MOPS, IUT St.-Avold, Common research on non-linear crystals and joint Ph.D. programs (K. Polgár and Á. Péter, 1999-open-end)

## Publications:

### Articles

- R.1. Franke\* I, Talik\* E, Roleder\* K, Polgár K, Salvestrini\* JP, Fontana\* MD; Temperature stability of elastic and piezoelectric properties of  $\text{LiNbO}_3$  single crystals; *J Phys D Appl Phys*; **38**, 4308-4312, 2005
- R.2. Divall\* M, Osvay\* K, Kurdi\* G, Divall\* EJ, Klebniczki\* J, Bohus\* J, Péter Á, Polgár K; Two-photon-absorption of frequency converter crystals at 248 nm; *Appl Phys B*; **81**, 1123-1126, 2005
- R.3. Szenes\* G, Fink\* D, Klaumünzer\* S, Pászti F\*, Péter Á; Ion-induced track in  $\text{Bi}_4\text{Ge}_3\text{O}_{12}$  and  $\text{Bi}_{12}\text{GeO}_{20}$  crystals; *Nucl Instr Meth Phys Res B*; **245**, 243-245, 2006
- R.4. Ravindra\* K, Bencs L, Wauters\* E, de Hoog\* J, Deutsch\* F, Roekens\* E, Bleux\* N, Berghmans\* P, Van Grieken\* R; Seasonal and site specific variation in vapour and

- aerosol phase polycyclic aromatic hydrocarbons over Flanders (Belgium) and their relation with anthropogenic activities; *Atmosph Environ*; **40**, 771-785, 2006
- R.5. Dravecz G, Péter Á, Polgár K, Kovács L; Alkali metal oxide solvents in the growth of stoichiometric LiNbO<sub>3</sub> single crystals; *J Cryst Growth*; **286**, 334-337, 2006
- R.6. Zhang\* Y, Guilbert\* L, Bourson\* P, Polgár K, Fontana\* MD; Characterization of short range heterogeneities in sub-congruent lithium niobate by micro-Raman spectroscopy; *J Phys Condens Matter*; **18**, 957-963, 2006
- R.7. Ravindra\* K, Godoi\* AFL, Bencs L, Van Grieken\* R; Low-pressure gas chromatography - ion trap mass spectrometry for the fast determination of polycyclic aromatic hydrocarbons in air samples; *J Chromatogr A*; **1114**, 278-281, 2006
- R.8. Földvári I, Baraldi\* A, Capelletti\* R, Magnani\* N, Sosa\* RF, Munoz\* AF, Kappers\* LA, Watterich A; Optical absorption and luminescence of Ho<sup>3+</sup> ions in Bi<sub>2</sub>TeO<sub>5</sub> single crystals; *Opt Mater*; accepted for publication
- R.9. Ajtony\* Zs, Bencs L, Haraszti\* R, Szigeti\* J, Szoboszlai\* N; Study of the simultaneous determination of some essential and toxic trace elements in honey by multielement graphite furnace atomic absorption spectroscopy; *Talanta*; accepted for publication
- R.10. Spolnik\* Z, Worobiec\* A, Samek\* L, Bencs L, Belikov\* K, Van Grieken\* R; Influence of different types of heating systems on particulate air pollutant deposition: the case of churches situated in a cold climate; *J Cultur Herit*; accepted for publication
- R.11. Földvári I, Beregi E, Solarz\* P, Dominiak-Dzik\* G, Ryba-Romanowski\* W, Watterich A; Luminescence of YAB:Er single crystal; *Phys Stat Sol (c)*; accepted for publication
- R.12. Baraldi\* A, Földvári I, Capelletti\* R, Magnani\* N, Mazzera\* M, Beregi E; High resolution FTIR absorption study of holmium doped yttrium aluminum borate single crystals; *Phys Stat Sol (c)*; accepted for publication
- R.13. Mazzera\* M, Baraldi\* A, Capelletti\* R, Beregi E, Földvári I; Electron - phonon interaction in Er and Dy doped YAl<sub>3</sub>(BO<sub>3</sub>)<sub>4</sub> single crystals; *Phys Stat Sol (c)*; accepted for publication
- R.14. Alvarez\* E, Sosa\* R, Földvári I, Polgár K, Péter Á, Munoz\* A; Co-emission of Tb<sup>3+</sup> and Eu<sup>3+</sup> ions in LiNbO<sub>3</sub>:Tb,Eu single crystals; *Phys Stat Sol (c)*; accepted for publication
- R.15. Dravecz G, Kovács L, Péter Á, Polgár K, Bourson\* P; Raman and IR spectroscopic characterization of LiNbO<sub>3</sub> crystals grown from alkali metal oxide solvents; *Phys Stat Sol (c)*; accepted for publication
- R.16. Kapljanskii\* AA, Kapphan\* E, Kutsenko\* AB, Polgár K, Skvortsov\* AP; Multitude of Eu centers in stoichiometric lithium niobate crystals; *Techn Phys Lett*; accepted for publication

### **Conference proceedings**

- R.17. Ravindra\* K, Bencs L, Wauters\* E, de Hoog\* J, Deutsch\* F, Roekens\* E, Bleux\* N, Berghmans\* P, Van Grieken\* R; Concentration trends and sources of polycyclic aromatic hydrocarbons (PAHs) in Belgium; In: *Proc. 4<sup>th</sup> Asian Aerosol Conference, AAC-2005, December 2005, Mumbai, India*; Ed.: H.S. Kuswaha, IASTA Bulletin; **17**, pp. 98-99, 2005
- R.18. Van Grieken\* R, Kontozova\* V, Godoi\*, R.H.M, Spolnik\* Z, Worobiec\* A, Deutsch\* F, Bencs L; Some studies of the effect of indoor and outdoor pollutants on cultural heritage items; In: *Proc First International Conference on Air Pollution & Combustion, June 2005, Ankara, Turkey*; pp. 1-11, 2005
- R.19. Dafinei\* I, Diemoz\* M, Fasoli\* M, Földvári I, Longo\* E, Moretti\* F, Péter Á, Somma\* F, Vedda A; TeO<sub>2</sub> scintillating crystals growth and properties; In: *Proc 8th Int Conf on Inorganic Scintillators and their use in Scientific and Industrial Applications, SCINT2005, September, 2005, Alushta, Ukraine*; Eds.: A. Getkin and B. Grinyov; pp. 106-108, 2006

### **Book chapters**

- R.20. Bencs L, Ravindra\* K, Van Grieken\* R; Spatial and temporal variation of anthropogenic palladium in the environment, In: *Palladium Emissions in the Environment: Analytical Methods, Environmental Assessment and Health Effects*; Eds.: F. Zereini and F. Alt, Springer, Berlin; pp. 433-454, 2006
- R.21. Bencs L, Ravindra\* K, Van Grieken\* R; Determination of ultra-trace levels of palladium in environmental samples by graphite furnace atomic spectrometry techniques, In: *Palladium Emissions in the Environment: Analytical Methods, Environmental Assessment and Health Effects*; Eds.: F. Zereini and F. Alt, Springer, Berlin; pp. 173-189, 2006

### **Other**

- R.22. Földvári I: A kristálytan szerepe a lézerek alkalmazásában (The role of crystallography in laser applications, in Hungarian); *ACTA Geographica ac Geologica et Meteorologica Debrecina*; accepted for publication

**See also: K.7., S.9., S.12., S.13.**

## S. CHARACTERIZATION AND POINT DEFECT STUDIES OF OPTICAL CRYSTALS

*L. Kovács, I. Bányász, G. Corradi, I. Hajdara<sup>#</sup>, E. Hartmann, K. Lengyel, L. Malicskó, G. Mandula, A. Watterich*

**Microscopic studies of planar defects in YAB crystals.** — On as-grown {110} type prism habit faces of both undoped and doped yttrium aluminium borate –  $\text{YAl}_3(\text{BO}_3)_4$ , YAB – single crystals microscopic rectilinear surface configurations, unknown earlier, were found and studied using optical and scanning electron microscopy. They were crystallographically oriented parallel to the edges between the {101} type pyramid and the {110} type prism faces and seemed to be surface traces of near-surface inner microcracks or intergrowth layers.

**Investigation of defects in  $\text{LiNbO}_3$  single crystals.** —  $\text{LiNbO}_3:\text{Mg}$  crystals doped with 0-8 mol% Mg with stoichiometric, intermediate and congruent compositions were systematically investigated by Raman spectroscopy. The damping of the  $\text{E}(\text{TO}_3)\text{-E}(\text{TO}_9)$  and  $\text{A}_1(\text{TO}_1)\text{-A}_1(\text{TO}_4)$  phonon modes was found to be very sensitive for the characterization of the crystal composition. For a given Li/Nb ratio, the change in the Mg concentration dependence of the Raman band parameters determines the same photorefractive threshold concentration as that concluded from IR and UV spectroscopic measurements. For high Mg concentrations the appearance of  $\text{Mg}_4\text{Nb}_2\text{O}_9$  defect clusters was shown.

Using the new interatomic potential determined for the undoped  $\text{LiNbO}_3$  crystal, solution energies for  $\text{M}^{2+}$  and  $\text{M}^{3+}$  dopant metal ions were calculated. A number of possible doping schemes were found depending on both the dopant ion and the temperature.

**Holography in  $\text{LiNbO}_3$  crystals and silver halide emulsions.** — We proposed and investigated a novel application of the thermal fixing of photorefractive holographic scattering in  $\text{LiNbO}_3$ . For thick dehydrated crystal samples with high photorefractive gain the effect helps to determine the hydrogen concentration  $N_H$ . The method uses the thermal dark decay times of the small-angle and the  $90^\circ$  scattering components. A cross-section  $\sigma = \alpha/N_H = (2.1 \pm 0.4) \times 10^{-19} \text{ cm}^2$  was determined, where  $\alpha$  is the maximum absorbance of the  $\text{OH}^-$  vibrational band at 2870 nm for ordinarily polarized light.

We studied the build-up of holographic gratings in Fe-doped  $\text{LiNbO}_3$  crystals for various grating constants and fringe visibilities, using interference microscopy. The experimental setup has been improved by attaching a PC-controlled digital photographic camera to the microscope.

Higher-order nonlinearities of holographic phase gratings recorded in silver halide emulsions and processed applying various schemes have been determined using Fourier-analysis of high-resolution phase contrast micrographs. These results make it possible to compare the processing schemes. The presence of a fourth-order harmonic in heavily modulated silver halide phase gratings, predicted by Slinger and Solymar, has been observed directly.

**Spectroscopy of other ferroelectric oxide crystals.** — The composition of potassium lithium niobate (KLN) crystals have been characterised by ultraviolet (UV) and infrared absorption spectroscopy completed by dielectric measurements. The UV absorption edge

---

<sup>#</sup> Ph.D. student

shifts to lower wavelengths with decreasing Nb content, independently of the K/Li ratio of the crystal, while the ratio of the intensities of the OH<sup>-</sup> stretching vibrational bands at about 3440 cm<sup>-1</sup> and 3520 cm<sup>-1</sup> depends on the K/Li ratio as well. The Curie temperature of the crystals and ceramics depends considerably on the Nb content, and slightly on the K/Li ratio. So the real crystal composition can be obtained combining all three methods.

The newly synthesized single-crystal relaxor ferroelectric Pb<sub>0.78</sub>Ba<sub>0.22</sub>Sc<sub>0.5</sub>Ta<sub>0.5</sub>O<sub>3</sub> compound has been studied by Raman and optical spectroscopies. The addition of Ba shifts the optical absorption edge to lower energies and gives rise to extra absorption peaks at 460 nm and 730 nm, the latter originating from electronic transitions in the ferroic species.

**Photochromism of gallium garnets.** — Terbium gallium garnet (TGG, Tb<sub>3</sub>Ga<sub>5</sub>O<sub>12</sub>) and its doped variants are magneto-optic materials for high-power applications. In order to understand the photochromic effect in TGG doubly doped with calcium and cerium, the spectral and kinetic properties of absorption changes induced by heating and irradiation have been characterised. Based on the findings it has been concluded that the photochromic band at 420 nm originates from defects involving Tb<sup>4+</sup>. Previously this band was attributed to Ce<sup>3+</sup>. Two possible models have been suggested and discussed, both of which are in agreement with the obtained experimental results.

The centrosymmetric gadolinium gallium garnet (GGG, Gd<sub>3</sub>Ga<sub>5</sub>O<sub>12</sub>) doped with calcium has also been found to be photosensitive. Mixed absorption and refractive index gratings can be recorded over a wide range of wavelengths in the visible spectral range. Charge transfer processes between complex color centers and F-centers may be responsible for the photochromic phenomena in GGG. However, the reason of the light-induced symmetry loss (i.e. the appearance of the photorefractive effect) is not yet known.

**Spectroscopy of Cu centres in lithium tetraborate single crystals.** — The spectroscopic properties of Cu centres in single crystals of the excellent neutron detector and tissue-equivalent thermoluminescent dosimeter material, Li<sub>2</sub>B<sub>4</sub>O<sub>7</sub>:Cu, have been characterised by EPR and also by time-resolved luminescence methods using synchrotron radiation and Xe flash lamp pulses. The two methods yielded complementary information on the incorporation and the electronic structure of paramagnetic Cu<sup>2+</sup> centres and luminescent Cu<sup>+</sup> centres, both involved in the electronic processes under ionising radiation.

**Hydroxyl ions in scheelite type crystals.** — The presence of hydroxyl ions has been detected for the first time in as-grown scheelite type molybdate and tungstate crystals. A number of stretching vibrational bands were observed in PbMoO<sub>4</sub> and BaWO<sub>4</sub> crystals at 8 K, while only very weak OH<sup>-</sup> absorption was found in CaMoO<sub>4</sub>, SrMoO<sub>4</sub> and SrWO<sub>4</sub> in the 3200 – 3600 cm<sup>-1</sup> wavenumber range. The anharmonicity of the stretching modes for all bands in PbMoO<sub>4</sub> and BaWO<sub>4</sub> was found to be in agreement with that observed in other oxides. The similarities of the spectra in those two crystals and the polarization dependence measurements allowed us to draw some conclusions about the possible lattice sites of hydroxyl ions in scheelite crystals.

**Investigation of X-ray storage phosphors and scintillators.** — In luminescence studies of a new generation of X-ray storage phosphors, expected to provide higher spatial resolution and low dose requirements for medical and industrial X-ray imaging applications, the luminescence properties of various Ce-doped single crystalline and nanocrystalline barium halides have been compared. The photostimulated luminescence of BaBr<sub>2</sub>:Ce single crystals, shown to be at least as efficient as that of commercially used BaFBr:Eu storage phosphors, was found to be mainly related to background oxygen and alkali impurities, the latter impurities being also active in the case of BaCl<sub>2</sub>:Ce.

**Design and fabrication of diffractive optical elements and waveguides by ion implantation.** — Waveguiding at visible (633 nm) and near IR (up to 1.2  $\mu\text{m}$ ) wavelength in buried channel waveguides in tellurite glass samples fabricated by implantation of 1.5 MeV  $\text{N}^+$  ions has been demonstrated for the first time. A 3D guiding effect is also confirmed observing a good confinement for the green up-conversion emission obtained by pumping the  $\text{Er}^{3+}$  ions at 977.8 nm along the waveguide. We also recorded buried channel waveguides in  $\text{Bi}_{12}\text{GeO}_{20}$  samples via implantation of 1.5 MeV  $\text{N}^+$  ions.

**History of science.** — The main accomplishments of the Gyulai-Tarján school were summarized. In the fifties Z. Gyulai obtained for the tensile strength of whiskers a value as high as the theoretical one for perfect crystals. The paper of I. Tarján (1966) about the growth of alkali halide crystals of high purity proved to be the most cited one in the journal “Kristall und Technik”. Hungarian crystal growers wrote the book “*Laboratory Manual on Crystal Growth*” (in 1972), “which should be in the hands of all teachers and students of crystal growth” according to C.W. Bunn. The pamphlet “*An Introduction to Crystal Physics*”(1984) was written for the Teaching Commission of IUCr.

### **E-Mail:**

István Bányász	banyasz@szfki.hu
Gábor Corradi	corradi@szfki.hu
Ivett Hajdara	hajdara@szfki.hu
Ervin Hartmann	hartmann@szfki.hu
László Kovács	lkovacs@szfki.hu
Krisztián Lengyel	klengyel@szfki.hu
Gábor Mandula	mandula@szfki.hu
László Malicskó	malicsko@szfki.hu
Andrea Watterich	watter@szfki.hu

### **Grants and international cooperations**

- OTKA T 037669 Geometrical, vibrational and electronic structure of borate crystals and their defects (A. Watterich, 2002-2006)
- OTKA T 047265 Photo- and neutronrefractive materials and phenomena (L. Kovács, 2004-2007)
- OTKA K 60086 Spectroscopic studies of photon-induced electron transport for data handling and medical applications (G. Corradi, 2006-2009)
- TÉT Italian-Hungarian Intergovernmental S & T Cooperation (I-46/03): Growth and FTIR spectroscopy of optical crystals (L. Kovács, 2004-2007)
- TÉT Italian-Hungarian Intergovernmental S & T Cooperation (I-15/03): Fabrication of active and passive integrated optical elements and devices by ion beam implantation (I. Bányász, 2004-2007)
- HAS – Polish Academy of Sciences joint project: Structure of real crystals (A. Watterich, 2005-2007)
- HAS – Estonian Academy of Sciences joint project: Electronic paramagnetic resonance and time-resolved luminescence spectroscopy of oxyanionic crystals (A. Watterich, 2004-2006)
- HAS – CNR joint project: Growth and spectroscopic investigation of self-frequency-doubling laser crystals (I. Földvári, contributor L. Kovács, 2004-2006)

HAS – Polish Academy of Sciences joint project: Growth and spectroscopic investigation of rare- earth-doped nonlinear optical crystals (I. Földvári, contributor L. Kovács, 2005-2007)

COST Action P8. Materials and Systems for Optical Data Storage and Processing (H.-J. Eichler (Berlin), Hungarian leader I. Földvári, contributor L. Kovács 2002-2006)

## Publications

### Articles

- S.1. Bányász I; Fourier analysis of high spatial frequency holographic phase gratings; *J Modern Optics*; **52**, 2443-2451, 2005
- S.2. Selling\* J, Corradi G, Secu\* M, Schweizer\* S; Comparison of the luminescence properties of the x-ray storage phosphors BaCl<sub>2</sub>:Ce<sup>3+</sup> and BaBr<sub>2</sub>:Ce<sup>3+</sup>; *J Phys: Condens Matter*; **17**, 8069-8078, 2005
- S.3. Bányász I; Higher-order harmonics in bleached silver halide holograms; *Optics and Lasers in Engineering*; **44**, 926-942, 2006
- S.4. Bányász I; Comparison of the effects of two bleaching agents on the recording of phase holograms in silver halide emulsions; *Optics Communications*; **267**, 356-361, 2006
- S.5. Marinova\* V, Mihailova\* B, Malcherek\* T, Paulmann\* C, Lengyel K, Kovács L, Veleva\* M, Gospodinov\* M, Güttler\* B, Stosch\* R and Bismayer\* U; Structural, optical and dielectric properties of relaxor-ferroelectric Pb<sub>0.78</sub>Ba<sub>0.22</sub>Sc<sub>0.5</sub>Ta<sub>0.5</sub>O<sub>3</sub>; *J Phys: Condens Matter*; **18**, L385-L393, 2006
- S.6. Dachraoui\* H, Rupp\* RA, Lengyel K, Ellabban\* MA, Fally\* M, Corradi G, Kovács L, Ackermann\* L; Photochromism of doped terbium gallium garnet; *Phys Rev B*; **74**, 144104/1-11, 2006
- S.7. Ellabban\* MA, Fally\* M, Rupp\* RA, Kovács L; Light-induced phase and amplitude gratings in centrosymmetric gadolinium gallium garnet doped with calcium; *Optics Express*; **14**, 593-602, 2006.
- S.8. Araujo\* RM, Amaral\* JB, Jackson\* RA, Valerio\* MG, Lengyel K, Kovács L; Computer modelling of substitutional defects and optical properties of the ferroelectric and paraelectric phases of LiNbO<sub>3</sub>; *phys stat sol (c)*; accepted for publication
- S.9. Hajdara I, Lengyel K, Dravecz G, Kovács L, Péter Á, Polgár K; Spectroscopic methods for the determination of the composition of potassium lithium niobate crystals; *phys stat sol (c)*; accepted for publication
- S.10. Corradi G, Watterich A, Polgár K, Nagirnyi\* V, Hofstaetter\* A, Rakitina\* LG, Meyer\* M; EPR of Cu<sup>2+</sup> in lithium tetraborate single crystals; *phys stat sol (c)*; accepted for publication

- S.11. Nagirnyi\* V, Kotlov\* A, Corradi G, Watterich A, Kirm\* M; Electronic transitions in  $\text{Li}_2\text{B}_4\text{O}_7:\text{Cu}$  single crystals; *phys stat sol (c)*; accepted for publication
- S.12. Lengyel K, Kovács L, Péter Á, Polgár K, Corradi G, Bourson\* P; The effect of Mg doping on the Raman spectra of  $\text{LiNbO}_3$  crystals; *phys stat sol (c)*; accepted for publication
- S.13. Kovács L, Péter Á, Ivleva\* LI, Baraldi\* A, Capelletti\* R; Hydroxyl ions in scheelite type molybdates and tungstates; *phys stat sol (c)*; accepted for publication
- S.14. Mandula G, Ellabban\* MA, Fally\* M; A method to determine  $\text{H}^+$  concentration in dehydrated iron doped lithium niobate using photorefractive beam fanning effect; *Ferroelectrics*; accepted for publication

### **Conference proceedings**

- S.15. Mandula G, Rupp\* RA, Balaskó\* M; Erasure of elementary holograms in  $\text{LiNbO}_3:\text{Fe}$  by neutron irradiation; In: *Proc. of Holography 2005, International Conference on Holography, Optical Recording, and Processing of Information, Varna, Bulgaria, 21-25 May 2005*; Eds.: Yury Denisyuk, Ventseslav Sainov, Elena Stoykova, SPIE, Bellingham, Washington, USA, Proceedings of SPIE; **6252**; 62520N/1-5, 2006
- S.16. Bánász I, Mandula G; Direct microscopic observation of hologram build-up in photorefractive crystals; In: *Proc. of Holography 2005, International Conference on Holography, Optical Recording, and Processing of Information, Varna, Bulgaria, 21-25 May 2005*; Eds.: Yury Denisyuk, Ventseslav Sainov, Elena Stoykova, SPIE, Bellingham, Washington, USA, Proceedings of SPIE; **6252**; 625209/1-6, 2006
- S.17. Selling\* J, Corradi G, Secu\* M, Schweizer\* S; Rare earth doped barium halide x-ray storage phosphors and scintillators; In: *Proc. of the Eighth International Conference on Inorganic Scintillators and their Use in Scientific and Industrial Applications (SCINT2005), Alushta, Crimea, Ukraine, 19-23 September, 2005*; Eds. Gektin A, Grinyov B; National Academy of Sciences of Ukraine, Kharkov; pp. 415-418, 2006

**See also: R.5., R.8., R.11., R.15.**

## T. NONLINEAR AND QUANTUM OPTICS

*P. Ádám, J. Asbóth<sup>#</sup>, P. Domokos, A. Gábris<sup>#</sup>, J. Janszky, A. Kárpáti, Zs. Kis, T. Kiss, M. Koniorczyk, Z. Kurucz<sup>#</sup>, D. Nagy<sup>#</sup>, V. Szalay, G. Tóth, A. Vukics<sup>#</sup>*

**Laser-induced dynamics of atoms, cavity QED.** – A gas of linearly polarizable particles transversely pumped by an off-resonant laser and interacting with the counterpropagating radiation modes of a ring cavity was studied. Depending on the pump intensity and the detunings the gas can form a self-organized density grating that enhances the feeding of the cavity. We investigated the system via a mean-field approach and found the thermodynamic phases of (i) uniform distribution, (ii) self-organized Bragg lattice, (iii) lattice with defects, and (iv) instability. The occurrence of these phases as a function of the pump intensity and atom density is fully mapped.

Recently we have developed efficient schemes for the quantum control of degenerate multi-state atomic systems. However, in a real experiment it is necessary to verify the prepared quantum state. Therefore, we have proposed a quantum state reconstruction procedure for retrieving the quantum state of a degenerate multi-state system, in particular the quantum states in Zeeman manifolds. The scheme is based on a coherent pumping technique, in which the initial state space is coupled to excited states by an elliptically polarized laser pulse: due to spontaneous emission the system relaxes into the dark states defined by the filter laser and into some other states outside the initial state space. The population pumped into the dark subspace is measured in a subsequent step. It is shown for a system with total angular momentum of  $J=2$ , that by varying the polarization state of the filter laser, the initial quantum state of the system can be retrieved from the measured populations with high fidelity.

The time-evolution operator of open quantum systems is determined generally via a stochastic operator sum representation. Quantum trajectories originating from any quantum trajectory method applicable to the system can be used for the construction. The result does apply to non-Markovian systems as well. The computational time reduction is in the order of the dimension of the Hilbert space compared to conventional quantum trajectory methods combined with algebraic reconstruction of the map. To demonstrate the efficiency of the method, the effects of decoherence are analysed for a C-NOT gate realized by two atoms in a cavity.

**Quantum information, entanglement and teleportation.** – We have considered translationally invariant states of an infinite one-dimensional chain of qubits or spin-1/2 particles. We have maximized the entanglement shared by nearest neighbors via a variational approach based on finitely correlated states. We have found an upper bound of nearest-neighbor concurrence very close to the conjectured maximum value known from the literature, and described the entanglement properties of the quantum state.

We investigated the dynamical features of iterated deterministic quantum maps which describe the measurement-induced conditional dynamics of one- and two qubit systems and which have been proposed recently in the context of quantum information. These qubit systems do not have a (trivial) classical limit. We presented a one-qubit scheme where the equation governing the time evolution is a complex-valued nonlinear map with one complex parameter. In contrast to the usual notion of quantum chaos, exponential sensitivity to the initial state occurs here. We calculated analytically the Lyapunov exponent based on the overlap of quantum states, and found that it is positive. We

---

<sup>#</sup> Ph.D student

determined numerically the Julia set of the initial values leading to chaos as well as the corresponding set in the parameter space in some illustrative cases.

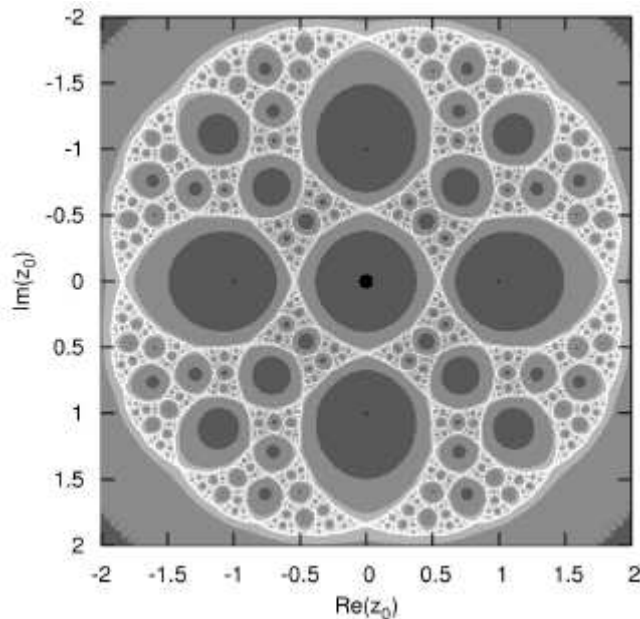


**Figure 1.** The Julia set of the initial states of a qubit undergoing measurement selected iterative dynamics, for a fixed value of the complex rotation parameter. Initial states, close to each other, may deviate exponentially fast, unlike in usual quantum chaos. Grayscale indicates how fast the map converges to the stable cycle (dark – fast, gray – slow convergence, white – no convergence).

We studied entanglement detection in various physical systems with a connection to recent experiments, e.g., with photonic systems realizing a four-qubit symmetric Dicke state with two excitations. We looked for temperature limits below which entanglement can be present in a spin chain.

**Nuclear motion in molecules: dynamics and spectroscopy.** – New results concerning the theory and applications of finite basis and discrete variable representations (FBR and DVR) and a number of subtle and confusing issues in large amplitude internal motions of molecules have been obtained. In particular, it has been shown how an optimal set of grid points can be obtained for an optimal generalized FBR/DVR calculation with a given truncated basis and the notions of Gaussian quadrature and Gaussian quadrature accuracy have been extended to general, multivariable basis functions.

### E-Mail:

Péter Ádám	adam@szfki.hu
János Asbóth	asboth@optics.szfki.kfki.hu
Péter Domokos	domokos@szfki.hu
Aurél Gábris	gabrisa@optics.szfki.kfki.hu
József Janszky	janszky@szfki.hu
Attila Kárpáti	karpati@optics.szfki.kfki.hu
Zsolt Kis	zsolt@szfki.hu
Tamás Kiss	tkiss@optics.szfki.kfki.hu
Mátyás Koniorczyk	kmatyas@optics.szfki.kfki.hu
Zoltán Kurucz	kurucz@szfki.kfki.hu
Dávid Nagy	nagyd@optics.szfki.kfki.hu,
Viktor Szalay	viktor@szfki.hu
Géza Tóth	toth@optics.szfki.kfki.hu,
András Vukics	vukics@optics.szfki.kfki.hu

## Grants and international cooperations

- OTKA T049234 Quantum optical systems and applications in quantum informatics (J. Janszky, 2005-2008)
- OTKA T043079 Moving atoms and molecules in strongly-coupled radiation fields (P. Domokos, 2003-2006)
- OTKA T043287 Adiabatic control in quantum optics and quantum informatics (Z. Kis, 2003-2006)
- OTKA T045955 Theoretical methods to describe vibrational-rotational motion of molecules (V. Szalay, 2004-2007)
- OTKA T049234 Detection of multipartite entanglement in quantum optical systems (G. Tóth, 2006-2008)
- TéT, Hungarian-Czech Bilateral Intergovernmental S&T Cooperation (CZ-2/2005): Quantum information and entanglement in quantum optical networks (T. Kiss, 2006-2007)
- TéT Hungarian-Greek Bilateral Intergovernmental S&T Cooperation (GR-42/03): Nonlinear and quantum optics in photonic band gap materials: phenomena and methods (Z. Kis, 2005-2006)
- FP6 Marie Curie European Reintegration Grant of the European Commission (MERC-CT-2005-029146): Detection of multipartite entanglement in quantum optical systems (G. Tóth, 2006)
- Öveges József program: Qubit dynamics in quantum optical networks (T. Kiss, 2006-2007)
- Öveges József program: Cavity Quantum Electrodynamics: from atoms to many-body systems (P. Domokos, 2006-2007)

## Publications

### Articles

- T.1. Allen<sup>\*</sup> WD, Bodi<sup>\*</sup> A, Szalay V, Császár<sup>\*</sup> AG; Adiabatic approximation to internal rotation; *J Chem Phys*; **124**, 224310/1-9, 2006
- T.2. Czakó<sup>\*</sup> G, Szalay V, Császár<sup>\*</sup> AG; Finite basis representations with nondirect product basis functions having structure similar to that of spherical harmonics; *J Chem Phys*; **124**, 014110/1-13, 2006
- T.3. Guhne<sup>\*</sup> O, Mechler<sup>\*</sup> M, Tóth G, Ádám P; Entanglement criteria based on local uncertainty relations are strictly stronger than the computable cross norm criterion; *Phys Rev A*; **74**, 010301(R)/1-4, 2006
- T.4. Guhne<sup>\*</sup> O, Tóth G; Energy and multipartite entanglement in multidimensional and frustrated spin models; *Phys Rev A*; **73**, 052319/1-9, 2006
- T.5. Hiesmayr<sup>\*</sup> H, Koniorczyk M, Narnhofer<sup>\*</sup> H; Maximizing nearest-neighbor entanglement in finitely correlated qubit chains; *Phys Rev A*; **73**, 032310/1-11, 2006
- T.6. Kárpáti A, Ádám P, Kis Z, Janszky J; Stochastic unraveling of the time-evolution operator of open quantum systems; *Europhys Lett*; **75**, 209-215, 2006

- T.7. Kiss T, Jex<sup>\*</sup> I, Alber<sup>\*</sup> G, Vymetal<sup>\*</sup> S; Complex chaos in the conditional dynamics of qubits; *Phys Rev A*; **74**, 040301R/1-4, 2006
- T.8. Kurucz Z, Ádám P, Janszky J; General criterion for oblivious remote state preparation; *Phys. Rev. A*; **73**, 062301/1-6, 2006
- T.9. Koniorczyk M, Buzek<sup>\*</sup> V, Ádám P; Simulation of generators of Markovian dynamics on programmable quantum processors; *Eur Phys J D*; **37**, 275-281, 2006
- T.10. Nagy D, Asbóth J, Domokos P, Ritsch<sup>\*</sup>; Self-organization of a laser-driven cold gas in a ring cavity; *Europhys. Lett*; **74**, 254-260, 2006
- T.11. Szalay V; Optimal grids for generalized finite basis and discrete variable representations: Definition and method of calculation; *J Chem Phys*; **125**, 154115/1-15, 2006
- T.12. Tóth G, Acin<sup>\*</sup> A; Genuine tripartite entangled states with a local hidden-variable model; *Phys Rev A*; **74**, 030306(R)/1-4, 2006
- T.13. Tóth G, Gühne<sup>\*</sup> O, Briegel<sup>\*</sup> HJ; Two-setting Bell inequalities for graph states; *Phys Rev A*; **73**, 022303/1-7, 2006
- T.14. Tóth G, Gühne<sup>\*</sup> O; Detection of multipartite entanglement with two-body correlations; *Appl Phys B: Lasers and Optics*; **82**, 237-241, 2006
- T.15. Czakó<sup>\*</sup> G, Császár<sup>\*</sup> AG, Szalay V, Sutcliffe<sup>\*</sup> BT; Adiabatic Jacobi corrections to  $H_2^+$ -like systems; *J Chem Phys*; accepted for publication
- T.16. Kiss T, Jex<sup>\*</sup> I, Alber<sup>\*</sup> G, Vymetal<sup>\*</sup> S; Complex chaos in conditional qubit dynamics and purification; *Acta Phys Hung B*; accepted for publication
- T.17. Kurucz Z, Ádám P, Janszky J; Remote state preparation in quadrature basis; *Acta Phys Hung B*; accepted for publication
- T.18. Nagy D, Asbóth J, Domokos P; Collective cooling of atoms in a ring cavity; *Acta Phys Hung B*; accepted for publication
- T.19. Stefanak<sup>\*</sup> M, Kiss T, Jex<sup>\*</sup> I, Mohring<sup>\*</sup> B; The meeting problem in the quantum walk; *J Phys A*; accepted for publication
- T.20. Tóth G; Detection of multipartite entanglement in the vicinity of symmetric Dicke states; *J Opt Soc Am B*; accepted for publication

#### ***Articles in Hungarian***

- T.21. Janszky J, Domokos P; Kvantumoptika és kvantuminformatika (Quantum optics and quantum information, in Hungarian); *Magyar Tudomány*; **166**, 1550-1557, 2005
- T.22. Domokos P; Az atom-foton molekula (The atom-photon molecule, in Hungarian); *Magyar Tudomány*; **167**, 531-535, 2006

***Book chapters in Hungarian***

- T.23. Ádám P, Kárpáti A.; Nyílt kvantumrendszerek Markov közelítésben: a sűrűségoperátor és a kvantumtrajektória módszerek (Open quantum systems in Markoff approximation: the density matrix and quantum trajectory methods, in Hungarian); In: *A kvantumoptika és elektronika legújabb eredményei*; eds.: Heiner Zs, Osvai K, SZTE TTK, ISBN:963 482 779 9, pp. 135-147, 2006
- T.24. Domokos P; A fény mechanikai hatása optikai rezonátorban (The mechanical effects of light in optical resonators, in Hungarian); In: *A kvantumoptika és elektronika legújabb eredményei*; eds.: Heiner Zs, Osvai K, SZTE TTK, ISBN:963 482 779 9, pp. 107-119, 2006
- T.25. Koniorczyk M, Tóth G; Bevezetés a kvantummechanikai összefonódottsághoz (An introduction to quantum entanglement, in Hungarian); in: *A kvantumoptika és elektronika legújabb eredményei*; eds.: Heiner Zs, Osvai K, SZTE TTK, ISBN:963 482 779 9, pp. 95-106, 2006

# EDUCATION

## Graduate and postgraduate courses, 2006

- Algebraic Bethe ansatz and its application (F. Woynarovich, ELTE<sup>1</sup>)
- Advanced solid-state physics (J. Sólyom, ELTE)
- Electrodynamics of continuous media (F. Woynarovich, ELTE)
- Renormalization methods for quantum systems (Ö. Legeza, ELTE)
- Solid-state physics (J. Sólyom, ELTE)
- Statistical physics (F. Iglói, SZTE<sup>2</sup>)
- Application of statistical physics (F. Iglói, SZTE)
- Disordered systems (F. Iglói, SZTE)
- Many body systems I. (P. Szépfalussy, ELTE)
- Many body systems II. (P. Szépfalussy, ELTE)
- The theory of magnetism I. (P. Fazekas, BME<sup>3</sup>)
- The theory of magnetism II. (P. Fazekas, BME)
- Electronic states in solids (J. Kollár, ELTE)
- Advanced solid state physics II. (I. Tüttő, ELTE)
- Solid state research I.-II. (I. Vincze, ELTE)
- Non-Equilibrium alloys (T. Kemény, ELTE)
- Spectroscopy and material structure (K. Kamarás, BME)
- Infrared and Raman spectroscopy (K. Kamarás, BME)
- Physics of liquid crystals and polymers (Á. Buka and N. Éber, ELTE)
- Pattern formation in complex systems (Á. Buka, ELTE)
- Non-conventional materials (Á. Buka, BME)
- Liquid crystals, their chemistry and chemical physics. (K. Fodor-Csorba)
- Nanophase metals (I. Bakonyi, ELTE)
- Advanced material technology (G. Konczos, BME and ELTE)
- NMR spectroscopy (K. Tompa, BME)
- Group theory in solid state research (G. Kriza, BME)
- Superconductivity (G. Kriza, BME)
- Application of thermal neutrons for study of condensed matter (L. Cser, ELTE).

---

<sup>1</sup> ELTE = Loránd Eötvös University, Budapest

<sup>2</sup> SZTE = University of Szeged

<sup>3</sup> BME = Budapest University of Technology and Economics

- Neutron beam methods in materials science, special course (L. Rosta, BME)
- Neutron Scattering in condensed matter, special course (L. Rosta, ME<sup>4</sup>)
- Disorder in condensed phases (L. Pusztai, ELTE)
- From femtosecond lasers to attophysics, special course (P. Dombi, BME)
- Medical application of lasers (Z. Gy. Horváth ; E-D Medical Laser Center)
- Physics of amorphous matter I. (M. Koós, SZTE)
- Physics of amorphous matter II. (M. Koós, SZTE)
- Optical signal processing (R. Szipócs, BME)
- Femtochemistry (R. Szipócs, ELTE)
- Growth, processing and characterization of nonlinear optical crystals (In: Applied Lasertechnics, I. Földvári, BME)
- Classic theories of crystal nucleation (L. Malicskó, BME)
- Theories of crystal growth (L. Malicskó, BME)
- Microscopy in materials science (L. Malicskó, BME)
- Technical application of crystals (E. Hartmann, BME)
- The characterization of crystals ( E. Hartmann, BME)
- Thermodynamics (P. Ádám, PTE<sup>5</sup>)
- Quantum mechanics I-II (P. Ádám, PTE)
- Quantum optics (P. Ádám, PTE)
- Resonant light-matter interaction (P. Ádám, PTE)
- Solid state physics (P. Ádám, J. Asbóth, PTE)
- Quantum mechanics (J. Janszky, PTE)
- Quantum information theory (J. Janszky, PTE)
- Applied optics (T. Kiss, ELTE)
- Information theory (M. Koniorczyk, PTE)
- Methods in theoretical quantum information (M. Koniorczyk, PTE)

### **Laboratory practice and seminars**

- Solid-state physics seminar (J. Sólyom, ELTE)
- Seminar in quantum mechanics (B. Lazarovits, BME)
- Infrared spectroscopy laboratory practice (V. Zólyomi, ELTE)
- Advanced molecular physics laboratory practice (V. Zólyomi, ELTE)

---

<sup>4</sup> ME = University of Miskolc

<sup>5</sup> PTE = University of Pécs

- Laboratory for solid state physics, Preparation and crystallization of metallic glasses (I. Vincze, ELTE)
- Lectures on vibrational spectroscopy (with laboratory practice), part of the course Experimental methods in materials science (K. Kamarás; BME)
- Infrared and Raman spectroscopy laboratory practice (K. Kamarás, BME)
- Infrared spectroscopy of fullerenes; part of the advanced Molecular Physics Laboratory, K. Kamarás, ELTE)
- Infrared and Raman spectroscopy of solids; part of the advanced Condensed Matter Laboratory (Á. Pekker, BME)
- Experiments on liquid crystals (Á. Buka and N. Éber, ELTE)
- NMR spectroscopy (K. Tompa, ELTE and BME)
- Physical chemistry laboratory practice (L. Péter, ELTE)
- Advanced solid state physics laboratory (Gy. Tóth, ELTE and BME)
- Radiation protection laboratory practices (L. Temleitner, BME)
- Environmental protection laboratory practices: radiation aspects (L. Temleitner, BME)
- Experimental physics classroom practice (Sz. Pothoczki, BME)
- Mathematical methods of physics I. (P. Ádám, PTE)
- Quantum statistical optics I. (Z. Kis, ELTE)
- Quantum mechanics (J. Asbóth, PTE)

### **Diploma works**

- J. Romhányi (BME): Competition of magnetic and dimer phases in Heisenberg models (Supervisor: P. Fazekas)
- G. Tátrai (ELTE): Effect of confined geometry on the electric and magnetic field induced instabilities in liquid crystals. (Supervisors: Á. Buka and N. Éber)
- Sz. Pothoczki (BME): Investigation of the structure of molecular liquids by neutron diffraction and Reverse Monte Carlo simulation (Supervisor: L. Pusztai)
- I. Hajdara (ELTE): Optical spectroscopic and dielectric measurements on potassium lithium niobate crystals (Supervisor: L. Kovács)
- K. Száraz (PTE): Gravitational field (Supervisor: P. Ádám)
- D. Nagy (BME): Collective effects in the laser cooling of neutral atoms (Supervisor: P. Domokos)

### **Ph. D. students**

- K. Buchta (ELTE): Phase transitions in low-dimensional spin and fermionic models (Supervisor: J. Sólyom)

- E. Szirmai (ELTE): Mott-transition in  $SU(n)$  symmetric Hubbard chains and ladders (Supervisor: J. Sólyom)
- L. Környei (SZTE): Statics and dynamics of random-field Ising models (Supervisor: F. Iglói)
- P. Nagy (SZTE): Relaxation in complex networks (Supervisor: F. Iglói)
- M. Karsai (SZTE): Cooperative behavior in complex networks (Supervisor: F. Iglói)
- F. Borondics (ELTE Graduate Program in Chemistry, supported by HAS): Raman spectroscopy of carbon nanotubes (Supervisor: K. Kamarás)
- Á. Pekker (BME Graduate Program in Physics): Spectroscopy of chemically functionalized carbon nanotubes (Supervisor: K. Kamarás)
- É. Kováts (ELTE): Addition reaction of fullerenes and related compounds in solid phase (Supervisor: S. Pekker)
- G. Tóth (ELTE): Field theoretic description of far-from-equilibrium solidification morphologies (Supervisor: L. Gránásy)
- É. Fazakas (ELTE): Preparation of bulk amorphous alloys by mechanical alloying (Supervisor: L.K. Varga)
- L. Németh (BME): NMR study of low-dimensional metals (Supervisor: G. Kriza)
- P. Matus (BME): NMR study of metals with correlated electronic system (Supervisor: G. Kriza)
- Á. Pallinger (ELTE): Dissipation in type-II superconductors (Supervisor: B. Sas)
- M. Markó (BME): Neutron holography (Supervisor: L. Cser)
- N.K. Székely (ELTE): Small angle neutron scattering study of polyol aqueous solutions, (Supervisor: L. Rosta)
- G. Nagy (ELTE): SANS study of model materials for photosynthesis (Supervisor: L. Rosta)
- J. Orbán (BME): Study and developing of readout electronic of position sensitive neutron detectors (Supervisor: L. Rosta)
- T. Veres (ELTE): Neutron Reflectometry (Supervisor: L. Cser)
- M. Fábrián (ELTE): The structure of borosilicate glasses (Supervisor: E. Sváb)
- L. Temleitner (BME): Diffraction and computer simulation studies of disordered molecular systems (Supervisor: L. Pusztai)
- Sz. Pothoczki (BME): Investigation of the structure of molecular liquids by neutron diffraction and computer simulation (Supervisor: L. Pusztai)

- P. Horváth (ELTE): Mass spectroscopic studies of radiofrequency H<sub>2</sub> and SiH<sub>4</sub>-H<sub>2</sub> plasmas (Supervisor: K. Rózsa)
- S. Tóth (SZTE): Light emission of carbon based films and nanoclusters (Supervisor: M. Koós)
- M. Füle (SZTE): Photoluminescence and optical absorption near the band edges in amorphous carbon thin films (Supervisor: M. Koós)
- P. Gál (BME): Development of light scattering instruments (Supervisor: A. Czitrovsky)
- D. Oszetzky (BME): Application of quantum-optical measurement methods (Supervisor: A. Czitrovsky)
- L. Vámos (BME): Statistics of scattered light (Supervisor: P. Jani)
- G. Dravecz (ELTE and Université de Metz): Study of the phase equilibria and crystal growth in the ternary system A<sub>2</sub>O-Li<sub>2</sub>O-M<sub>2</sub>O<sub>5</sub> (A= K,Rb,Cs, M=Nb,Ta) (Supervisor: K. Polgár)
- I. Hajdara (PTE): Spectroscopy of ferroelectric oxide crystals (Supervisor: L. Kovács)
- G. Czakó (ELTE): High-accuracy ab initio (ro)-vibrational spectroscopy; Non-born-Oppenheimer calculations (Supervisor: V. Szalay)
- A. Gábris (SZTE): Nonlinear photonic crystals and quantum optical processes therein (Supervisor: J. Janszky)
- Z. Kurucz (SZTE): Quantum state manipulation and quantum information theory (Supervisor: J. Janszky)
- A. Vukics (SZTE): Dissipative motion of atoms in strongly-coupled light fields (Supervisor: P. Domokos)
- J. Asbóth (SZTE): Atom-atom interactions mediated by optical resonator fields (Supervisor: P. Domokos)

## **Dissertations**

- V. Zólyomi: Theoretical investigation of small diameter carbon nanotubes (Ph.D., ELTE, supervisor: J. Kúrti, ELTE)
- F. Bagaméry: Critical behaviour of 2d models with inhomogeneous perturbations (Ph.D., SZTE, supervisor: F. Iglói)
- Gy. Pergerné-Klupp: Study of the Jahn-Teller effect in alkali fullerenes (PhD, ELTE Graduate Program in Chemistry, supervisor: K. Kamarás)
- Gy. Bényei: Synthesis of caged compounds and investigation of their mesomorphic properties (Ph.D., ELTE, co-supervisor: K. Fodor-Csorba)

- A. Bárdos: Preparation and investigation of Fe-based bulk amorphous alloys (Ph.D., BME, co-supervisor: L.K. Varga)
- A. Kákay: Numerical investigations of micromagnetic structures (Ph.D., ELTE, supervisor: L.K. Varga)
- A. Mikó: Preparation of nanostructured and amorphous Fe-based thin layers and Fe/Fe-oxide multilayers by non-stationary electrochemical methods (Ph.D., ELTE, co-supervisor: L.K. Varga)
- I. Harsányi: Investigation of the structure of aqueous electrolyte solutions using computer simulation methods (Ph.D, ELTE, supervisor: L. Pusztai)
- M.Füle: Photoluminescence and optical absorption near the band edges in amorphous carbon thin films (Ph.D., SZTE, supervisor: M. Koós)
- Á Bányász: Model-free deconvolution of ultrafast kinetic data, and singlet excited state behaviour of uracil derivatives (PhD, ELTE, supervisor: R. Szipőcs)

## AWARDS

- Gy. Farkas, Károly Simonyi Award 2006 (Founders: Hungarian-American Coalition and the János Arany Foundation)
- P. Fazekas, Physics Award of the Hungarian Academy of Sciences (2006)
- B. Lazarovits, Burgen Scholarship 2006, awarded by Academia Europaea (2006)
- I. Bakonyi, SZFKI Annual Publication Award (2006)
- S. Tóth, M. Veres, M. Füle, SZFKI Annual Award for Applied Research (2006)
- Gy. Török, L.Cser, Gy. Káli, 3rd award of the Petersburg Nuclear Physics Institute for the best publication of 2005 in Solid State Physics (2006)
- Sz. Pothoczki, 1<sup>st</sup> prize and the Dean's Award, Young Investigators' Conference (2006)
- G. Bortel, Bolyai Grant (2003-2006)
- G. Oszlányi, Bolyai Grant (2003-2006)
- T. Pusztai, Bolyai Grant (2003-2006)
- T. Börzsönyi, Bolyai Grant (2005-2008)
- L. Péter, Bolyai Grant (2004-2006)
- M. Veres, Bolyai Grant (2006-2008)
- R. Szipőcs, Bolyai Grant (2005-2006)
- P. Domokos, Bolyai Grant (2003-2006)

## CONFERENCES

The **Introductory course and training – neutron applications at IBR-2 pulsed reactor** has been held on October 1-8 in the Joint Institute for Nuclear Research (JINR), Dubna, Russia. This was the first joint school organization by the Neutron Spectroscopy Department of our Institute and the Frank Laboratory of Neutron Physics of JINR. The aim of this course was to provide insight into various neutron scattering techniques and their application for studies on structure and dynamics of condensed matter. The 12 hours of lectures were delivered by scientists of the Neutron Spectroscopy Department and the Frank Laboratory of Neutron Physics, they gave an introduction on various neutron scattering techniques. Hands-on-training on neutron spectrometers led by the local instrument scientists, demonstrated to the students the art of utilization of instruments at a large scale facility. 15 students participated in the training, young physicists and chemists from 6 Hungarian research institutes universities.

**3<sup>rd</sup> Reverse Monte Carlo Conference and Tutorial**; Hotel Normafa, Budapest; 26-30 September 2006; organised by L. Pusztai (Department of Neutron Physics). 44 participants (28 from abroad). Proceedings volume will be published in *Journal of Physics: Condensed Matter*.

## TABLE of CONTENTS

<b>PREFACE</b>	
<b>KEY FIGURES</b>	<b>1</b>
<b>A. STRONGLY CORRELATED SYSTEMS</b>	<b>7</b>
<b>B. COMPLEX SYSTEMS</b>	<b>11</b>
<b>C. ELECTRONIC STATES IN SOLIDS</b>	<b>14</b>
<b>D. NON-EQUILIBRIUM ALLOYS</b>	<b>20</b>
<b>E. X-RAY DIFFRACTION</b>	<b>23</b>
<b>F. LIQUID CRYSTALS</b>	<b>29</b>
<b>G. ELECTRON CRYSTALS</b>	<b>34</b>
<b>H. METAL PHYSICS</b>	<b>36</b>
<b>I. METALLURGY AND MAGNETISM</b>	<b>41</b>
<b>J. NEUTRON SPECTROSCOPY IN CONDENSED MATTER</b>	<b>46</b>
<b>K. NEUTRON SCATTERING</b>	<b>53</b>
<b>L. INTERACTIONS OF INTENSE LASER FIELDS WITH MATTER</b>	<b>58</b>
<b>M. LASER PHYSICS</b>	<b>62</b>
<b>O. LASER APPLICATION</b>	<b>66</b>
<b>P. FEMTOSECOND LASERS</b>	<b>73</b>
<b>Q. OPTICAL THIN FILMS</b>	<b>77</b>
<b>R. GROWTH AND CHARACTERIZATION OF OPTICAL CRYSTALS</b>	<b>79</b>
<b>S. CHARACTERIZATION AND POINT DEFECT STUDIES OF OPTICAL CRYSTALS</b>	<b>85</b>
<b>T. NONLINEAR AND QUANTUM OPTICS</b>	<b>90</b>
<b>EDUCATION</b>	<b>95</b>
<b>AWARDS</b>	<b>101</b>
<b>CONFERENCES</b>	<b>102</b>